New light Sources for Biomedical Applications

Argyraki, Aikaterini

Publication date:
2017

Document Version
Publisher's PDF, also known as Version of record

DTU Fotonik
Department of Photonics Engineering

Technical University of Denmark DTU

New light Sources for Biomedical Applications

PhD Thesis

Aikaterini Argyraki

May 26, 2017

Main supervisor: Prof. Paul Michael Petersen

Supervisor: Senior scientist Carsten Dam-Hansen

Resumé

LED teknologien giver helt nye muligheder for spektralt design, som er attraktivt inden for mange medicinske anvendelser. Ph.d. afhandlingen udforsker de potentielle sundhedsmæssige fordele, man kan opnå med ultraviolette og synlige LED lyskilder.

Afhandlingen benytter en tværfaglig tilgang, der kombinerer kompetencer fra forskellige videnskabelige områder som fotonik, mikrobiologi, fotokemi, kronobiologi og obstetrik. Det er afhandlingens formål at undersøge de biologisk relevante effekter, som LED-belysning har, samt at give statistisk evidens for at disse LED-systemer kan forbedre menneskers sundhed.

Et bærbar ultraviolet LED UV-belysningssystem blev fremstillet i ph.d. projektet. Belysningssystemet blev benyttet til at undersøge hvorledes bakterier i biofilm kunne inaktiveres ved at benytte smalbåndet UV-bestråling i intervallet 250-340 nm. Det blev observeret at genvækst blev mest effektivt undertrykt af lyset i UVB-området. Blandt alle de undersøgte bølgelængder fremviste 296 nm det største potentiale for biofilm inaktivering. En strålingseksponering på 20.000 J/m^2 var tilstrækkelig til at opnå fuldstændig inaktivering af biofilmen. Denne optiske behandlingsform viste sig at være mere effektiv til inaktivering af bakterier end: 1) fotodynamisk terapi, 2) antibiotika og 3) lige så effektive som kombinatoriske antibiotika. I ph.d. projektet er udviklet en ny metode "lys assisteret antibiotika", som giver en effektiv inaktivering på 99.9 % for modne biofilm. Sidstnævnte behandlingsform kan få stor betydning for behandling af infektionssygdomme i fremtiden, fordi mængden af antibiotika kan reduceres betydeligt.

I projektet er ligeledes undersøgt, hvorledes UV LED kan benyttes til D-vitaminberigelse af forskellige fødevarer. Indholdet af D-vitamin i svinehud kunne øges til et niveau på 0.5 µg/cm^2 efter blot 7 sekunders eksponering, og D-vitamin indholdet i æggeblommer blev øget med en faktor 4.

Den sidste del af ph.d. projektet omhandler, hvorledes synligt LED lys kan forbedre menneskers søvn, sundhed og præstationsevne. Konkrete eksempler er forbedring af ældre kvinders søvn, OL atleters reaktionsevne, samt inden for hospitalsanvendelser at reducere antallet af kejsersnit samt at øge evnen til at identificere blodårer.

Abstract

LED technology offers flexibility of spectral design and comfort in operation. This PhD thesis explores the potential health benefits that can be imposed by light interventions performed with ultraviolet (UV) light emitting diodes (LEDs) or visible (VIS) LED lighting systems.

Based on a cross-disciplinary approach, combining competences from diverse scientific fields such as photonics, microbiology, photochemistry, chronobiology, and obstetrics the scope of this PhD project was 1) to investigate, by a systematic approach, effects imposed by narrowband UV irradiation, as emitted by LEDs, on systems with biological relevance and 2) to generate statistically significant evidence that VIS LED lighting systems, when used in a suitable manner, can improve several dimensions of human health and human performance.

A portable UV irradiation setup was fabricated and characterized. Bacterial communities forming biofilms and their inactivation by narrowband UV irradiation in the range 250-340 nm, was investigated. It was observed that regrowth was suppressed more effectively after UVB irradiation. Among the UVB LEDs tested, the diode at 296 nm showed the greatest potential for biofilm inactivation; radiant exposure at 20.000 J/m^2 was proven adequate to totally inactivate immature biofilms. This treatment was shown to be more effective than 1) photodynamic therapy, $p=0.002$ 2) conventional antibiotics, $p<<0.001$; and 3) equally effective to combinatory antibiotics, $p=0.12$. However, effective inactivation (99.9%) on mature biofilms was only achieved after a novel treatment was invented, namely “light assisted antibiotics”. Additionally, significant vitamin D enrichment of various food products was achieved. Especially the content of vitamin D in pig skin could reach 0.5 μg/cm^2 after 7 sec. exposure versus the 0.005 μg/cm^2 of not exposed samples, and 4 fold increase of vitamin D in egg yolk was demonstrated by direct illumination.

Applying VIS LED illuminants with specific spectral power distribution in elderly houses resulted in better sleep for elderly women ($p=0.007$). Light interventions enabled elite athletes to conserve their sleep quantity and quality, despite their shifted circadian rhythm. Easier vein identification-access was achieved by applying a special LED illuminant and a statistic evaluation of the human eye ability to identify veins was performed. Finally, lower risks for C-section (OR= 0.57; 95% CI 0.33-0.97) were attained when labor rooms were equipped with dynamic illumination.

Note: The holistic approach of benefits on human health induced by LED interventions followed throughout the present PhD study is not following the conventional path of contemporary academic work governed by high degree of specialization. This is a consequence of the project's scope and the author's diverse background.

Preface

This thesis is submitted in partial fulfillment of the requirements for obtaining a Doctor of Philosophy degree at the Technical University of Denmark (DTU). The work has been carried out mainly at the Department of Photonics Engineering, Technical University of Denmark (DTU Fotonik) in the Diode Lasers and LED Systems group. Four month research stay was spent at the National Food Institute, Technical University of Denmark (DTU Food) and at the Department of International Health, Immunology and Microbiology Costerton biofilm Center at University of Copenhagen. Main supervisor of the PhD project is Prof. Paul Michael Petersen, Professor and group leader of the Diode Lasers and LED systems group at DTU Fotonik and co-supervisor the Senior Researcher Carsten Dam-Hansen. The project was co-financed by Region Zealand Denmark “Doll project”(project no. 2075008) and DTU Fotonik.

Acknowledgement

This project has been completed with the support and assistance from several individuals. I hereby wish to express my appreciation and gratitude for their help and collaboration to the following:

First of all I would like to thank my main supervisor Prof. Paul Michael Petersen for his intelligent guidance throughout the project, for inspiring me to work in a cross-disciplinary environment and for always supporting my personal development and showing interest in my work. Paul Michael I would like to thank you for always allowing me to pursue my ideas, sharing your knowledge with me; and for always inventing time for me.

I would also like to thank Carsten Dam-Hansen for his guidance and for always answering my questions. I would like to express my gratitude to Anders Kragh Hansen for proof reading part of my thesis. Dennis Dan Corell and Anders Thorseth, I would like to thank you for your help and assistance in the lab, Maria Louisa Rosenberg Welling thank you for checking the written quality of the thesis and for always helping with practicalities. Dominik Marti I would like to thank you for proof reading my first PhD publication. My warm thanks to Haiyan Ou and Yiyu Ou for introducing me to the world of LEDs, and helping me with the transition from nanoscience to photonics. I would also like to thank Weifang Lu for the contact angle measurements and scanning electron microscopy pictures of nanostructured polymer. Jakob Munkgaard Andersen, Søren Hansen and Peter Jensen for providing assistance and helping me several times with moving the UV irradiation setup at several locations in Copenhagen area. Stubager Jørgen thanks for helping with the fabrication of highly reflective orifices. Anders Stockmarr and Bo F. Nielsen I would like to thank you for your feedback on statistical analysis of biofilms. Linda Christel thank you for your warm smile at the times that was most needed. My thanks also embrace all members of the Diode Lasers and LED Systems Group for their usefull suggestions and all my colleagues from DTU Fotonik for our interesting discussions.

I am indebted to all great collaborators from different Institutes and hospitals, for enlightening me with their expertise, as well as for our constructive cross-disciplinary discussions and debates: Jette Jakobsen, Line L. Barnkob, Anja H. Pedersen; from the National Food Institute (DTU), Merete Markvart, Lars Bjørndal; from the Department of Odontology (KU), Thomas Bjarnsholt, Camilla Stavnsbjerg, Anne Nielsen, Maria Alhede; from

the Department of Immunology and Microbiology, Costerton biofilm Center (KU), Birgit. A. Sander and Line Kessel; from the Department of Ophthalmology, Rigshospitalet – Glostrup (KU), Tine Wrønding and Ellen C. L. Løkkegaard; from the Department of Obstetrics and Gynecology, Nordsjællands Hospital – Hillerød, Line K. H. Clemmensen; from DTU Compute, Kjeld Johnsen and Jakob Markvart; from Aalborg University, Lars Johansen, Andreas T. Adler; from Team Denmark, Jes Broeng and Jakob H. Andersen; from the Innovation Team of DTU Fotonik.

I would also like to acknowledge Region Zealand Denmark “DOLL project” and DTU Fotonik for the financial support of my PhD project, and Otto Mønsted's Foundation for the financial support for travelling.

Finally, I would like to thank my parents in Greece, Dimitrio Argyraki and Kassiani Gouni, and my brother Labro for always supporting my choices and for placing in me the seed of curiosity; and my family in Denmark for the unlimited love and for shining light my life.

Kgs. Lyngby, May 26, 2017

Aikaterini Argyraki

PhD Publication List

Journal articles

0.1. **Argyraki, A**., Clemmensen, L.K.H. and Petersen, P.M.,. 2016. Does correlated color temperature affect the ability of humans to identify veins?. JOSA A, 33(1), pp.141-148.

Author's contribution: Design of experiments, execution of experiments, generation of idea, analysis of data and writing the manuscript.

0.2. Barnkob, L.L., **Argyraki, A.**, Petersen, P.M. and Jakobsen, J.,. 2016. Investigation of the effect of UV-LED exposure conditions on the production of vitamin D in pig skin. Food Chemistry, 212, pp.386-391.

Author's contribution: Design of irradiation protocols, execution of irradiation experiments, UV LEDs characterization, Fabrication of experimental setup, and writing the manuscript sections related to irradiation.

0.3. Sander, B., Markvart, J., Kessel, L., **Argyraki, A**. and Johnsen, K.,. 2015. Can sleep quality and wellbeing be improved by changing the indoor lighting in the homes of healthy, elderly citizens?. Chronobiology international, 32(8), pp.1049-1060.

Author's contribution: Light characterization, formulation of the manuscript sections related to light conditions.

0.4. Ou, H., Ou, Y., **Argyraki, A.**, Schimmel, S., Kaiser, M., Wellmann, P., Linnarsson, M.K., Jokubavicius, V., Sun, J., Liljedahl, R. and Syväjärvi, M.,. 2014. Advances in wide bandgap SiC for optoelectronics. The European Physical Journal B, 87(3), pp.1-16.

Author's contribution: Development of new low cost method (thin Al mask) to form nanostructures for enhancing LED light extraction efficiency, fabrication, characterization, optical measurements.

0.5. **Argyraki, A.**, Markvart, M., Bjarnsholt, T., Bjørndal, L. and Petersen, P.M., 2017. Inactivation of Pseudomonas aeruginosa (P. aeruginosa) biofilm after UV LED treatment: a comparative study between UVC and UVB. Submitted to Journal of Biomedical Optics.

Author's contribution: Design of irradiation experiments, execution of irradiation treatments, fabrication of experimental setup, characterization, modelling, analysis of data and writing the manuscript.

0.6. Markvart, M., **Argyraki, A.**, Bjarnsholt, T., Petersen, P.M., and Bjørndal, L., UVB irradiation is more efficient than photodynamic therapy on uni-microbial biofilms" (to be submitted).

Author's contribution: Design of irradiation experiments, execution of irradiation treatments, fabrication of experimental setup, characterization, analysis of data (UV treated samples).

0.7. Wrønding, T., **Argyraki, A.**, Petersen, P. M., Løkkegaard E.C.L. "The association between light conditions in a delivery room and risk of obstetrician interventions " (to be submitted)

Author's contribution: Light characterization, formulation of the manuscript sections related to light conditions.

0.8. **Argyraki, A.**, Stavnsbjerg. C., Markvart, M., Bjarnsholt, T., Bjørndal, L. and Petersen, P. M., 2017. "Light assisted antibiotics" (in preparation)

Author's contribution: Conceptualization of novel treatment for combating resistant biofilms, design of experiments, execution of irradiation treatments, fabrication of experimental setup, characterization, analysis of data and writing the manuscript.

Published Proceedings

0.9. **Argyraki, A.,** Markvart, M., Nielsen, A., Bjarnsholt, T., Bjørndal, L. and Petersen, P.M., 2016. Comparison of UVB and UVC irradiation disinfection efficacies on Pseudomonas Aeruginosa (P. aeruginosa) biofilm. Proc. SPIE 9887, Biophotonics: Photonic Solutions for Better Health Care V, pp. 988730-988730.

Author's contribution: Design of irradiation experiments, execution of irradiation treatments, fabrication of experimental setup, modelling, analysis of data and writing the manuscript.

0.10. **Argyraki, A.,** Lu, W., Petersen, P.M. and Ou, H.,. 2015. Scalable nanostructuring on polymer by a SiC stamp: optical and wetting effects. "Proc. SPIE 9556, Nanoengineering: Fabrication, Properties, Optics, and Devices XII, pp. 955607-955607.

Author's contribution: Design of experiment, fabrication, characterization, optical measurements, and writing the manuscript.

0.11. **Argyraki, A.,** Clemmensen, L.K.H. and Petersen, P.M., 2015. Development of LED Light Sources for Improved Visualization of Veins: a statistical approach. In 3rd European-Asian workshop on Light-Emitting Diodes.

Author's contribution: Design of experiment, fabrication of setup, optical measurements, analysis and writing the manuscript.

Conferences (Poster sessions and talks)

0.12. **Argyraki, A.,** Andersen, J.M., Hansen, S.S., Stubager, J., Corell, D.D. and Petersen, P.M., 2014. Development of New LED

Light Sources for Improved Visualization of Bio-samples. In 35th Progress In Electromagnetics Research Symposium. (talk)

0.13. **Argyraki, A.,** Stavnsbjerg, C, Markvart, M., Bjarnsholt, T., Bjørndal, L. and Petersen, P.M., 2016, Inactivation of biofilms with UV LEDs. Annual Danish Optical Society meeting. (poster)

0.14. **Argyraki, A.,** Lu, W., Petersen, P.M. and Ou, H., 2015. Scalable nanostructuring on polymer by a SiC stamp: optical and wetting effects. SPIE 9556, Nanoengineering: Fabrication, Properties, Optics, and Devices XII, San Diego, California. (talk)

0.15. **Argyraki, A.,** Andersen, J. H., Johansen, L., Adler A.T., Broeng J., Petersen P. M. 2017. Light interventions: a novel approach for sustaining sleep quality and quantity of elite swimmers under conditions of shifted circadian rhythm. CSS Conference, Calgary AB, Canada. (poster)

0.16. Markvart, M., **Argyraki, A.,** Bjarnsholt, T., Petersen, P.M. and Bjørndal, L., 2017. UV treatment is Superior to Photodynamic Therapy on Enterococcus Faecalis. 18th Biennial ESE Congress, 14-16 Sept. Brussels, Belgium. (poster)

0.17. **Argyraki, A.,** Markvart, M., Nielsen, A., Bjarnsholt, T., Bjørndal, L. and Petersen, P.M., 2016. Comparison of UVB and UVC irradiation disinfection efficacies on Pseudomonas Aeruginosa (P. aeruginosa) biofilm. SPIE Photonics Europe, Brussels, 4-7 April. (poster)

Patent

- **Argyraki, A.,** Petersen, P. M., Bjarnsholt, T., Markvart, M., Bjørndal, L. Stavnsbjerg. C., 2017. Light assisted antibiotics. DTU ref.: 96036 (not filed yet)

Award

- 2016 Annual Danish Optical Society (DOPS), Best Poster Award.

Contents

1. Introduction

1.1. Motivation

Modern living separates humans from their natural surroundings and many might claim that this behavior is happening due to evolution mechanisms. However, when this separation is abrupt, it can have negative consequences. One vital element that is shaping or/and giving form to the natural surroundings is sunlight. Humans evolved in outdoor environments and therefore under the exposure of natural light, over millions of years. Nowadays, most hours of the day are spent indoors and for this reason it is important to try to optimize the artificial light sources with the scope to support wellbeing.

In the past, the gamut of available light sources for indoor illumination was quite limited. Technological development though, has brought us from the usage of torches and oil lamps, to three milestones of illumination: incandescent, fluorescent and LEDs. Incandescent and fluorescent lamps provide a spectral power distribution which is fixed, and as shown in Fig. 1.1 their spectral power distribution is distinct from sunlight. Incandescent lamps provide a continuous spectrum but lack the blue-ish contents; while fluorescent lamps exhibit discontinuity. Sunlight exhibits blue enriched and blue suppressed phases during the diurnal period, which cannot be achieved either by incandescent or fluorescent lamps.

On the contrary, solid state lighting (LEDs) offers the possibility to the light engineers to be creative with the spectral content and dynamically modulate it throughout a day. However, evidence for the possible positive effects of using a “spectrally creative” and time modulated indoor illumination, has not yet been extensively confirmed.

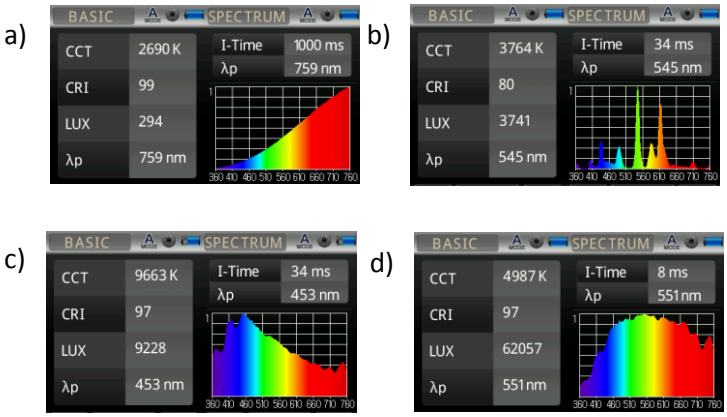

Fig. 1.1: Power spectral distributions as measured by a handheld spectrometer of a) an incadescent lamp b) a flourescent lamp c) morning sunlight d) afternoon sunlight.

Furthermore, LEDs also open the road for performing narrowband exposures in the UV range. This asset offered by solid state lighting could be used for bio-application purposes, but requires extensive knowledge about the specific wavelength dependent effects induced by UV light and a more mature UV LED market.

There is massive evidence that the LED markets both in the visible and UV region will continue growing primarily due to the energy saving benefits. Therefore, the (LED) costs are expected to fall drastically, enforcing wide acceptance of LEDs and out-phasing of the alternative lighting technologies. One must not forget that market development is a wheel of components: discovery, reflection, focusing, connection and enrichment that circulate creating a loop of feedback and progress [1.1]. This project focuses separately on VIS and on UV LEDs.

Visible LEDs

When this PhD project was initiated it was a moment where dynamic solid state lighting has matured in terms of technological development and several commercial products were available suggesting positive effects. However, the statistical demonstration of its possible positive effects on wellbeing and evidence that general health can be benefited by their usage was poor. The opinion, of the Illumination Engineering Society of North

America, that further research on the topic is essential, and not only with focus at LEDs, was clearly stated in 2008 [1.2, 1.3]. Concerning VIS LEDs, the purpose of this PhD thesis was to bridge that gap by generating more evidence and demonstrate statistically that the health benefits suggested were significant; by testing and characterizing existing commercially available LED systems. Populations with special healthcare needs were particularly in focus, since these groups are more vulnerable to negative consequences of inadequate lighting and attempts were made to even suggest novel light interventions. A scalable nanostructuring method for improving light extraction efficiency of LEDs was also suggested.

UV LEDs

In comparison to VIS solid state lighting, UV LEDs are still in the process of technological development and the effects of narrowband UV LED exposure are still unexplored. In this thesis, a systematic approach was implemented to investigate/discover the imposed effects of UV narrowband irradiation, as emitted by UV LEDs, in two critical areas which are indirectly connected to human health, namely vitamin D biofortification and biofilm disinfection/inactivation. By enriching the fields where UV LEDs can be used and connecting them to real life applications this PhD thesis contributes to re-enforce the loop of UV LED development.

In conclusion, this study has been based on a cross-disciplinary approach, with the scope to explore the potential health benefits that can be imposed by VIS and UV interventions, as provided by solid state lighting (LEDs).

1.2. Objectives

The main objectives of the present PhD thesis are:

- To explore the potential health benefits that can be imposed by LEDs as providers of electromagnetic radiation in the VIS and UV range
- To propose and implement an irradiation method for inactivating resistant bacteria (target to achieve a 99.9% inactivation) and

investigate, in a systematic approach, the ability of UV LEDs to be used as biofilm disinfection tools
- To systematically investigate the potential of vitamin D enrichment on a variety of food products by LEDs
- To perform light characterization of commercially available LED systems on experimental location and in the lab
- To generate evidence of possible beneficial effects of (LED) light interventions including better sleep quality of elderly and athletes; easier labor process for the mothers and the medical personnel
- To develop an LED illuminant for improved visualization of veins that only minimally disturbs the circadian rhythm
- To explore possible potential of nanoengineering into biomedical LED applications
- To merge knowledge coming from diverse medical fields and identify how photonics can make a positive impact.

1.3. Project Background and Collaborations

The project is interdisciplinary and covers topics within the fields of LEDs and biophotonic applications for improved health and performance, as such, it combines competences coming from diverse scientific fields such photonics, analytical chemistry, performance analytics, chronobiology, photochemistry, odontology, microbiology and obstetrics.

The project was carried out at the Department of Photonics Engineering, Technical University of Denmark (DTU) in collaboration with: PANUM Institute (Costerton Biofilm center and Department of Odontology, University of Copenhagen), medical doctors from Danish Hospitals (Nordsjællands Hospital – Hillerød and Glostrup Hospital), Aalborg University, Gate 21, DTU Food, DTU Compute, Team Denmark, as well as Danish industry (Hedegård Foods A/S, U-Vivo Aps, Hesalight etc.).

The holistic approach followed throughout the present PhD study, to identify possible benefits on human health induced by light, required that skills and competences from diverse expertise were brought together. The present project would not be possible without the collaborations among

the different Institutions mentioned above; and the irreplaceable contribution of the following persons:

- Chapter 3: Main collaborators: M. Markvart and L. Bjørndal and T. Bjarnsholt and for their assistance: C. Stavnsbjerg, A. Nielsen and M. Alhede. Section 3.6: H. Ou, Y. Ou and W. Lu.
- Chapter 4: Main collaborators: J. Jakobsen and L. L. Barnkob and for her assistance: A. H. Pedersen.
- Chapter 5.2: Main collaborators: B. A. Sander, J. Markvart, L. Kessel, K. Johnsen and Gate 21 , Chapter 5.3: T. Wrønding and E. C. L. Løkkegaard, Chapter 5.4: J. H. Andersen, J. Broeng and from Team Denmark: L. Johansen and A. T. Adler. Chapter 5.5: L. K. H. Clemmensen.

1.4. Thesis outline

The key aspect of this thesis was to investigate how VIS and UV LEDs can be used to promote wellbeing. In the first part of the thesis, chapter 2, a basic introduction to the VIS and UV LEDs is given, together with the direct and indirect impact of UV/VIS electromagnetic radiation on human health. Moreover, since the results of this thesis are often statistical, some basic statistical tools are introduced. All the important findings produced during the PhD project are documented in the present thesis (divided in chapters), and in scientific publications or patent applications (see Publication list). The content of the peer reviewed scientific publications and the PhD chapters, is in some cases overlapping; in those cases the relevant publication is cited. The outline of the chapters and their novelty are shortly introduced.

Chapter 3 is concerned with the usage of UV LEDs for biofilm inactivation. Biofilms are assemblies of microorganisms that join together into communities in order to enhance their survival chances against external treats, and are known for their antibiotic resistance and shielding mechanisms against immune response. The role of biofilms is central in infectious diseases, therefore alternative methods for achieving biofilm eradication is of vital importance. A systematic investigation about how UV LED light sources can be implemented to eliminate biofilms has not been reported in the past. Moreover, the inactivation efficacy of the suggested

approach of UV irradiation is compared to conventional treatments namely antibiotics [0.13] and photodynamic therapy [0.6, 0.16]. Finally a novel treatment is suggested to combat resistant biofilms [0.8], and discussed together with future possibilities of improving implants by exploiting nanoscale topography [0.4, 0.10].

In chapter 4, irradiation processes with UV LEDs for increasing the vitamin D content of a variety of food products (pig skin [0.2], salmon skin, eggs), are described. Vitamin D deficiency and insufficiency are common problems that have broad negative impact on general health status. Biofortification of food products with UV LEDs could be a way to circumvent this problem. Consumption of biofortified edible products produced with UV LEDs is excluding all dangers (cancer development, irritation of skin etc.) of direct skin exposure to UVB. Moreover, in terms of market product development the solution provided here adds an innovative aspect that has not been presented before, and has several advantages over the solutions presented in the past. Furthermore, the possibility of biofortifying farmed salmon skin with blue light as suggested by Pierens et al [1.4], was investigated, however, such a response was not observed.

Chapter 5 is presenting the potential benefit that can be achieved with VIS LED lighting systems to populations with special health care needs. Interventions with VIS lighting are noninvasive, have minimal side effects and are easy to fit into everyday activities. Therefore the proof of the concept is expected to have big impact to society. Focus is put on elderly people [0.3], women in labor [0.7], midwives, and elite athletes [0.15]. According to our knowledge lighting has never been used in the past as an intervention for the labor process, neither as a tool for sustaining sleep quality of elite athletes under conditions of shifted circadian rhythm (jetlag). The chapter is finishing with the statistical demonstration that white illumination settings can affect the human ability to identify veins in the inner hand vasculature [0.1]. Veins are used as an “easy to handle” example that direct visual perception of biosamples can be improved if suitable general lighting is applied.

Chapter 6 summarizes the main conclusions of the study together with the presentation of the future perspectives.

References

1.1. Knowledge based Entrepreneurship. Heebøll, John. 3rd revised ed. Copenhagen: Polyteknisk Forlag, 2008.
1.2. Illuminating Engineering society. 2008, November. Light and Human health: An Overview of the impact of Light on Visual, Circadian, Neuroscience and Neurobehavioral Responses. IES.
1.3. Illuminating Engineering Society. n.d. Effects of ExteriorLighting on Human Health. New York: IES.
1.4. Pierens, S.L. and Fraser, D.R., 2015. The origin and metabolism of vitamin D in rainbow trout. The Journal of steroid biochemistry and molecular biology, 145, pp.58-64.

2. Theoretical background

2.1. UV LEDs

The ultraviolet (UV) LED market has grown noticeably the last years and both the number of companies manufacturing UV LEDs and UV LED adoption continue to accelerate [2.1]. UV-LEDs are LEDs that emit UV radiation with a wavelength of approximately 400 nm or shorter. Near UV LEDs, are having an emission wavelength of 300–400 nm, and deep UV LEDs at 200–300 nm. Technology and research developed for visible LEDs provide an existing infrastructure for near UV-LEDs, and progress in nitride semiconductors has driven commercial UV LEDs well into the 200–280 nm (UVC) band.

In comparison to fluorescent UV lamps, UV-LEDs exhibit several advantages and therefore are expected to prevail in the future. UV LEDs are mercury free, have a longer lifetime and a more stable light intensity, as well as higher energy efficiency. It is easy to control their temperature, they are more compact, and most importantly they exhibit a narrow spectrum.

The bandgap of pure gallium nitride (GaN) corresponds to 365 nm (Fig 2.1). The emitted wavelength can be increased towards violet and blue, by adding indium, while addition of aluminum decreases the wavelength towards deeper UVC wavelengths. Pure aluminum nitride (AlN) has a bandgap wavelength of 210 nm, which remains the shortest wavelength achieved by LEDs [2.2].

UV LEDs are typically grown on sapphire (Al2O3) substrates. The choice of substrate is very important for the performance in the deep UV region. A lattice mismatch between the substrate and the active AlGaN layer results

in a high defect density in the crystal and therefore a poor performance of deep UV LED devices [2.3]. As the aluminum concentration increases, reducing the LED wavelength, the lattice mismatch with sapphire becomes bigger and the external quantum efficiency decreases. Other substrates more rarely used are SiC [2.4], GaN [2.5, 2.6] and AlN [2.7, 2.8].

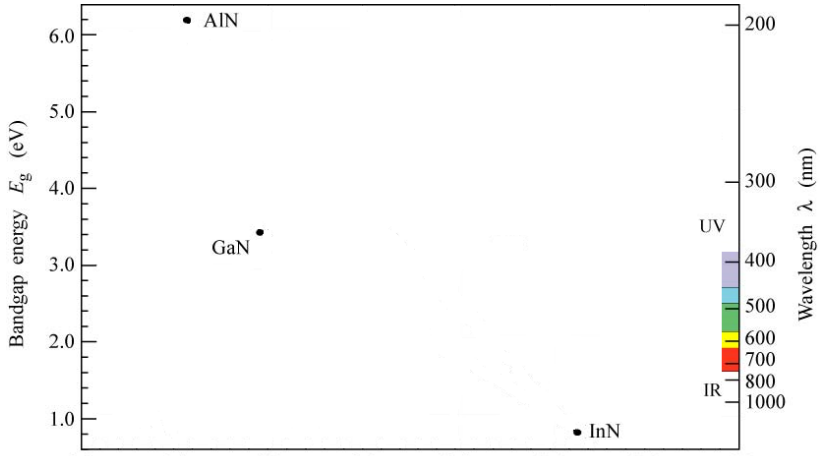

Fig. 2.1: Bandgaps of the most common semiconductors used for UV LED production. The scale to the right presents the light wavelength, corresponding to the band gap energy.

Researchers are exploring various manufacturing processes to gain better performance for UV LEDs [2.9] considering all efficiency parameters [2.10]: internal quantum efficiency, electron injection efficiency and light extraction efficiency. Approaches like photonic structures [2.11], novel chip geometries [2.12], and epitaxial lateral overgrowth [2.13] have been reported to substantially improve performance. The current state-of-the-art external quantum efficiency as obtained for LEDs in the UV region is presented in Fig. 2.2 [2.14-2.25].

UV LEDs have strong potential for applications in water [2.26] and air purification [2.27], phototherapy [2.28], biotechnology [2.29], UV curing [2.30, 2.31], banknote detection [2.32], sterilization [2.33], sensing [2.34, 2.35], lithography [2.36, 2.37], microscopy [2.38], and many more.

It is expected that due to the strong demand for an environmentally friendly, reliable, and energy efficient light source in the UV region,

researchers will be able to overcome the hindering challenges in the near future and provide users with UV LEDs at reasonable prices and satisfactory output power.

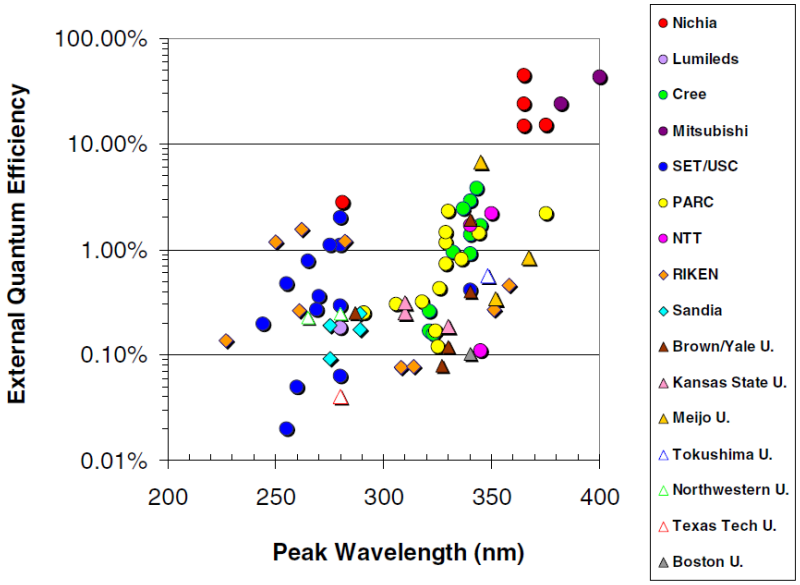

Fig. 2.2: External quantum efficiency as a function of peak wavelength, as reported for state-of-the-art UV LEDs [2.14-2.25]. The figure is from Kneissl et al [2.14].

2.2 VIS LEDs

LEDs are widely adopted in various environments and are accepted as an environmentally friendly light source [2.39]. Contrary to other light sources, LEDs are directly transforming electrical energy into light (electroluminescence), and therefore are considered as the ultimate form of lamp that theoretically can achieve almost 100% power to light conversion [2.40]. The current status for external quantum efficacy of InGaN and AlGaInP LEDs [2.41] is presented in Fig 2.3. The luminous efficacy of conventional light sources and LEDs, as expected to improve by 2020, was reported by Tsao et al. in 2004 [2.42].

When electric current flows through the junction, holes and electrons are injected into the depletion region and into the neutral n- and p-type regions, these diffused excess holes and electrons get potential energy equal to the band gap energy and can recombine causing light emission. The light emitted exhibits relatively narrow-band spectra, meaning that inherently LEDs are colored light sources. However, white light with a dynamic broad spectrum can be produced by LEDs, offering again the ability to the modern human, which is usually acting in indoor environment, to enjoy an illumination setting that resembles natural sunlight. The dynamic broad spectrum can be achieved by using color mixing of independently controlled LEDs and the full potential of this type of lighting remain still to be explored. The biggest challenge for this approach is the gap in the efficiency in the green-yellow region (see Fig. 1.3, dotted line) [2.43]. Recent advances indicate that this issue can be overcome [2.44-2.47].

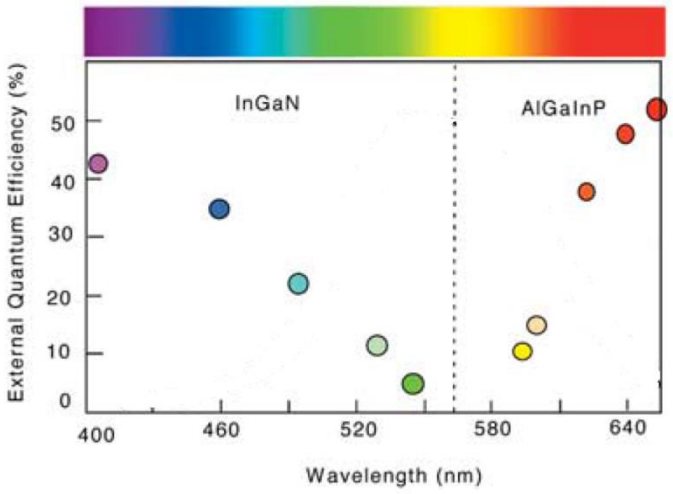

Fig. 2.3: External quantum efficacy of InGaN and AlGaInP LEDs. The figure is from Shur et al [2.41].

Microscale implantable and wireless controlled LEDs are expected to push the frontiers of potential applications beyond imagination. LED systems at the microscale have already been reported to find success in optogenetics for brain stimulation and cellular imaging [2.48-2.51].

2.3. VIS and UV electromagnetic radiation: direct and indirect impact on human health

Electromagnetic radiation refers to the photons or waves (particle-wave duality) of the electromagnetic field, propagating through space carrying electromagnetic radiant energy [2.52, 2.53]. The electromagnetic spectrum in sequence of increasing wavelength (and decreasing frequency) consists of gamma rays, X-rays, UV radiation (UVC, UVB, and UVA), visible light, infrared radiation, microwaves, and radio waves (Fig. 2.4).

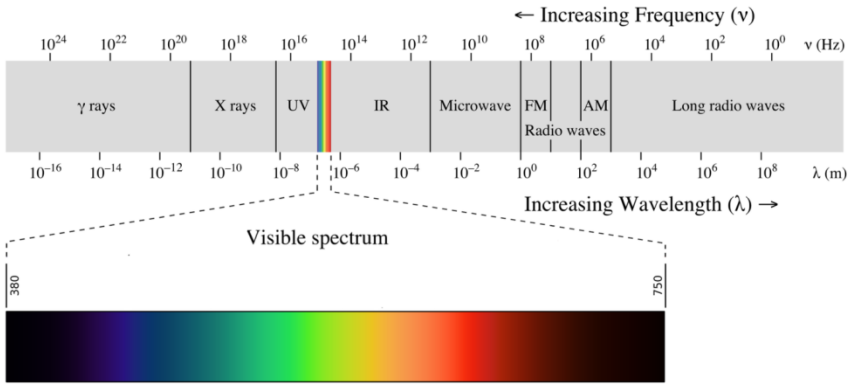

Fig. 2.4: Electromagnetic radiation classification.

Electromagnetic radiation in the visible wavelength region is an influential environmental factor and acts on the human body by two pathways 1) the primary optic tract which governs visual perception [2.54-2.55], and 2) the retinohypothalamic tract which governs endocrine, neurobehavioral, and circadian functions [2.56, 2.57]. Another pathway, namely direct brain stimulation, induced by VIS electromagnetic radiation is also discussed as a possibility with increasing evidence [2.58-2.60].

It was recently shown that for women whose melatonin release was repeatedly suppressed during their pregnancy weeks 37-40, by usage of light, the period for arriving at the labor stage was significantly prolonged

[2.61]. These facts should alert us for the quantity and quality of light human beings need, in order to function optimally during the day, and in various circumstances. Especially nowadays, that most of our lifetime is spent indoors, and thus we are mostly exposed to artificial light.

Since the human race evolved in sunlight one would expect that the artificial light sources should mimic as closely as possible the natural light for promoting wellbeing.

UV radiation has played a major role in the development of early life by providing the "praise" of mutation which is the underlying genetic mechanism of evolution [2.62]. UV radiation is also the best natural source of vitamin D. Vitamin D insufficiency could have a major impact on general health. Diminished bone mineralization, muscular weakness, hypertension, autoimmune diseases, multiple sclerosis, type 1 diabetes, schizophrenia, and depression are some of the diseases that could be attributed to vitamin D deficiency [2.63].

However, UV radiation can also be harmful, especially the shortest wavelengths (more energetic radiation). Skin cancer is one of the major negative effects that UV radiation is accused for [2.64]. The tradeoff between positive and negative effects of UV radiation is not easy to resolve and it is a matter of finding the proper balance among the parameters: UV wavelength, radiant exposure, and sensitivity of the organism involved.

For microorganisms, which are quite often antagonists of human wellbeing, the effects of UV radiation can be fatal. The exact nature of the effect of ultraviolet light on microorganisms at the molecular level is a matter of intensive research. All UV wavelengths cause some photochemical effects, though, the UVC wavelengths are considered to be particularly harmful to cells because they are absorbed by DNA [2.65]. The inactivation effectiveness of UV wavelengths can vary between species. UVA inactivation effects are expected to be significantly less effective than UVC and UVB. The biological effects of UVA are generally credited to enhanced production of reactive oxygen species (ROS), which results in oxidative damage to lipids, proteins and DNA [2.66]. UVB and UVC photons cause more direct damage by inducing formation of DNA lesions (photoproducts), mainly pyrimidine dimers, which block DNA replication and RNA transcription [2.67]. DNA and RNA are responsible for microbial replication and protein synthesis and damage to these nucleic acids cause inactivation or failure to reproduce. Exposure to UVB also causes oxidative stress, therefore, UVB induced damage comprises elements of both direct and

indirect pathways of damage [2.68]. Ultraviolet light also causes photochemical reactions/damages in proteins (UV absorption peaks at about 280 nm). Absorption in the peptide bonds within proteins can happen at wavelengths below 240 nm. For bacteria in planktonic state, the germicidal effectiveness of UV radiation demonstrates a peak at around 260–265 nm and this corresponds to the peak of UV absorption by bacterial DNA [2.69]. UV light could become a disinfection tool for medical instruments and devices [2.70] or even against bacterial infections.

2.4. Statistical tools

In this paragraph statistical tools used throughout this thesis are introduced. A common question often rising up during this work was "Is the response, of a parameter X, different among groups receiving diverse treatments?". If Y_{ki} is the observation of response for experimental unit i in group k, $i \in \{1, \ldots, m\}$ and $k \in \{1, \ldots, l\}$ we assume:

$$Y_{ki} = \mu_k + \epsilon_{ki}$$

where μ_k is the mean in group k and ϵ_{ki} is the individual variation, and the observations are assumed to follow a normal distribution within each group with a common variance σ^2 ($\epsilon_{ki} \sim N(0, \sigma^2)$, $Y_{ki} \sim N(\mu_k, \sigma^2)$). In one way analysis of variance (ANOVA) [2.71] there is only one hypothesis (null hypothesis), namely, "are the groups the same?"

$$H_0 = \mu_1 = \mu_2 = \cdots = \mu_m$$

If the hypothesis is accepted, p≥ 0.01 or 0.05 (depending on where the significance level is set to 1% or 5%) then we can assume a simpler model:

$$Y_{ki} = \mu + \epsilon_{ki}$$

where all responses are described by the common overall average or "grand mean" and the variance observed is only attributed to random error. The null hypothesis of equal means is rejected if p <0.01 or 0.05, i.e.

when the variation between groups is too large compared to the variation within the groups:

$$\sum_{ki}(y_{ki} - y_{mean})^2 = \sum_{ki}(y_{ki} - y_{kmean})^2 + \sum_{ki}(y_{kmean} - y_{mean})^2$$

Total variation Variation within groups Variation between groups

then the differences induced by the different treatments are significant.

A low p. value suggests that the sample tested (representing the entire population) provides enough evidence that we can reject the null hypothesis for the entire population. A specific p. value can be interpreted as following, (for example) p=0.001 means: assuming that the treatment applied had no effect, we would obtain the observed difference or more, in 0.1% of tests due to random sampling error. For identifying where the differences are to be found (among which treatments) pairwise t-tests [2.72] can be performed and confidence interval (CI) limits can be used to determine how big or how little difference is enacted by a treatment compared to another [2.73]. The assumptions for variance homogeneity and normally distributed observations can be tested with Levene's test [2.74] and QQ-plots [2.75], respectively.

The experimental units used in this thesis were quite diverse: biofilms, pig skin, salmon skin, eggs, elderly people, women in labor, elite athletes, gamers, and vein observers. Similarly, the responses tested were also diverse: colony forming units (CFUs), vitamin D content, sleep pattern factors, several parameters of labor like acute caesarean section and use of additional syntocinon, reaction time, and vein identification output. The treatments on the other hand were all VIS or UV exposures, delivered mostly by LEDs and always intending to improve health and wellbeing. The amount of replications was determined by the resources available in each project and by time restrains.

References

2.1) http://www.yole.fr/UVLED_MarketOverview.aspx#.WNuEjm-LTX6

2.2) Taniyasu, Y., Kasu, M. and Makimoto, T., 2006. An aluminium nitride light-emitting diode with a wavelength of 210 nanometres. Nature, 441(7091), pp.325-328.

2.3) Novikov, S.V., Staddon, C.R., Sahonta, S.L., Oliver, R.A., Humphreys, C.J. and Foxon, C.T., 2016. Growth of free-standing bulk wurtzite Al x Ga 1− x N layers by molecular beam epitaxy using a highly efficient RF plasma source. Journal of Crystal Growth, 456, pp.151-154.

2.4) Nothern, D.M., 2016. Inverted vertical algan deep ultraviolet leds grown on p-SiC substrates by molecular beam epitaxy (Doctoral dissertation, Boston University).

2.5) Akita, K., Nakamura, T. and Hirayama, H., 2004. Advantages of gan substrates in InAlGan quaternary ultraviolet-light-emitting diodes. Japanese journal of applied physics, 43(12R), pp.8030.

2.6) Nishida, T., Saito, H. and Kobayashi, N., 2001. Efficient and high-power AlGaN-based ultraviolet light-emitting diode grown on bulk GaN. Applied Physics Letters, 79(6), pp.711-712.

2.7) Guo, Y., Zhang, Y., Wang, J., Yan, J., Tian, Y., Chen, X., Sun, L., Wei, T. and Li, J., 2015, November. Development of AlGaN-based deep ultraviolet light-emitting diodes and laser diodes. In Solid State Lighting (SSLCHINA), 2015 12th China International Forum on (pp. 4-7). IEEE.

2.8) Islam, S.M., Protasenko, V., Jena, D. and Xing, G., 2016, June. 250 nm deep UV LED using GaN/AlN heterostructures on bulk AlN substrates. In CLEO: Science and Innovations (pp. STu3R-5). Optical Society of America.

2.9) Hirayama, H., Maeda, N., Fujikawa, S., Toyoda, S. and Kamata, N., 2014. Recent progress and future prospects of AlGaN-based high-efficiency deep-ultraviolet light-emitting diodes. Japanese Journal of Applied Physics, 53(10), p.100209.

2.10) Pimputkar, S., Speck, J.S., DenBaars, S.P. and Nakamura, S., 2009. Prospects for LED lighting. Nature Photonics, 3(4), pp.180-182.

2.11) Oder, T.N., Kim, K.H., Lin, J.Y. and Jiang, H.X., 2004. III-nitride blue and ultraviolet photonic crystal light emitting diodes. Applied Physics Letters, 84(4), pp.466-468.

2.12) Kim, D.Y., Park, J.H., Lee, J.W., Hwang, S., Oh, S.J., Kim, J., Sone, C., Schubert, E.F. and Kim, J.K., 2015. Overcoming the fundamental light-extraction efficiency limitations of deep ultraviolet light-emitting diodes by utilizing transverse-magnetic-dominant emission. Light: Science & Applications, 4(4), p.e263.

2.13) Muramoto, Y., Kimura, M. and Nouda, S., 2014. Development and future of ultraviolet light-emitting diodes: UV-LED will replace the UV lamp. Semiconductor Science and Technology, 29(8), p.084004.

2.14) Kneissl, M., Kolbe, T., Chua, C., Kueller, V., Lobo, N., Stellmach, J., Knauer, A., Rodriguez, H., Einfeldt, S., Yang, Z. and Johnson, N.M., 2010. Advances in group III-nitride-based deep UV light-emitting diode technology. Semiconductor Science and Technology, 26(1), p.014036.

2.15) Nishida, T., Kobayashi, N. and Ban, T., 2003. GaN-free transparent ultraviolet light-emitting diodes. Applied physics letters, 82(1), pp.1-3.

2.16) Edmond, J., Abare, A., Bergman, M., Bharathan, J., Bunker, K.L., Emerson, D., Haberern, K., Ibbetson, J., Leung, M., Russel, P. and Slater, D., 2004. High efficiency GaN-based LEDs and lasers on SiC. Journal of Crystal Growth, 272(1), pp.242-250.

2.17) Kneissl M., Yang Z., Teepe M., Knollenberg C., Johnson N. M., Usikov A. and Dmitriev V., 2006. Ultraviolet InAlGaN light emitting diodes grown on hydride vapor phase epitaxy AlGaN/sapphire template Japan. J. Appl. Phys. **45** 3905.

2.18) Tsuzuki H. et al, 2009. High-performance UV emitter grown on high-crystalline quality AlGaN underlying layer Phys. Status Solidi **a 206** 1199.

2.19) Zhang J. P., Chitnis A., Adivarahan V., Wu S., Mandavilli V., Pachipulusu R., Shatalov M., Simin G., Yang J. W. and Kahn M. A., 2002. Milliwatt power deep ultra-violet light-emitting diodes over sapphire with emission at 278 nm Appl. Phys. Lett. **81** 4910.

2.20) Adivarahan V., Wu S., Zhang J. P., Chitnis R. A., Shatalov M., Mandavilli V., Gaska R. and Khan M. A., 2004. High-efficiency 269 nm emission deep ultraviolet light-emitting diodes Appl. Phys. Lett. **84** 4762.

2.21) Zhang J., Hu X., Lunev A., Deng J., Bilenko Y., Katona T. M., Shur M. S., Gaska R. and Khan M. A, 2005. AlGaN deep-ultraviolet light-emitting diodes Japan. J. Appl. Phys. **44** 7250.

2.22) Khan A., Balakrishnan K. and Katona T., 2008. Ultraviolet light-emitting diodes based on group three nitrides Nat. Photonics **2** 77.

2.23) Hirayama H., Fujikawa S., Noguchi N., Norimatsu J., Takano T., Tsubaki K. and Kamata N., 2009. 222-282 nm AlGaN and InAlGaN-based deep-UV LEDs fabricated on high-quality AlN on sapphire Phys. Status. Solidi a 206 1176.

2.24) Hirayama H., Tsukada Y., Maeda T. and Kamata N., 2010. Marked enhancement in the efficiency of deep-ultraviolet AlGaN light-emitting diodes by using a multiquantum-barrier electron blocking layer Appl. Phys. Express 3 031002.

2.25) Fujioka A., Misaki T., Murayama T., Narukawa Y. and Mukai T., 2010. Improvement in output power of 280-nm deep ultraviolet light-emitting diode by using AlGaN multi quantum wells Appl. Phys. Express 3 041001.

2.26) Sauska, C., Csoknyai, G. and Packlocok, D., George Csokneyai, 1993. Ultraviolet water purification system with variable intensity control. U.S. Patent 5,230,792.

2.27) Huang, X., Wang, H., Yin, S., Chen, X., Chen, W. and Yang, H., 2009. Sterilization system for air purifier by combining ultraviolet light emitting diodes with TiO2. Journal of chemical technology and biotechnology, 84(10), pp.1437-1440.

2.28) Smith, K.C., 2005. Laser (and LED) therapy is phototherapy. Photomedicine and Laser Therapy, 23(1), pp.78-80.

2.29) Lee, J. and Tripathi, A., 2007. Measurements of Label Free Protein Concentration and Conformational Changes Using a Microfluidic UV-LED Method. Biotechnology progress, 23(6), pp.1506-1512.

2.30) Kennedy, J., Kennedy and John, 1995. Portable led photocuring device. U.S. Patent 5,420,768.

2.31) Nomoto, R., McCabe, J.F. and Hirano, S., 2003. Comparison of halogen, plasma and LED curing units. Operative dentistry, 29(3), pp.287-294.

2.32) Sandhu, A., 2007. The future of ultraviolet LEDs. Nature Photonics, 1(1), pp.38-38.

2.33) Bak, J., Ladefoged, S.D., Tvede, M., Begovic, T. and Gregersen, A., 2010. Disinfection of Pseudomonas aeruginosa biofilm contaminated tube lumens with ultraviolet C light emitting diodes. Biofouling, 26(1), pp.31-38.

2.34) de Lacy Costello, B.P.J., Ewen, R.J., Ratcliffe, N.M. and Richards, M., 2008. Highly sensitive room temperature sensors based on the UV-LED activation of zinc oxide nanoparticles. Sensors and Actuators B: Chemical, 134(2), pp.945-952.

2.35) Fan, S.W., Srivastava, A.K. and Dravid, V.P., 2009. UV-activated room-temperature gas sensing mechanism of polycrystalline ZnO. Applied Physics Letters, 95(14), p.142106.

2.36) Guijt, R.M. and Breadmore, M.C., 2008. Maskless photolithography using UV LEDs. Lab on a Chip, 8(8), pp.1402-1404.

2.37) Suzuki, S. and Matsumoto, Y., 2008. Lithography with UV-LED array for curved surface structure. Microsystem Technologies, 14(9-11), pp.1291-1297.

2.38) Connally, R., Jin, D. and Piper, J., 2006. High intensity solid-state UV source for time-gated luminescence microscopy. Cytometry Part A, 69(9), pp.1020-1027.

2.39) Steigerwald, D.A., Bhat, J.C., Collins, D., Fletcher, R.M., Holcomb, M.O., Ludowise, M.J., Martin, P.S. and Rudaz, S.L., 2002. Illumination with solid state lighting technology. IEEE journal of selected topics in quantum electronics, 8(2), pp.310-320.

2.40) N. Holonyak Jr., 2000. Is the light emitting diode (LED) an ultimate lamp?, Amer. J. Phys., vol. 68, pp. 864–866.

2.41) Shur, M.S. and Zukauskas, R., 2005. Solid-state lighting: toward superior illumination. Proceedings of the IEEE, 93(10), pp.1691-1703.

2.42) Tsao, J.Y., 2004. Solid-state lighting: lamps, chips, and materials for tomorrow. IEEE Circuits and Devices Magazine, 20(3), pp.28-37.

2.43) Crawford, M.H., 2009. LEDs for solid-state lighting: performance challenges and recent advances. IEEE Journal of Selected Topics in Quantum Electronics, 15(4), pp.1028-1040.

2.44) Pleasants, S., 2013. LEDs: Overcoming the'green gap'. Nature Photonics, 7(8), p.585.

2.45) Fadil, A., Ou, Y., Zhan, T., Wu, K., Suyatin, D., Lu, W., Petersen, P.M., Liu, Z. and Ou, H., 2015. Fabrication and improvement of nanopillar InGaN/GaN light-emitting diodes using nanosphere lithography. Journal of Nanophotonics, 9(1), pp.093062-093062.

2.46) R. Mueller-Mach, G. O. Mueller,M. R. Krames, and T. Trottier, 2002. High-power phosphor-converted light-emitting diodes based on III-nitrides, IEEE J. Sel. Topics Quantum Electron., vol. 8, no. 2, pp. 339–3452002.

2.47) Organic Light-Emitting Devices J. Shinar Ed. New York: Springer-Verlag, 2004.

2.48) Wu, F., Stark, E., Ku, P.C., Wise, K.D., Buzsáki, G. and Yoon, E., 2015. Monolithically integrated µLEDs on silicon neural probes for high-resolution optogenetic studies in behaving animals. *Neuron*, *88*(6), pp.1136-1148.

2.49) McGovern, B., Palmini, R.B., Grossman, N., Drakakis, E.M., Poher, V., Neil, M.A.A. and Degenaar, P., 2010. A new individually addressable micro-LED array for photogenetic neural stimulation. IEEE transactions on biomedical circuits and systems, 4(6), pp.469-476.

2.50) Rossi, M.A., Go, V., Murphy, T., Fu, Q., Morizio, J. and Yin, H.H., 2015. A wirelessly controlled implantable LED system for deep brain optogenetic stimulation. Frontiers in integrative neuroscience, 9, p.8.

2.51) Pisanello, F., Sileo, L. and De Vittorio, M., 2016. Micro-and nanotechnologies for optical neural interfaces. Frontiers in neuroscience, 10, p.70.

2.52) Maxwell, J.C., 1863. A Dynamical Theory of the Electromagnetic Field. Proceedings of the Royal Society of London, 13, pp.531-536.

2.53) Einstein, A., 1965. Concerning an heuristic point of view toward the emission and transformation of light. American Journal of Physics, 33(5), p.367.

2.54) Maffei, L. and Fiorentini, A., 1973. The visual cortex as a spatial frequency analyser. Vision research, 13(7), pp.1255-1267.

2.55) Gibson, James J. "The perception of the visual world." Oxford, England: Houghton Mifflin (1950).

2.56) Brainard, G.C., Hanifin, J.P., Warfield, B., Stone, M.K., James, M.E., Ayers, M., Kubey, A., Byrne, B. and Rollag, M., 2015. Short-wavelength enrichment of polychromatic light enhances human melatonin suppression potency. Journal of pineal research, 58(3), pp.352-361.

2.57) Gomes, C.C. and Preto, S., 2015. Blue Light: A Blessing or a Curse?. Procedia Manufacturing, 3, pp.4472-4479.

2.58) Alkozei, A., Smith, R., Pisner, D.A., Vanuk, J.R., Markowski, S.M., Fridman, A., Shane, B.R., Knight, S.A. and Killgore, W.D., 2016. Exposure to Blue Light Increases Subsequent Functional Activation of the Prefrontal Cortex During Performance of a Working Memory Task. Sleep. 39(9), pp.1671-80.

2.59) Knaier, R., Meister, S., Aeschbacher, T., Gemperle, D., Rossmeissl, A., Cajochen, C. and Schmidt-Trucksäss, A., 2015. Dose–response relationship between light exposure and cycling performance. Scandinavian journal of medicine & science in sports 26, pp. 794–801.

2.60) Lehrl, S., Gerstmeyer, K., Jacob, J.H., Frieling, H., Henkel, A.W., Meyrer, R., Wiltfang, J., Kornhuber, J. and Bleich, S., 2007. Blue light

improves cognitive performance. Journal of neural transmission, 114(4), pp.457-460.

2.61) Reiter, R.J., Tan, D.X., Korkmaz, A. and Rosales-Corral, S.A., 2013. Melatonin and stable circadian rhythms optimize maternal, placental and fetal physiology. Human reproduction update, p.dmt054.

2.62) Hessen, D.O., 2008. Solar radiation and the evolution of life. Solar radiation and human health, pp.123-136.

2.63) Huotari, A. and Herzig, K.H., 2008. Vitamin D and living in northern latitudes--an endemic risk area for vitamin D deficiency. International Journal of Circumpolar Health, 67(2-3).

2.64) Armstrong, B.K. and Kricker, A., 2001. The epidemiology of UV induced skin cancer. Journal of Photochemistry and Photobiology B: Biology, 63(1), pp.8-18.

2.65) Bolton JR, Cotton CA. 2008. Ultraviolet Disinfection Handbook.American Water Works Association. Denver, CO: and Rauth AM., 1965. The physical state of viral nucleic acid and the sensitivity of viruses to ultraviolet light. Biophys J 5, pp.257–273.

2.66) Chamberlain, J. and Moss, S.H., 1987. LIPID PEROXIDATION AND OTHER MEMBRANE DAMAGE PRODUCED IN Escherichia coli K1060 BY NEAR-UV RADIATION AND DEUTERIUM OXIDE. Photochemistry and photobiology, 45(5), pp.625-630.

2.67) Pfeifer GP., (1997). Formation and processing of UV photoproducts: effects of DNA sequence and chromatin environment. Photochem Photobiol 65, pp.270–283

2.68) Qiu X., Sundin G.W., Wu L., Zhou J., Tiedje J.M., (2005). Comparative analysis of differentially expressed genes in Shewanella oneidensis MR-1 following exposure to UVC, UVB, and UVA radiation. J Bacteriol 187, pp. 3556–3564.

2.69) Harm W., “Biological Effects of Ultraviolet Radiation.” New York: Cambridge University Press (1980).

2.70) Bak, J., Ladefoged, S.D., Tvede, M., Begovic, T. and Gregersen, A., 2010. Disinfection of Pseudomonas aeruginosa biofilm contaminated tube lumens with ultraviolet C light emitting diodes. Biofouling, 26(1), pp.31-38.

2.71) Aphalo, P.J., Albert, A., Björn, L.O., McLeod, A., Robson, T.M. and Rosenqvist, E. eds., 2012. Beyond the visible: a handbook of best practice in plant UV photobiology. Helsingin yliopisto.

2.72) https://stat.ethz.ch/R-manual/R-devel/library/stats/html/pairwise.t.test.html

2.73) Machler, M., 2007. Statistics: An Introduction using R, Michael J. Crawley. The American Statistician, 61, pp.100-101.
2.74) Fox, J. *Applied Regression, Linear Models, and Related Methods.* Sage (1997)
2.75) www.rprimer.dk

Chapter 3

3. Biofilm inactivation by UV LEDs and light assisted antibiotics

Motivation

Disinfection is a major issue in health care and especially disinfection of biofilms is a difficult task since the biofilm state is the mechanism implemented by bacteria in order to increase their chances of survival. A light based approach, for disinfection of biofilms, founded on implementation of UV LEDs could offer an alternative, additional tool to conventional treatments, which often are proven not to be adequate.

Related PhD publications: ***0.4, 0.5, 0.6, 0.8, 0.9, 0.10, 0.13, 0.14, 0.16, 0.17***

3.1. Introduction

In the present chapter the ability of UV LEDs to inactivate biofilms is investigated. Biofilm survival of two different species of bacteria (*Pseudomonas aeruginosa* and *Enterococcus faecalis*) was studied as a function of UV radiant exposure. The maturity of the biofilm (growth stage) was considered as a factor that could affect the outcome of the UV treatment. Moreover, the inactivation efficacy was systematically tested in a wavelength dependent manner for both bacterial species (*P. Aeruginosa; E.faecalis* [0.6]). Conventional antibiotic treatments were compared for their efficacy in killing *P. aeruginosa* biofilms with a treatment comprising of specific exposure to UVB irradiation [0.13].

The transmission properties of biofilms were also studied in order to develop a better understanding of how UV light interacts with bacteria in a biofilm state. A novel method "light assisted antibiotics" is suggested as an alternative approach for improving the killing efficacy of antibiotics on mature/persistent biofilms. Finally, this chapter contains a description of how nanoengineering, as a tool for implant improvement, may be used; and a method for fabricating cost effectively nanotopographies is introduced.

UV light treatments are non-invasive and are expected to have a growing potential in medical disciplines like dermatology and dentistry, where the confinement due to the limited penetration depth is not prohibitive. However, UV irradiation can also be detrimental if applied in a non-suitable way. During the present study, the focus of the UV treatments applied was towards UV wavelengths and exposures that could be realized in summer sunlight in the Nordic countries. UVC treatments were also part of the investigation, but not with the intention to be used in vivo, due to the probable harmful consequences for the patients.

The present chapter is the result of interdisciplinary research collaboration between DTU Fotonik, Department of Odontology and Department of Immunology and Microbiology, University of Copenhagen (M. Markvart, L. Bjørndal, T. Bjarnsholt). The antibiotic treatments were performed by Camilla Stavnsbjerg.

3.2. Irradiation treatments of *P. aeruginosa* and *E. faecalis* biofilms with UV LEDs

The present section focuses on the ability of UV LEDs to inactivate biofilms. The bacterial species studied were *Enterococcus faecalis (E. faecalis)* and *Pseudomonas aeruginosa* (*P. aeruginosa)*. *E. faecalis* is a gram positive bacterium [3.1] and has a thick cell wall of peptidoglycan, while *P. aeruginosa* is a gram negative bacterium with a thin layer of peptidoglycan and an outer lipid bilayer into which porins and specific uptake channels are embedded [3.2].

The inactivation of the biofilms was systematically investigated as a function of radiant exposure, in the range (approx.) from 70 J/m^2 to 10.000 J/m^2, as well as in a wavelength dependent manner in the wavelength range 250-340 nm. Furthermore, the effect of maturity of the biofilm on the effectiveness of the treatments was tested, more specifically biofilms were left to grow for 24, 48 of 72hours before the treatment took place [0.6].

The efficacy of UVB (above 290 nm) or UVA irradiation to inactivate biofilms could be particularly interesting. For these wavelengths, the intervention can be performed in a way that could be characterized as “natural”, since they are part of daylight. The quantum flux density below 290 nm reaching the earth’s surface is about 1016 photons/cm2 per month, and can be considered negligible [3.3]. At extreme latitudes such as in Norway there is no detectable UVB irradiation below 300 nm [3.4]. During a summer day in Nordic countries the intensity of UV irradiance at noon is around 0.7 W/m^2 [3.5]. Therefore an exposure around 20.000 J/m^2 could be reached after 6 days in summer sunlight at noon time (2hours per day).

The way of design of indoor illumination for environments that require high standards of sterility could be revolutionized by enriching them with UV LEDs, or UV transparent windows, or a combination of the two depending on the orientation of the location. Especially one of the two bacterial species tested here, *P. aeruginosa*, is frequently the reason for hospital acquired infections [3.6, 3.7].

3.2.1. Materials and Methods

The LEDs that were used to deliver the UV irradiation to the biofilms were purchased from Sensor Electronic Technology, Inc (SETi, Columbia, SC, USA; TO3 package, hemispherical lens window). A schematic representation of the setup is shown in Fig. 3.1a. The UV LEDs were operated in constant current mode. The UV irradiation measurement protocol is described in pages 82-83 [0.2]. The irradiance delivered on the biofilms was also cross validated with measurements on location (Fig. 3.1b) with a portable radiometer (NIST Certified UV Radiometer) at distance 1.5±0.1 cm. The biofilms were circular with diameter 1.0±0.2 cm (Fig. 3.2). In all exposures, the distance between the LED and the biofilm was kept constant at 1.5±0.2 cm. All biofilms, before and after treatments, were stored in a UV-free environment. As a standard all treatments were performed on three different biological replicates in order to test the reproducibility. A biological replicate is either generated when biofilms are grown on different dates or when biofilms are grown on the same date but from different overnight (ON) cultures. Technical replicates were also generated, most of the time in triplicates. The outcome from the technical replicates is assumed to follow a normal distribution and only the mean value is presented.

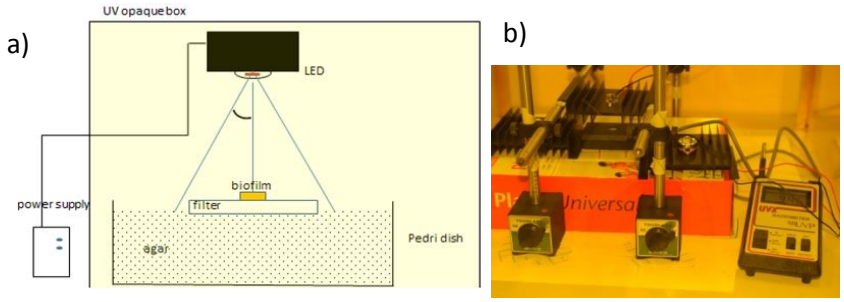

Fig. 3.1: a) Schematic representation of the UV irradiation set up. The agar plate carrying the biofilm is illuminated by the UV LED in a UV opaque box. b) The setup with portable radiometer to cross-validate irradiances delivered by the UV LEDs.

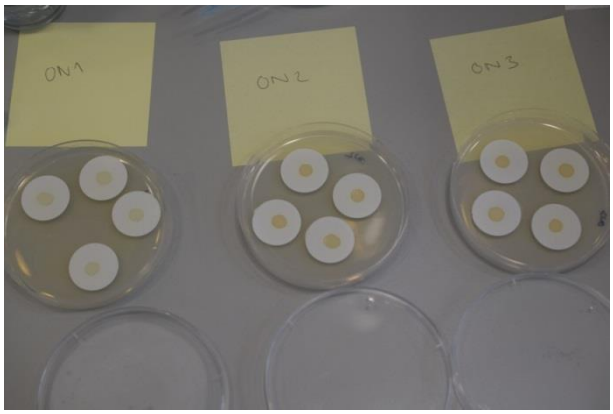

Fig. 3.2: Typical picture of prepared filter biofilms from three different overnight cultures. The biofilms are circular (diameter of 1 cm). The color of the biofilm and therefore their optical properties are not identical among overnight cultures. ON 1 appears not as dark as ON 2 and ON 3.

Bacteria were grown ON in Luria Broth (LB) medium at 37°C. The filter biofilms were grown on agar (2%) plates containing ABT minimal media supplemented with 0.5 w/v % glucose (ABTG plates). The Cellulose Nitrate Membrane (pores: 0.2μm, diameter: 25 mm, Whatman GmbH, Germany) filter was placed directly on the agar plate. The plate and filter were dried for 30 minutes at 37°C before the bacterial ON culture was added in a single spot on the membrane filter [3.8]. The biofilms were incubated for 24 hours (h), 48h or 72h, at 37°C. For a mature biofilm to develop, the membrane filter containing the growing biofilm was transferred to a fresh, dried ABTG plate every 24 h [0.6].

In order to perform the colony forming units (CFU) determination, the filters with the biofilms growing on top were transferred with sterile forceps to a 15 mL Falcon tube containing 5 mL of saline (0.9% NaCl). Samples were mixed for 15 seconds, degassed for 5 minutes (min) and sonicated for 5 min in an ultra-sonication bath to release the bacteria from the filter. Sonication fluids were serially diluted from 10^{-1} to 10^{-8}, and 20 μL of all dilutions were spotted on LB agar plates followed by overnight incubation at 37°C. The system followed for the different dilutions plated on the agar disks is depicted in Fig. 3.3 a.

The CFUs were counted after 24h of incubation in the dark. The plates that exhibited zero counts were left in the incubation room for another 24h and checked again for possible delayed formation of CFUs. The CFUs included in the data set were as determined by the final counting. Control samples, i.e. biofilms which were not exposed to UV irradiation, were plated every hour and included in the study as a reference for growth. A typical example of an agar plate with regrown CFUs under the counting process is presented in Fig. 3.3 b.

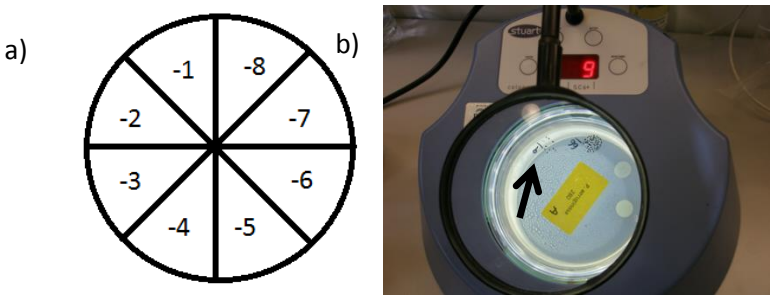

Fig. 3.3 a): Schematic explaining the way the serial dilutions were plated on the agar discs. b) Picture showing the counting machine for the CFUs loaded with a typical example of regrown CFUs after a moderately successful treatment. At higher dilutions well separated CFUs are formed and therefore are countable. At dilution order 4, nine CFUs are formed indicated by the arrow. At dilution order 3, sixty six CFUs are formed.

Apart from quantitatively assessing the effectiveness of the various treatments by comparing CFU counts, another commonly used method in this work is comparing the log survival or log inactivation where the log survival stands for:

$$Log\ survival = Log\frac{N_{treated}}{N_{control}} = -(LogN_{control} - LogN_{treated}) =$$

$$-Log\ inactivation = f\ (radiant\ expose\ or\ wavelength) \quad (1)$$

$N_{treated}$ is the number of CFUs after a UV radiant exposure (J/m^2) is delivered to the biofilm, and $N_{control}$ is the number of CFUs on the controls (not UV exposed).

The number of CFUs can be calculated by the following formula:

$$T_m = V[\frac{C_m}{D_m u}] \quad (2)$$

T_m is the estimated density of bacteria per initial volume, V is the original volume of the liquid the biofilm was placed into after the treatment, C_m is the CFU counts at the m order dilution, D_m is the dilution (=10^{-m}, m is the dilution order), and u is the volume of the aliquot transferred (spotted) to each agar plate location (for the specific dilution, see Fig. 3.3.a) from the m^{th} dilution tube.

The *E. faecalis* biofilms were significantly thinner compared to *P.aeruginosa* biofilms. A possible reason for the poorer growth of *E. faecalis* could be the choice of growth media, which might have not been optimal for supporting growth.

3.2.1.1. UV Irradiation details for biofilm survival dependence on radiant exposure

The influence of radiant exposure on the viability of biofilms was tested in the range 70-10.000 J/m^2 for one UVB and one UVC LED. The spectral distribution of the two LEDs is shown in Fig. 3.4. The irradiance delivered on the biofilms, was varied between 19 and 108 W/m^2 for the UVC LED;

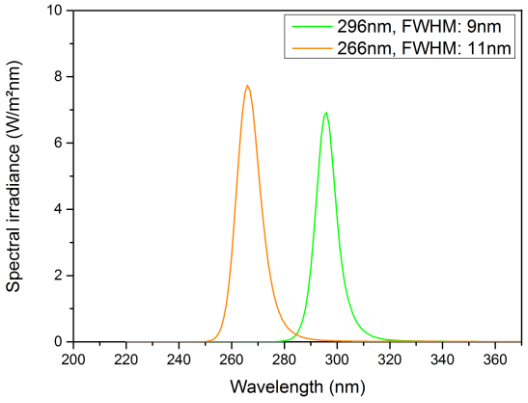

Fig. 3.4: Spectral distribution of UVB and UVC LEDs used for studying the effect of incident radiant exposure on the viability of biofilms, as measured in contact with the detector.

and between 1 and 15 W/m^2 for the UVB LED. For all treatments, the exposure time was below twelve minutes.

3.2.1.2. UV Irradiation details for biofilm survival dependence on UV wavelength

The inactivation on the biofilms induced by UV irradiation treatments was investigated as a function of the central UV wavelength applied. The UV range investigated was from 250 nm to 380 nm, covering the whole UVB region, and partially the UVA and UVC regions of the UV spectrum. The spectral distribution of the LEDs used, is presented in Fig. 3.5.

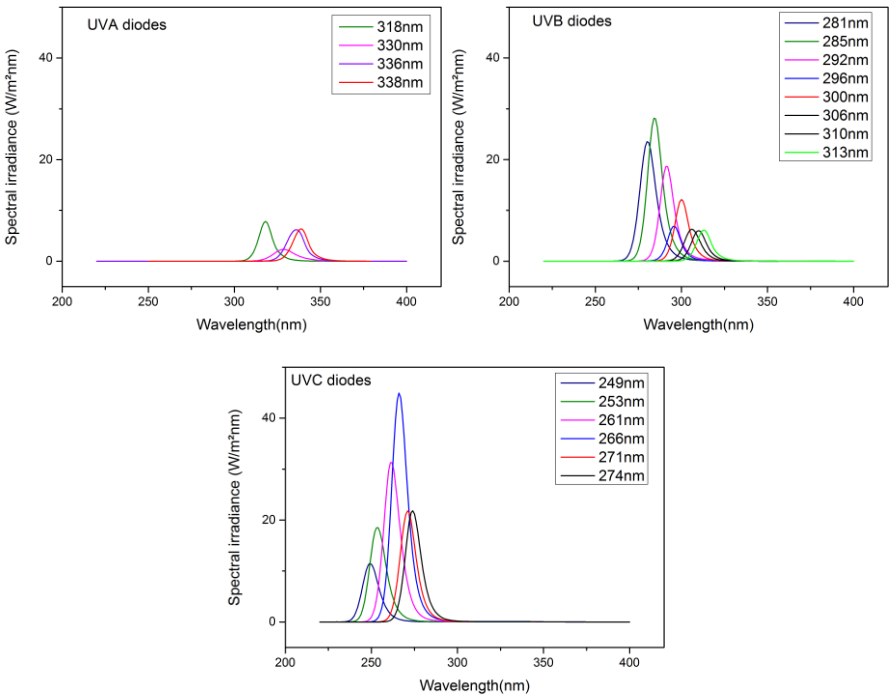

Fig. 3.5: Spectral distribution of UV LEDs used to investigate the effect of wavelength on the induced biofilm inactivation, as measured in contact with the detector. The central wavelengths are indicated in the respective label boxes.

Photochemistry occurs on a photon-by-photon basis, therefore, we intended to deliver equal amount of photons on the biofilm surface with the various light sources (instead of equal radiant energy). In order to achieve that the radiant exposure delivered to the biofilm surface was varying with the central wavelength of the diode (equations 3 and 4).

$$\frac{Energy\ exposure}{E_{mol}} = Photon\ exposure \quad (3)$$

$$E_{mol} = \frac{hc}{\lambda} N_A \quad (4)$$

E_{mol} is the energy of a mol of photons, N_A is Avogadro's number, c is the speed of light in vacuum, h is Planck's constant and λ is the irradiation wavelength in meters.

With a central wavelength at 296 nm, a radiant exposure around 1.450 J/m^2 (similar radiant exposure is received in sunlight after approx. 50min) should induce a moderate inactivation effect on a 24h grown P. Aeruginosa biofilm. Choosing a UV radiant exposure where moderate inactivation effects are observed, could prevent observing saturation (observe total killing for all central wavelengths), and therefore, make it possible to identify if an optimum wavelength exists. Consequently, for the smallest central wavelength at 249 nm, a radiant exposure around 1.700 J/m^2 was delivered; and for the longest central wavelength at 338 nm, a radiant exposure around 1.260 J/m^2 was delivered. All exposures were kept within a timeframe up to two minutes.

Similarly, for *E.faecalis* biofilms [0.6] a moderate total radiant exposure applied for identifying the optimal wavelength for inactivation was around 480 J/m^2 (this value was for the central wavelength at 281 nm). Exposures lasted less than one minute each.

Finally, the prospect to achieve a total inactivation effect (no bacteria left) of 24h grown biofilms with UVB or UVA irradiation would be beneficial in numerous clinical related circumstances; advantage of "natural" treatment as described in section 3.2. Therefore, UVB and UVA treatments were also delivered at higher radiant exposures (similar UV is delivered in 12h of noon sunlight, in Denmark). For the LED with central wavelength at 296 nm the radiant exposure delivered was around 20.000 J/m^2. As above, the radiant exposure delivered on the samples was modified with the different central

wavelength of the LEDs. However, in this occasion it was not possible to apply all the treatments in a consistent time frame, due to the different power profile of the LEDs. The longest treatment was 36min and 32sec (8 W/m^2, 330 nm) and the shortest 5min and 12sec (67 W/m^2, 285 nm).

3.2.1.3. Growth of biofilm

For *E. faecalis* the maturity as an additional parameter was tested for the outcome of UVB irradiation at radiant exposure of 20.000 J/m^2 [0.6]. Additionally, *P. aeruginosa* biofilms at different growth stages (grown for 24, 48 and 72 hours), were treated with a radiant exposure around 20.000 J/m^2 (both with UVB and UVC irradiation), to investigate if and how the maturity of the biofilm might alter the outcome of the irradiation.

3.2.2. Results

3.2.2.1. Log survival of non-mature biofilms as a function of radiant exposure

The log survival values of *P. aeruginosa* biofilms (24h grown), after being exposed to UVB or UVC irradiation with a central wavelength at 296 nm or 266 nm, respectively, as a function of UV radiant exposure (dose) are presented in Fig 3.6. It was observed that UVB irradiation (Fig. 3.6 a) was much more efficient than UVC (Fig. 3.6 b) to inhibit regrowth *P. aeruginosa* biofilms.

No counts were found for all replicates after a UVB exposure of 10.000 J/m^2. A similar exposure with UVC resulted in a log survival = -1 or 10 fold decrease in amount of bacteria compared to control samples. The log survival values for *E. faecalis* (24hours grown biofilm) are presented in Table 3.1. It was observed that it was much easier to inactivate *E. faecalis* biofilms compared to *P. aeruginosa* biofilms. No counts were observed for biological replicates 2 and 3, for exposures at 720J/m^2 or above [0.6]. Moreover, for *E. faecalis* biofilms it was not so clear from the present experiments whether UVB or UVC irradiation is more efficient, since from biological replicate 2 and 3, UVC seems to work more effectively than UVB,

but for biological replicate 1 some inconsistency was observed at the higher delivered exposures.

a)

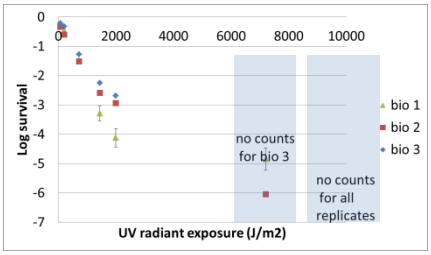

b)

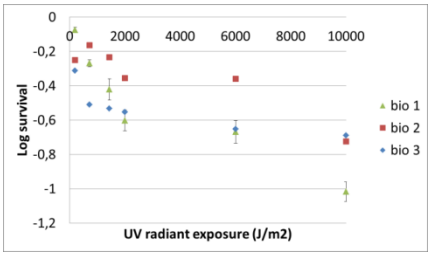

Fig. 3.6: The log survival of the *P. aeruginosa* biofilms as a function of a) UVB (296 nm central wavelength) radiant exposure and b) UVC (266 nm central wavelength) radiant exposure. The results from the three different biological replicates are indicated by different colors (green, red and blue). Notice the difference in y axis. UVB irradiation was observed to be much more efficient in inactivating *P.aeruginosa* biofilms than UVC. The error bar for biological replicate 1 is showing the deviation observed among the technical replicates.

Table 3.1: Log survival values for *E. faecalis* after different exposures to UVB and UVC irradiation. It is not clear from the present results if UVB or UVC irradiation is more efficient in inactivating *E. faecalis* biofilms grown for 24h. Data adapted from Markvart et al. [0.6].

Radiant exposure (J/m^2)	Log survival of biological replicate 1		Log survival of biological replicate 2		Log survival of biological replicate 3	
	UVB	UVC	UVB	UVC	UVB	UVC
70	-0.05	-1.06	-0.15	-1.45	-0.06	-1.34
200	-0.70	-2.40	-1.03	-3.13	-1.11	-1.96
720	-3.44	-1.89	no counts	no counts	no counts	no counts
1.440	-3.09	no counts	no counts	no counts	no counts	no counts
2.000	no counts	no counts	no counts	no counts	no counts	no counts
6.000	no counts	-3.89	no counts	no counts	no counts	no counts
10.000	no counts	-2.70	no counts	no counts	no counts	no counts

3.2.2.2. Log survival of non-mature biofilms as a function of UV wavelength

The bacterial survival as observed for 24h grown *P. aeruginosa* biofilms, after the treatments by the different central-wavelength UV-LEDs were applied (0.0036 mol/m^2 photon rate, corresponding to a radiant exposure around 1.450 J/m^2 at the 296 nm), is presented in Fig. 3.7. Despite the differences at the specific values of log survival found for the different biological replicates, it was interesting to observe that the best inactivation performance was always attained with the same LED (with central wavelength at 296 nm).

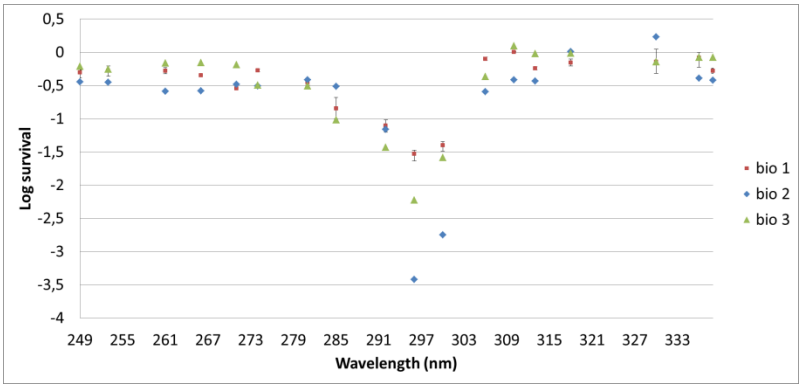

Fig. 3.7: Log survival of the 24hours grown *P. Aeruginosa* biofilms as a function of wavelength of the applied treatment (moderate radiant exposure; 1.260-1.700 J/m^2). The results from the three different biological replicates are indicated by different colors (red, blue and green). Independently of biological replicate, the optimal wavelength range for reducing survival of *P. Aeruginosa* biofilms grown for 24h is 290-300 nm.

For 24h grown *E. faecalis* biofilms, the bacterial survival values as a function of central wavelength of treatment applied are presented in Fig. 3.8 [0.6]. The radiant exposure applied ranged from 400-550 J/m^2, depending on the central wavelength of the treatment, in order to deliver equal amount of

photons to the biofilm surface (see equations 3 and 4). The optimal wavelength region (for the central wavelength of the LEDs) for achieving maximal inactivation as experienced in the three biological replicates is 280-296 nm. The peak performance was achieved with the LED, central wavelength at 285 nm, that resulted in zero counts for all biological and all technical replicates [0.6]. For one of the biological replicates (bio 3) of *E.faecalis* biofilms, all wavelengths in the range 249-296 nm resulted in zero counts. This result may indicate that satisfactory growth of *E. feacalis* biofilms (before treatment) was sometimes hindered [0.6].

By combining graphs in figures 3.7 and 3.8 (search for overlapping region where both bacterial are killed) one can conclude that for disinfecting an area infected with non-mature biofilms comprising of both gram negative and gram positive bacteria, the best LEDs to irradiate the area with, would be those exhibiting central wavelength at 290-296 nm.

From the section 3.2.2.1 it was made clear that an increase in exposure could improve the disinfection potential. As discussed in section 3.2., the goal of the present study was to determine a UV treatment that could be characterized as natural, while resulting (if possible) no regrowth, therefore, a high exposure treatment (20.000 J/m^2) was attempted with UVB and UVA wavelengths existing in sunlight.

For *E. faecalis* only UVB and UVA treatments (around 20.000 J/m^2) with central wavelength in the range 280-306 nm, resulted in no counts [0.6]. The results for *P. aeruginosa* non-mature biofilms are presented in Fig 3.9.

For *P. aeruginosa* it was observed that when the higher exposure was delivered, the range of wavelengths that resulted in no regrowth was 290-306 nm. However, one observation (see black arrow Fig. 3.9) was opposed to the trend observed in all other experiments (optimal wavelength for inactivation at 296nm, Fig. 3.7). Therefore, the specific experiment (296 nm central wavelength and 20.000 J/m^2 exposure) was repeated with another 2 biological replicates, with 2 technical replicates each; no regrowth was observed.

The combination of all the above information indicated that a UVB treatment with the LED exhibiting central wavelength at 296 nm and a radiant exposure around 20.000 J/m^2 could be a good candidate for disinfecting both gram negative and gram positive biofilms.

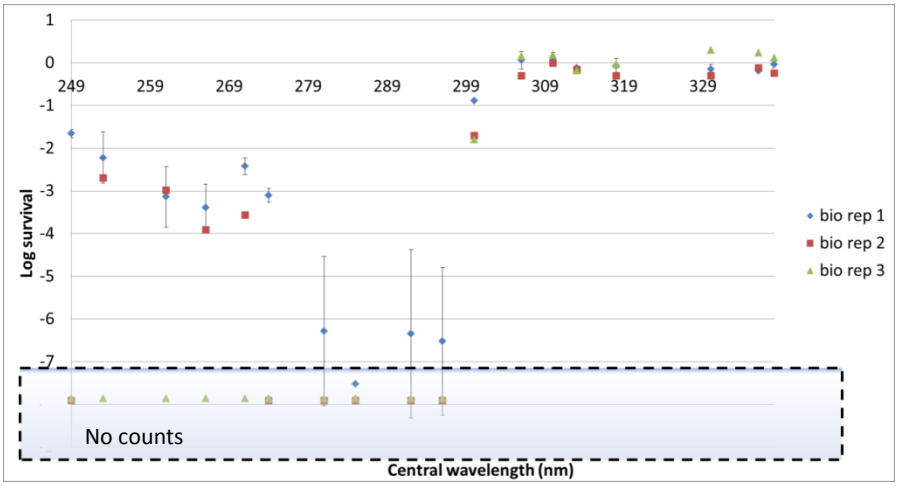

Fig. 3.8: Log survival of the 24h grown *E. faecalis* biofilms as a function of wavelength (moderate radiant exposure; 400-550 J/m^2) of the applied treatment. The results from the three different biological replicates are indicated by different colors (blue, red, and green). For all the points in the blue transparent box no colony forming units were regrown after treatment. Adapted from Markvart et al. [0.6].

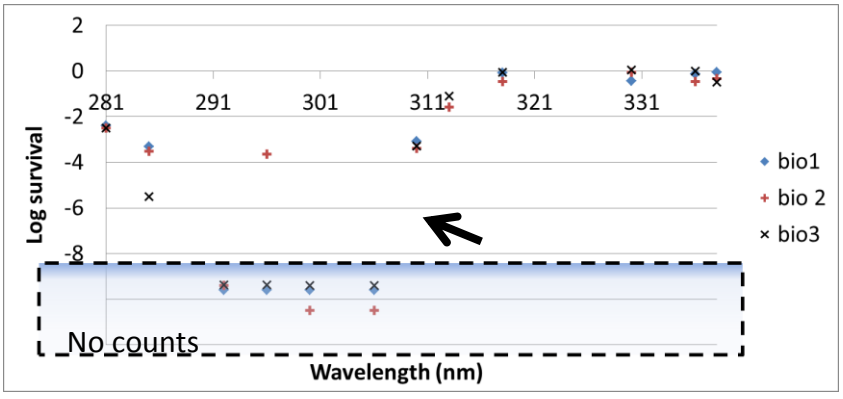

Fig. 3.9: Log survival of the 24h grown *P. aeruginosa* biofilms as a function of wavelength of the applied treatment (around 20.000 J/m2 radiant exposure). No regrowth was observed in the wavelength range 290-306 nm. The black arrow indicates an observation that was opposed to the trends observed in all other occasions, demonstrating that biological variance is something that cannot be easily controlled or predicted.

3.2.2.3. Effect of growth

For *E.faecalis* no regrowth (zero CFUs) was observed after the treatment (20.000 J/m^2, central wavelength of LED at 296 nm) independently of the maturity of the treated biofilm [0.6]. The log CFU outcome for the *P. aeruginosa* mature biofilms (either 48 or 72 hours grown) after the UVB "natural" treatment was applied (20.000 J/m^2, central wavelength of LED at 296 nm), is presented in Fig. 3.10. The more mature the biofilm is, the less effective the treatment becomes.

The inactivation, for the *P. Aeruginosa* mature biofilms (48hours grown) after UVC treatment (central wavelength at 266 nm, 22.200 J/m^2), was for all biological replicates negligible, no reduction was observed for CFUs of treated samples compared to control/non-treated samples (Fig. 3.10). For non-mature biofilms, the UVC treatment resulted in around 1 log reduction.

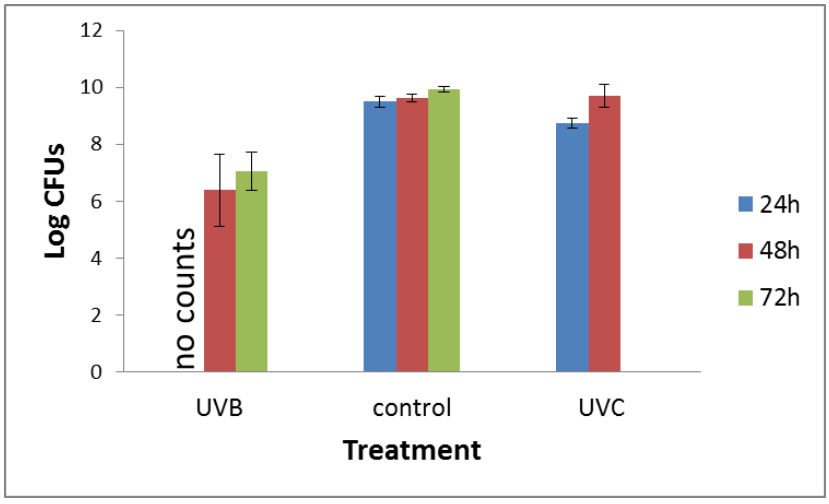

Fig. 3.10: Log CFUs of *P. aeruginosa* biofilms (either grown for 24, 48 or 72 hours) after UVB (20.000 J/m^2, central wavelength of LED at 296 nm), UVC (22.000 J/m^2, central wavelength of LED at 266 nm) and no treatment (control). It is observed that the longer the growth of the biofilm before the treatment is applied, the lower the inactivation achieved. UVC was not tested on 72h grown biofilms (missing green column).

3.2.3. Discussion and Conclusion

The systematic investigation, to identify the optimal UV irradiation treatment with LEDs in order to inactivate biofilms, showed that the potential optimal treatments might not be identical for different bacterial species. Moreover, the maturity of the biofilm was also proven to be an additional factor affecting the inactivation outcome of the UV treatments.

In the case of the gram negative and gram positive species studied here, namely *P. aeruginosa,* and *E. faecalis* [0.6]*,* it was found that treatments at moderate radiant exposure in the region 290-296 were resulting in very high inactivation for both species (specifically the LED with central wavelength 296 nm was the best for *P. aeruginosa* inactivation). Total inactivation (no regrowth), at a higher radiant exposure (around 20.000 J/m^2), was observed for both species in the region 290-306 nm.

The high exposure treatment with the UVB LED, central wavelength at 296 nm was considered a good candidate for achieving biofilm inactivation in a "natural" way, for biofilms expected to grow in thick biofilms like *P. aeruginosa*.

The effectiveness of treatments involving UV irradiation clearly depends on the opaqueness of the biofilm, which is dependent on the thickness. Unfortunately, in the present work it was not possible to control the thickness of the biofilms; and especially for *E. faecalis* the growth of the biofilm was such that resulted in thinner biofilms, compared to *P. aeruginosa* biofilms. In future studies, it would be interesting to investigate the correlations among the variables: biofilm thickness, biofilm opaqueness for various UV wavelengths, biofilm maturity, species of bacteria present in the biofilm, and inactivation efficiency of UV wavelengths. In the present work some fundamental steps were taken towards inactivation of biofilms with UV LEDs and a first foundation was shaped for developing irradiation treatments.

Finally, it was demonstrated for the first time that UVC irradiation is less efficient than UVB in inactivating thick *P. Aeruginosa* biofilms, independent of the growth stage of the biofilm [0.9]. The reason must be the better penetration depth of the UVB photons to the complex structure of the biofilm. UVC photons are expected to "experience" very low transmission through biofilms [3.9].

3.3. Comparison of inactivation: UV versus antibiotics

Biofilm infections are highly resistive to the immune response and are known for their tolerance to antibiotic treatments [3.10]. Moreover, the emergence of antibiotic resistance has evoked a turn towards antibiotics control programs [3.11]. For the mentioned reasons, alternative approaches different from conventional antibiotic treatments, are gaining increasing interest. Light-based treatments [3.2] are unconventional strategies for biofilm eradication that have met some success. Photodynamic therapy is a useful approach in inactivation of biofilms [3.12-3.14], but requires light, photosensitizer and oxygen [3.12] for ensuring adequate efficiency. Blue light treatments, without the usage of exogenous photosensitizers, have been reported to reduce *P. aeruginosa* infection in a mouse model of burn wounds mice burns and prevent bacteremia [3.15].

In the present section the "natural" UVB irradiation treatment defined in the previous section, namely 20.000 J/m^2 radiant exposure, with central wavelength at 296 nm, is compared in vitro to conventional antibiotic treatments (monotherapies and combinatory treatment)[0.13].

3.3.1. Materials and Methods

A summary of the antibiotic treatments tested in vitro on *P.Aeruginosa* biofilms can be found in table 3.2. For testing the antibiotic treatments filter biofilms were transferred to ABTG agar plates supplemented with either tobramycin (Eurocept International, Netherlands), or colistin sulfate salt (Sigma-Aldrich, USA) or a combination of the two. The filter biofilms were subsequently incubated at 37°C for 24 hours. The rest of the process for determining the CFUs and thereafter the log survival/log inactivation, was as described in section "Materials and Methods" 3.2.1; apart from 1) the serial dilutions which in this case were performed from no dilution to 10^{-7} (instead of dilutions 10^{-1} to 10^{-8}) and 2) the spotted volume which was 10 μL (instead of 20 μL). The statistical analysis was performed with the R software package [3.16]. Pairwise t-tests were used to detect (inactivation efficacy) differences among the treatments. The tests with irradiation and

antibiotics were performed on different days; controls were produced on both days to assure that the comparison between treatments was reasonable. Target for the treatments was to achieve a 99.9% inactivation (3 log reduction).

Table: 3.2: Summary of the antibiotic treatments tested. MIC stands for minimal inhibitory concentration.

Antibiotic	Concentration
Tobramycin	100 MIC
Colistin	100 MIC
Tobramycin and colistin	100 MIC and 100 MIC

3.3.2. Results

The number of regrown CFU after the different treatments, both for 24hours and 48hours grown *P. aeruginosa* biofilms is presented in Fig. 3.11. The difference in counted CFUs was insignificant

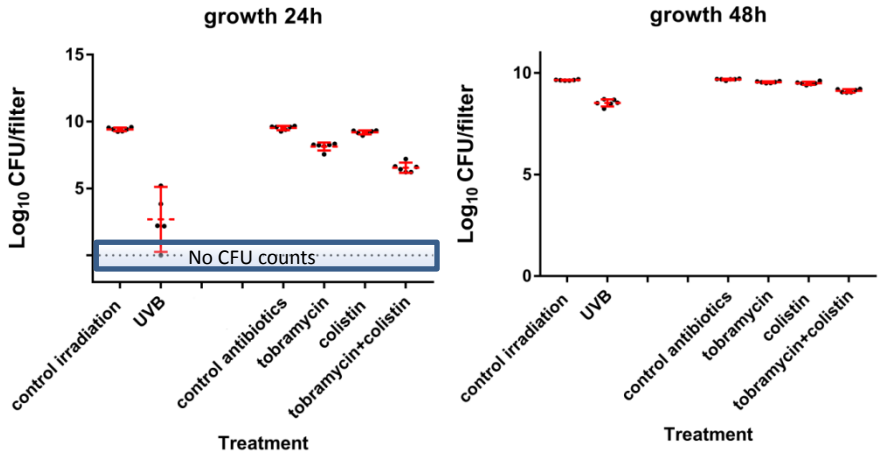

Fig. 3.11: Regrowth of *P. aeruginosa* (log of CFUs per filter) after different treatments were applied on three biological replicates (2 technical replicates each); on 24h grown or 48h grown biofilms. One UVB sample (24h) was destroyed.

between the controls (p=0,87) therefore for the "log inactivation analysis" the controls were assembled in one group. A summary of the analysis for biofilms grown for 24hours is shown in table 3.3. For mature biofilms the analysis is presented in table 3.4.

The UVB treatment was the most efficient of all for non-mature biofilms. For mature biofilms the combinatory antibiotic treatment and the UVB treatment were equally successful (p=0.12, hypothesis that the two treatment are similar is accepted).

Table 3.3: Summary of log inactivation analysis of the different treatments on non-mature biofilms. The 95% confidence interval (CI) is also presented for the log inactivation. P. values are from t-pairwise tests, where treatments are compared to the control. The values reported in parenthesis are after Bonferroni adjustment is applied.

Treatment	Log inactivation	95% CI	p. value
Control	0.0	-0.58 – 1.16	Not applicable
Tobramycin	1.40	0.03 – 2.20	0.03 (0.11)
Colistin	0.33	-0.40 – 1.10	0.50 (1.0)
Tobramycin and colistin	2.97	1.57 – 3.71	3.6^{-7} (1.3^{-5})
UVB	7.18	5.78 – 7.91	8.0^{-15} (2.9^{-13})

Table 3.4: Summary of log inactivation analysis of the different treatments on mature biofilms. The 95% CI is also presented for the log inactivation. P. values are from t-pairwise tests where treatments are compared to the control. The values reported in parenthesis are after Bonferroni adjustment is applied. The goal of 99.9% inactivation (3 log inactivation) was not achieved by none of the treatments applied.

Treatment	Log inactivation	95% CI	p.value
Control	0.0	-0.47 – 0.1	Not applicable
Tobramycin	0.1	-0.40 – 0.3	0.34 (1.0)
Colistin	0.2	-0.06 – 0.44	0.19 (1.0)
Tobramycin and colistin	0.6	0.02 – 0.73	0.0005 (0.02)
UVB	1.1	0.58 – 1.30	3.0-8 (1.1^{-6})

3.3.3. Discussion and Conclusion

It was demonstrated that the suggested UVB treatment was adequate to inactivate non mature biofilms, in comparison to antibiotic monotherapies that induced only minor inactivation effects for the concentrations tested (100 MIC). The combinatory antibiotic treatment managed to reach a 3 log inactivation on non-mature biofilms, though it was significantly less effective than UVB treatment ($p=8.5^{-7}$).

For mature biofilms the combinatory antibiotic treatment and the UVB treatment were equally successful ($p=0.12$). However, none of the treatments can be characterized as adequate to inactivate mature biofilms, since none of the treatments reached the 99.9% inactivation goal (3 log inactivation).

The inconsistency between the inactivation outcomes on the 48h grown biofilms, after UVB, observed in this paragraph (1.1±0.1 log inactivation) and paragraph 3.2.2.3. (3.2±1.3 log inactivation could not be explained.

Colistin and tobramycin, both as monotherapies and combinatory treatment, were administrated directly onto the biofilm surface. Therefore, the conclusion drawn here that colistin and tobramycin impose an insignificant inactivation effect on biofilms, only refers to the specific method of administration and the concentration used here. Colistin and tobramycin were reported to be successfully used for the treatment of multidrug resistant *P. aeruginosa* in the past [3.17, 3.18].

3.4. Optical properties of biofilms

The transmission of biofilms in the UV region was studied on quartz. Unfortunately, the membrane filters where the original biofilms were grown on were not transparent in the UV range. The transmission measurements were performed with a Cary 50 spectrophotometer. To grow the biofilms on quartz, quartz surfaces were embedded in bacterial culture for 28h. The biofilms grown on quartz were not expected to attain

the same thickness or structure as biofilms grown on membranes. However, still the transmission measurement could assist to get a better understanding of the UV wavelength dependent penetration ability into a thin layer of bacteria existing in a "biofilm state". Especially the ratio of transmission properties at different wavelengths would provide valid information for understanding the process.

Moreover, the biofilm thickness was not expected to be the same over the whole quartz surface, confirmed by observation of the samples by bare eye. The thickness variation of the biofilm grown at different locations of one quartz plate ("biofilm spot") is attributed to the biological aspects of biofilm formation. Therefore, large variation for the absolute values of the transmission was expected; the location on the biofilm where the transmission measurement was taking place was not controllable.

It was observed that in average (3 different spots, each on a different biofilm quartz sample, were measured) 10% less UV light was transmitted at a wavelength of 266 nm than at 296 nm, the transmission curve slope was found to be 0.33±0.07 (Fig. 3.12).

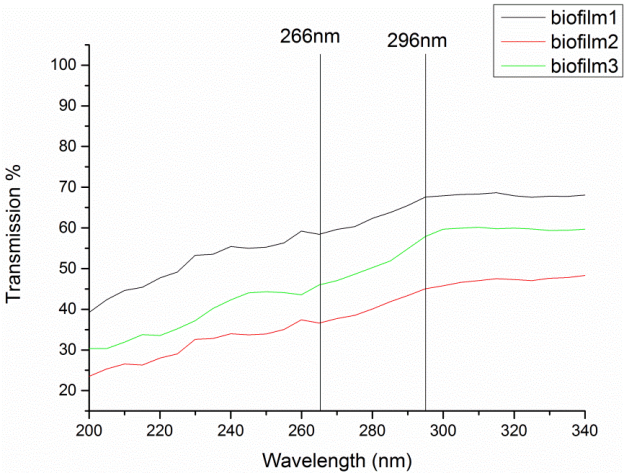

Fig. 3.12: Transmission spectra of biofilms grown on quartz under the exact same conditions. It is observed that in average 10% more UV light is transmitted at a wavelength of 296 nm than at 266 nm.

In case of biofilm 2 (obviously the thickest among the "biofilm spots" measured) only 37% was transmitted, at a wavelength of 266 nm. It is

believed that in the case of the biofilms grown on filters, which were much thicker, the UVC irradiation did not penetrate through the whole biofilm volume.

Limited penetration depth of UVC photons to the biofilm means lower delivered dose, especially at the deepest layers of the biofilm, therefore presence of intact bacteria and significant regrowth.

3.5. Light assisted antibiotics: a novel concept for disinfection

Combinatory antibiotic therapies seem to be the solution for combating resistant biofilms present in chronic infections [3.19, 3.20]. On the other hand, the need to reduce the amount of antibiotics used for treatment, by identifying other methods that would increase the vulnerability of bacteria is increasing, since the overuse of antibiotics has stimulated bacterial resistance [3.21].

In the present study, an alternative combinatory treatment is proposed for the first time, where the antibiotic administration is complemented by exposure to light. We call the treatment “light assisted antibiotics” and we believe that it will lead to new possibilities in treatment of a large number of infectious diseases, related to biofilms, in the future.

The inactivation efficacy of light assisted antibiotics is compared to highly concentrated monotherapies and combinatory antibiotic treatments at high and lower concentrations.

3.5.1. Materials and Methods

A summary of the antibiotic treatments compared to the light assisted antibiotic treatment in vitro can be found in table 3.5. The *P. aeruginosa* biofilms used for the experiments were left to grow for 24 or 48 hours. The biofilm assay was prepared as explained previously and the process for preparing the CFU counting was the same as described in section 3.3.1. Also

here, the treatments were applied on filter biofilms from three different overnight cultures, and in doublet determination as a standard for testing reproducibility. The CFU counts per filter were calculated with the weighted average method. The antibiotics were purchased as described in section 3.3.1. Experiments involving irradiation, described in paragraph 3.3 were performed on the same day as the light assisted antibiotic treatment (performed on biofilms grown from same ON cultures.)

In the light assisted antibiotic treatment, UVB irradiation was delivered first on the biofilm and then the antibiotic treatment (tobramycin at 100MIC; 100μg/mL). UVB irradiation was delivered on the samples with the help of a LED (SETi, Columbia, SC, USA; central wavelength: 296 nm, and full width half maximum: 9 nm). The radiant exposure was 20.000 J/m^2.

Table 3.5: Summary of the antibiotic treatments compared to the light assisted antibiotic treatment in vitro. MIC stands for minimal inhibitory concentration.

Antibiotic	Concentration	Symbol/ Acronym
Tobramycin	1.000 MIC (1000 μg/mL)	t*1000
Colistin	300 MIC (250 μg/mL)	c*300
Tobramycin and colistin	1.000 MIC and 300MIC	c*300+t*1000
	100 MIC (100 μg/mL) and 100 MIC (80 μg/mL) [same results as presented in section 3.2.2]	c*100+t*100

3.5.2. Results

The number of regrown CFU after the different treatments, both for 24h and 48h grown *P. aeruginosa* biofilms is presented in Fig. 3.13.

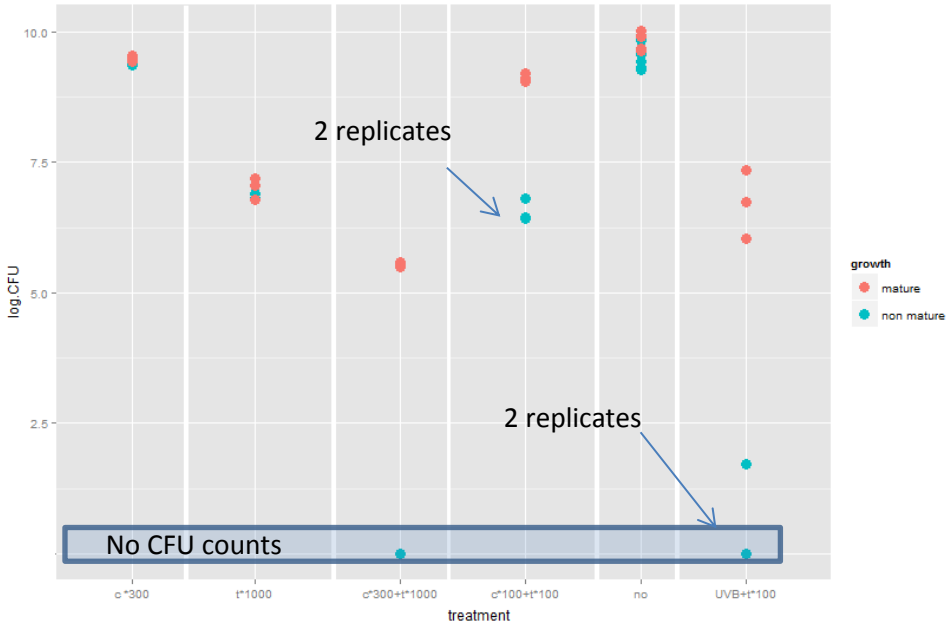

Fig. 3.13: Regrown CFUs (Log CFUs) after the different treatments were applied. The points can represent more than one biological replicate as indicated in some cases by the arrows. Points inside the blue marked area indicate that no CFUs were formed after regrowth. Each treatment was repeated on three biological replicates.

A summary of the log inactivation analysis for biofilms (*P.aeruginosa*) grown for 24h is shown in table 3.6. The p. value results from all possible pairwise t-test comparisons among the tested treatments are presented in table 3.7. For mature biofilms, the log inactivation analysis is presented in table 3.8. and p. value results from pairwise t-tests in table 3.9.

Table 3.6: Summary of log inactivation analysis of the different treatments on non-mature biofilms. The 95% CI is also presented for the log inactivation.

Acronym	Treatment	Log inactivation	95% CI
No	Control	0.0	-1.0 – 0.5
t*1000	Tobramycin (1.000 MIC)	2.9	1.5 – 3.6
c*300	Colistin (300 MIC)	0.4	0.9 – 1.2
c*300+t*1000	Tobramycin (1.000 MIC) and colistin (300 MIC)	No regrowth	
c*100+t*100	Tobramycin (100 MIC) and colistin (100 MIC)	3.0	1.6 – 3.7
UVB+t*100	Light assisted antibiotic (UVB+100 MIC tobramycin)	No regrowth for 2 samples;3rd sample 7.9	

Table 3.7: P. values from the pairwise t-tests among various treatment applied on 24h grown *P. aeruginosa* biofilms.

P. values	Control	t*1000	c*300	c*300+t*1000	c*100+t*100
t*1000	1.9^{-5}	-	-	-	-
c*300	1.0	0.0025	-	-	-
c*300+t*1000	2.3^{-16}	4.7^{-11}	5.7^{-14}	-	-
c*100+t*100	1.3^{-5}	1.0	0.002	5.8^{-11}	-
UVB+t*100	2.5^{-15}	1.1^{-9}	6.5^{-13}	Not applicable	1.4^{-9}

Table 3.8: Summary of log inactivation analysis of the different treatments on mature biofilms. The 95% CI is also presented for the log inactivation.

Acronym	Treatment	Log inactivation	95% CI
No	Control	0.0	-0.5 – 0.1
t*1000	Tobramycin (1.000 MIC)	2.9	2.4 –3.1
c*300	Colistin (300 MIC)	0.5	-0.1 – 0.6
c*300+t*1000	Tobramycin (1.000 MIC) and colistin (300 MIC)	4.4	3.9 –4.6
c*100+t*100	Tobramycin (100 MIC) and colistin (100 MIC)	0.6	0.0 –0.7
UVB+t*100	Light assisted antibiotic (UVB+100 MIC tobramycin)	2.9	2.4 –3.1

Table 3.9: P. values from the pairwise t-tests among various treatment applied on 48h grown *P. aeruginosa* biofilms.

P. values	Control	t*1000	c*300	c*300+t*1000	c*100+t*100
t*1000	1.9^{-15}	-	-	-	-
c*300	0.08	8.9^{-12}	-	-	-
c*300+t*1000	$<2.16^{-16}$	2.6^{-7}	2.3^{-16}	-	-
c*100+t*100	0.02	1.9^{-11}	1.0	3.8^{-16}	-
UVB+t*100	2.0^{-15}	1.0	9.4^{-12}	2.4^{-7}	2.0^{-11}

3.5.3. Discussion and Conclusion

Here, for the first time it was demonstrated that when antibiotics (tobramycin) are combined with light (UVB irradiation) the concentration of the antibiotic could be reduced by ten-fold without compromising the inactivation output even for mature biofilms. Moreover, the inactivation achieved by the light assisted tobramycin (100 MIC), was observed to be significantly more effective than the conventional combinatory antibiotic treatment tobramycin (100 MIC) and colistin (100 MIC) independently of the maturity of the biofilm. Tobramycin and colistin are known to have a synergetic action against gram negative bacteria [3.22].

The combinatory treatment comprised of high concentration tobramycin (ten-fold more concentrated) and colistin (3-fold) resulted in a significantly more effective inactivation than the light assisted antibiotic, as expected. However, such high concentration antibiotic treatments can be challenging, due to potential side effects or accumulated toxicity [3.23].

Especially for mature biofilms, tobramycin alone at a concentration of 100 MIC had no significant inactivation effect (see table 3.4), but when the same treatment was assisted by light the inactivation output was 3.0 log. The UVB treatment alone on a mature biofilm as shown in table 3.4 resulted in a 1.1 log inactivation. This indicates that there is a synergetic effect of light and antibiotics. These treatments were all performed on biofilms grown from the same three ON cultures.

In future, further research could enable the optimization of light assisted antibiotic treatments for combating persistent biofilms. The exact combination of wavelength and type of antibiotic is expected to be dictated by the taxonomic diversity present in the biofilm to be eradicated.

The present achievement could motivate the development of light assisted treatments to successfully reduce the amount of antibiotics for treating infections, as well as to reduce successfully the bacterial load of persistent biofilms.

3.6. Nanoscale topography: future possibilities for implants and biofilm disinfection

Nano and microscale topography exists in several circumstances in nature (lizard skin [3.24], butterfly [3.25], dental tubuli [3.26]) and with the rise of nano engineering the modification of surfaces at the nanoscale are becoming popular for improving performance of devices like implants [3.27, 3.28], biosensors [3.29], photovoltaics [0.4], LEDs [0.4, 3.30], and many more. Specifically in the case of implants, a nano modification of the surface could impact both the cell proliferation enhancing the chances for acceptance and integration of the implant, but also affect (hinder) bacterial adhesion [3.31].

The main barrier for nano engineering is the high cost. In the present PhD thesis a cost effective method for fabricating scalable nanostructures on surfaces was presented together with the effect of the presence of nanostructures on the optical and wetting properties of the material [0.10].

The various nano structured landscapes attained by the method could be used in the future as a template for studying biofilm growth and cell proliferation; both becoming relevant in dental and implant science.

In Argyraki et al. [0.10] aluminum was used as a coating for the nano landscapes and it was shown that the coating was following the morphology of the underlying surface. The prospect of using titanium dioxide (TiO_2) instead and combine it with UV irradiation would open new possibilities in understanding the biofilm eradication, since several interactions should be expected among the biofilm growth/attachment, the nano landscape, the TiO_2 photocatalyst and the UV irradiation (generated by LEDs). TiO_2 is known as a photocatalytic disinfectant applied in medicine [3.32-3.36].

3.7. Novelty of the Chapter

Disinfection processes are vital in all clinical environments in order to reduce the incidence of hospital acquired infections [3.37, 3.38]. More specifically, biofilm contaminated medical devices are regularly the reason for infectious diseases [3.39, 3.40]. Traditionally, microbial infections are

treated by antibiotics however this approach raised the problem of antibiotic resistance [3.41, 3.42]. Therefore, the interest of the scientific community was directed towards alternative disinfection methods [3.2, 3.43, 3.44]. Light based methods, which offer the advantage of non-invasiveness, have been reported in the past to be able to inactivate microorganisms [3.45-3.51]. Extensive research on UVC LED disinfection of catheter biofilms has been reported by Bak et al [3.52-3.56]. UV wavelength dependent sensitivity and comparison of the different wavelengths killing efficacy has been reported before for bacteria in suspension both with broadband light sources [3.57, 3.58] and narrowband light sources [3.59].

Biofilms are less prone to antibiotics and other antimicrobial agents than their planktonic counterparts [3.60]. It is validated that the minimal inhibitory concentration (MIC) for biofilms is considerably higher (approx. 10–1.000 times) compared to planktonic bacterial cells [3.61]. Tobramycin specifically is an antibiotic often used in management of chronic P. aeruginosa infections [3.62] and colistin has been currently reestablished in clinical practice due to the emergence of multidrug-resistant gram-negative bacteria [3.63]. Therefore comparison of these well-established antibiotics to light based UV irradiations treatments would have considerable impact in the field.

The novelties, related to UV LEDs and disinfection, achieved by the author of this thesis are presented below:

- systematic investigation of the inactivation efficacy of UV LEDs on biofilms in the whole UV range
- discovery of the fact that UVB wavelengths which exists in sunlight can be more efficient in killing biofilms than UVC wavelengths [0.9]; transmission properties of biofilms
- killing efficacy comparison of UVB irradiation to conventional antibiotic, and combinatory antibiotic treatment [0.13]
- proposal of a novel method for disinfection comprising of UVB pretreatment (central wavelength 296 nm) and topical administration of antibiotic (tobramycin) for combating resistant biofilms
- Development of a new low cost method, which uses thin aluminum film as the etching mask to form nanostructures. The method could easily fit to existing LED production lines [0.4] to enhance LED light extraction efficacy or for changing optical, wetting or attachment surface properties [0.10].

3.6. Summary

In this Chapter of the thesis, the ability of UV LEDs to inactivate biofilms was systematically investigated. The bacterial survival/inactivation was studied as a function of radiant exposure [0.9] and wavelength, for two different bacterial species (*P. aeruginosa; E. faecalis* [0.6]). Moreover, the maturity stage of the biofilm was considered as a parameter that could affect the inactivation ability of the treatment. The transmission properties of biofilms were investigated in the UV range, showing that UVC has limited penetration ability.

A UVB treatment was specified as a good candidate for disinfection and its inactivation efficacy was compared to conventional antibiotic treatments [0.13]. It was shown that the treatment suggested was more efficient than the antibiotic treatments and photodynamic therapy [0.6, 0.16].

A novel method "light assisted antibiotics" was suggested for fighting persistent biofilms and it was demonstrated for the first time that the concentration of the antibiotic could be reduced by ten- fold without compromising the inactivation output.

As a final point, a "diverse toolbox" was assembled consisting of: 1) the UV LED (wavelength range 250-340 nm) treatments; 2) a method to fabricate different nano landscapes [0.4, 0.10] (optimally with a TiO_2 coating); 3) knowhow in biofilm growth and inactivation (also on different bacterial species); and 4) their relevance in dentistry and implantology that could contribute to an optimized and all-embracing disinfection approach.

References

3.1) Siddiqui, S.H., Awan, K.H. and Javed, F., 2013. Bactericidal efficacy of photodynamic therapy against Enterococcus faecalis in infected root canals: a systematic literature review. Photodiagnosis and photodynamic therapy, 10(4), pp.632-643.

3.2) Yin, R., Dai, T., Avci, P., Jorge, A.E.S., de Melo, W.C., Vecchio, D., Huang, Y.Y., Gupta, A. and Hamblin, M.R., 2013. Light based anti-infectives: ultraviolet C irradiation, photodynamic therapy, blue

light, and beyond. Current opinion in pharmacology, 13(5), pp.731-762.

3.3) Barker, R.E., 1968. The availability of solar radiation below 290 nm and its importance in photomodification of polymers. Photochemistry and Photobiology, 7(3), pp.275-295.

3.4) Henriksen, K., Stamnes, K., Volden, G. and Falk, E.S., 1989. Ultraviolet radiation at high latitudes and the risk of skin cancer. Photo-dermatology, 6(3), pp.110-117.

3.5) Kolari, P.J., Lauharanta, J. and Hoikkala, M., 1986. Midsummer solar UV-radiation in Finland compared with the UV-radiation from phototherapeutic devices measured by different techniques. Photo-dermatology, 3(6), pp. 340-345.

3.6) Morrison, A. J., Jr., and R. P. Wenzel, 1984. Epidemiology of infection due to Pseudomonas aeruginosa. Rev. Infect. Dis. 6(Suppl. 3), pp. 627-642.

3.7) National Nosocomial Infection Surveillance System. National Nosocomial Infection Surveillance (NNIS) System report, data summary from January 1992 through June 2004, issued October 2004. Am. J. Infect. Control 32, pp. 470-485.

3.8) Bjarnsholt, T., Alhede, M., Jensen, P.Ø., Nielsen, A.K., Johansen, H.K., Homøe, P., Høiby, N., Givskov, M. and Kirketerp-Møller, K., 2015. Antibiofilm properties of acetic acid. Advances in wound care 4(7), pp. 363-372.

3.9) Argyraki, A., Markvart, M., Nielsen, A., Bjarnsholt, T., Bjørndal, L. and Petersen, P.M., 2016, April. Comparison of UVB and UVC irradiation disinfection efficacies on Pseudomonas Aeruginosa (P. aeruginosa) biofilm. In SPIE Photonics Europe. International Society for Optics and Photonics, pp. 988730-988730.

3.10) Høiby, N., Bjarnsholt, T., Givskov, M., Molin, S. and Ciofu, O., 2010. Antibiotic resistance of bacterial biofilms. International journal of antimicrobial agents, 35(4), pp. 322-332.

3.11) Neu, H.C., 1992. The crisis in antibiotic resistance. Science, 257(5073), pp. 1064-1074.

3.12) Sharma, M., Visai, L., Bragheri, F., Cristiani, I., Gupta, P.K. and Speziale, P., 2008. Toluidine blue-mediated photodynamic effects on staphylococcal biofilms. Antimicrobial agents and chemotherapy, 52(1), pp. 299-305.

3.13) Cieplik, F., Tabenski, L.K., Buchalla, W. and Maisch, T., 2014. Antimicrobial photodynamic therapy for inactivation of biofilms formed by oral key pathogens. Frontiers in microbiology, 5 (405), pp. 1-17.

3.14) Biel MA, 2010. Photodynamic therapy of bacterial and fungal biofilm infections. Photodynamic Therapy, 635 (Methods and Protocols), Humana Press, pp. 175-194.

3.15) Dai, Tianhong, Asheesh Gupta, Ying-Ying Huang, Rui Yin, Clinton K. Murray, Mark S. Vrahas, Margaret E. Sherwood, George P. Tegos, and Michael R. Hamblin, 2013. Blue light rescues mice from potentially fatal Pseudomonas aeruginosa burn infection: efficacy, safety, and mechanism of action. Antimicrobial agents and chemotherapy 57(3), pp. 1238-1245.

3.16) R Core Team, "R: A language and environment for statistical computing. R foundation for statistical computing," Vienna, Austria, 2014, http://www.R‐project.org/.

3.17) DM.. Sabuda, K. Laupland, J. Pitout, B. Dalton, H. Rabin, T. Louie and J. Conly. 2008. Utilization of colistin for treatment of multidrug-resistant Pseudomonas aeruginosa. Can J Infect Dis Med Microbiol 19(6), pp. 413-418.

3.18) Ratjen, F., Munck, A., Kho, P. and Angyalosi, G., 2010. Treatment of early Pseudomonas aeruginosa infection in patients with cystic fibrosis: the ELITE trial. Thorax, 65(4), pp. 286-291.

3.19) Wu, H., Moser, C., Wang, H.Z., Høiby, N. and Song, Z.J., 2015. Strategies for combating bacterial biofilm infections. International journal of oral science, 7(1), pp.1-7.

3.20) Herrmann, G., Yang, L., Wu, H., Song, Z., Wang, H., Høiby, N., Ulrich, M., Molin, S., Riethmüller, J. and Döring, G., 2010. Colistin-tobramycin combinations are superior to monotherapy concerning the killing of biofilm Pseudomonas aeruginosa. Journal of Infectious Diseases, 202(10), pp.1585-1592.

3.21) Taraszkiewicz, A., Fila, G., Grinholc, M. and Nakonieczna, J., 2012. Innovative strategies to overcome biofilm resistance. BioMed research international, 2013 (ID: 150653), 13 pages.

3.22) Ozbek, B., Mataracı-Kara, E., Er, S., Ozdamar, M. and Yilmaz, M., 2015. In vitro activities of colistin, tigecycline and tobramycin, alone or in combination, against carbapenem-resistant Enterobacteriaceae strains. Journal of Global Antimicrobial Resistance, 3(4), pp.278-282.

3.23) Patrick, B.N., Rivey, M.P. and Allington, D.R., 2006. Acute renal failure associated with vancomycin-and tobramycin-laden cement in total hip arthroplasty. Annals of Pharmacotherapy, 40(11), pp.2037-2042.

3.24) Ge, L., Sethi, S., Ci, L., Ajayan, P.M. and Dhinojwala, A., 2007. Carbon nanotube-based synthetic gecko tapes. Proceedings of the National Academy of Sciences, 104(26), pp. 10792-10795.

3.25) Nishimoto, S. and Bhushan, B., 2013. Bioinspired self-cleaning surfaces with superhydrophobicity, superoleophobicity, and superhydrophilicity. Rsc Advances, 3(3), pp.671-690.

3.26) Kienle, A., Forster, F.K., Diebolder, R. and Hibst, R., 2002. Light propagation in dentin: influence of microstructure on anisotropy. Physics in medicine and biology, 48(2), p.N7.

3.27) Lavenus, S., Louarn, G. and Layrolle, P., 2010. Nanotechnology and dental implants. International Journal of Biomaterials 2010, Article ID 915327, 9 pages.

3.28) Streicher, R. M., Schmidt, M. and Fiorito, S., 2007. Nanosurfaces and nanostructures for artificial orthopedic implants. Nanomedicine 2(6), pp. 861–74.

3.29) Soleymani, L., Fang, Z., Sargent, E. H. and Kelley, S. O., 2009. Programming the detection limits of biosensors through controlled nanostructuring. Nature Nanotechnology 4(12), pp. 844-848.

3.30) Argyraki, A., Ou, Y., & Ou, H., 2013. Broadband antireflective silicon carbide surface produced by cost-effective method. Optical Materials Express 3(8), pp. 1119-1126.

3.31) Thakral, G., Thakral, R., Sharma, N., Seth, J. and Vashisht, P., 2014. Nanosurface–the future of implants. J Clin Diagn Res, 8(5), pp.7-10.

3.32) Dunlop, P.S.M., Sheeran, C.P., Byrne, J.A., McMahon, M.A.S., Boyle, M.A. and McGuigan, K.G., 2010. Inactivation of clinically relevant pathogens by photocatalytic coatings. Journal of Photochemistry and Photobiology A: Chemistry, 216(2), pp.303-310.

3.33) Sawase, T., Jimbo, R., Wennerberg, A., Suketa, N., Tanaka, Y. and Atsuta, M., 2007. A novel characteristic of porous titanium oxide implants. Clinical Oral Implants Research, 18(6), pp.680-685.

3.34) Marchi J, Amorim EM, Lazar DR, Ussui V, Bressiani AH, Cesar PF. 2013. Physicochemical characterization of zirconia-titania composites coated with an apatite layer for dental implants. Dent Mater. 29(9), pp. 954–62.

3.35) Singer J, Merz A, Frommelt L, Fink B. 2012. High rate of infection control with one-stage revision of septic knee prostheses excluding MRSA and MRSE. Clin Orthop Relat Res. 470(5), pp. 1461–71.

3.36) Bogdan, J., Jackowska-Tracz, A., Zarzyńska, J. and Pławińska-Czarnak, J., 2015. Chances and limitations of nanosized titanium dioxide practical application in view of its physicochemical properties. Nanoscale research letters, 10(1), p.57.

3.37) Rutala, W.A. and Weber, D.J., 1999. Infection control: the role of disinfection and sterilization. Journal of Hospital Infection, 43, pp.S43-S55.

3.38) Page, K., Wilson, M. and Parkin, I.P., 2009. Antimicrobial surfaces and their potential in reducing the role of the inanimate environment in the incidence of hospital-acquired infections. Journal of Materials Chemistry, 19(23), pp.3819-3831.

3.39) Guggenbichler, Josef Peter et al, 2011. Incidence and Clinical Implication of Nosocomial Infections Associated with Implantable Biomaterials – Catheters, Ventilator-Associated Pneumonia, Urinary Tract Infections. GMS Krankenhaushygiene interdisziplinär 6 (1), pp. 1-19.

3.40) Hall-Stoodley, L., Costerton, J.W. and Stoodley, P., 2004. Bacterial biofilms: from the natural environment to infectious diseases. Nature reviews microbiology, 2(2), pp.95-108.

3.41) Stewart, P.S. and Costerton, J.W., 2001. Antibiotic resistance of bacteria in biofilms. The lancet, 358(9276), pp.135-138.

3.42) Geddes A., 2000. Infection in the twenty-first century: Predictions and postulates. J. Antimicrob. Chemother 46 (6), pp. 873–878.

3.43) Jassim, Sabah A. A., and Richard G. Limoges., 2014. Natural Solution to Antibiotic Resistance: Bacteriophages 'The Living Drugs'. World Journal of Microbiology & Biotechnology 30 (8), pp. 2153–2170.

3.44) Cotter, Paul D., R. Paul Ross, and Colin Hill., 2013. Bacteriocins—a viable alternative to antibiotics?. Nature Reviews Microbiology 11(2), pp. 95-105.

3.45) Thai, Thao P., Pamela E. Houghton, David H. Keast, Karen E. Campbell, and M. Gail Woodbury., 2002. ULTRAVIOLET LIGHT Cin THE TREATMENT OF CHRONIC WOUNDS WITH MRSA: ACase STUDY. Ostomy/wound management 48 (11), pp. 52-60.

3.46) Thai, Thao P., David H. Keast, Karen E. Campbell, M. Gail Woodbury, and Pamela E. Houghton., 2005. Effect of ultraviolet light C on bacterial colonization in chronic wounds. Ostomy/wound management 51(10), pp. 32-45.

3.47) Hamblin, Michael R., and Tayyaba Hasan., 2004. Photodynamic therapy: a new antimicrobial approach to infectious disease?, Photochemical & Photobiological Sciences 3(5), pp. 436-450.

3.48) Maisch, Tim, J. Wagner, V. Papastamou, H-J. Nerl, K-A. Hiller, R-M. Szeimies, and Gottfried Schmalz., 2009. Combination of 10% EDTA, Photosan, and a blue light hand-held photopolymerizer to inactivate leading oral bacteria in dentistry in vitro. Journal of applied microbiology 107(5), pp. 1569-1578.

3.49) Enwemeka, Chukuka S., Deborah Williams, Sombiri K. Enwemeka, Steve Hollosi, and David Yens, 2009. Blue 470-nm light kills methicillin-resistant Staphylococcus aureus (MRSA) in vitro. Photomedicine and laser surgery 27 (2), pp. 221-226.

3.50) Tsen K. T., Fu T.S., Lindsay Q., Kibler S.M., Jacobs K., Wu B., Karanam T.C., Jagu B., Roden S.R.B. et al., 2009. Photonic approach to the selective inactivation of viruses with a near-infrared subpicosecond fiber laser. J Biomed Opt 14, p. 064042.

3.51) Tsen, Kong T., Shaw-Wei D. Tsen, Otto F. Sankey, and Juliann G. Kiang, "Selective inactivation of micro-organisms with near-infrared femtosecond laser pulses," Journal of Physics: Condensed Matter 19 (47), 472201 (2007).

3.52) Bak, J., Ladefoged, S.D., Tvede, M., Begovic, T. and Gregersen, A., 2010. Disinfection of Pseudomonas aeruginosa biofilm contaminated tube lumens with ultraviolet C light emitting diodes. Biofouling, 26(1), pp.31-38.

3.53) Bak, J., Begovic, T., Bjarnsholt, T. and Nielsen, A., 2011. A UVC Device for Intra-luminal Disinfection of Catheters: In Vitro Tests on Soft Polymer Tubes Contaminated with Pseudomonas aeruginosa, Staphylococcus aureus, Escherichia coli and Candida albicans. Photochemistry and photobiology, 87(5), pp.1123-1128.

3.54) Bak, J., Ladefoged, S.D., Begovic, T. and Winding, A., 2010. UVC fluencies for preventative treatment of Pseudomonas aeruginosa contaminated polymer tubes. Biofouling, 26(7), pp.821-828.

3.55) Bak, J., Jørgensen, T.M., Helfmann, J., Gravemann, U. and Vorontsova, I., 2011. Potential in vivo UVC disinfection of catheter lumens: estimation of the doses received by the blood flow outside the catheter tip hole. Photochemistry and photobiology, 87(2), pp.350-356.

3.56) Bak, J., 2009. Assembly and method for disinfecting lumens of medical devices. U.S. Patent Application 13/060,768.

3.57) Santos, A.L., Oliveira, V., Baptista, I., Henriques, I., Gomes, N.C., Almeida, A., Correia, A. and Cunha, Â., 2013. Wavelength dependence of biological damage induced by UV radiation on bacteria. Archives of microbiology, 195(1), pp.63-74.

3.58) Murphy, T.M., Hurrell, H.C. and Sasaki, T.L., 1985. WAVELENGTH DEPENDENCE OF ULTRAVIOLET RADIATION-INDUCED MORTALITY AND K+ EFFLUX IN CULTURED CELLS OF Rosa damascene. Photochemistry and photobiology 42(3), pp. 281-286.

3.59) http://www.s-et.com/cleantech-manuscript.pdf (Clean Technology 2010, www.ct-si.org, ISBN 978-1-4398-3419-0).

3.60) Wilson, M., 1996. Susceptibility of oral bacterial biofilms to antimicrobial agents. Journal of Medical Microbiology 44(2), pp. 79-87.

3.61) Hengzhuang, W., Wu, H., Ciofu, O., Song, Z. and Høiby, N., 2011. Pharmacokinetics/pharmacodynamics of colistin and imipenem on mucoid and nonmucoid Pseudomonas aeruginosa biofilms. Antimicrobial agents and chemotherapy, 55(9), pp.4469-4474.

3.62) Lam J, Vaughan S, Parkins MD, 2013. Tobramycin Inhalation Powder (TIP): An Efficient Treatment Strategy for the Management of Chronic Pseudomonas Aeruginosa Infection in Cystic Fibrosis. Clinical Medicine Insights Circulatory, Respiratory and Pulmonary Medicine 7, pp. 61-77.

3.63) Kasiakou, S. K., Michalopoulos, A., Soteriades, E. S., Samonis, G., Sermaides, G. J., & Falagas, M. E., 2005. Combination therapy with intravenous colistin for management of infections due to multidrug-resistant Gram-negative bacteria in patients without cystic fibrosis. Antimicrobial agents and chemotherapy, 49(8), pp. 3136-3146.

Chapter 4

4. Vitamin D increase in food products using UV LEDs (biofortification)

Motivation

Vitamin D deficiency is a global health problem. Vitamin D can be synthesized by exposure to UV light or taken by food intake or vitamin supplements. Fortification of food with vitamin D is a public health policy that aims to reduce the population suffering from hypovitaminosis D. However, vitamin D fortification of food is highly regulated and judged in Europe and vitamin D supplement intake may often lead to unwanted side effects, while direct UV exposure of humans can result in skin cancer.

UV exposure of farm animals with UV lamps was proposed in the past as an alternative approach (biofortification) to solve the vitamin D deficiency problem. However, UV lamps do not provide enough control of the exposure process and exhibit several disadvantages as light sources (see theoretical background, section 2.1).

UV LED technology would be a more appropriate approach for this concept. At the moment, UV lamps are much cheaper than UV LED, although, it is believed that this fact will change within the next years, as UV LED technology follows an exponential growth development.

***Related PhD publications:* 0.2**

4.1. Introduction

The present chapter includes several aspects related to the development of LED irradiation protocols to bio-fortify with vitamin D a variety of food products. There is strong evidence that having insufficient vitamin D levels or deficiency, have broad negative influence on the general health and therefore more attention should be given to improve the vitamin D status of the general population [4.1]. We investigated the vitamin D response spectra of pig skin in a wavelength range 280-340 nm. For the optimal UV region identified, the vitamin D production was studied as a function of radiant exposure. Moreover, the reciprocity hypothesis [4.2] was tested within a 2 fold range for irradiance. Apart from pig skin, we proposed to biofortify (with vitamin D) by using LEDs, eggs and salmon skin. Egg bio-fortification can be intended either by direct UV exposure; or indirectly by illuminating the egg-laying hens. Each method has advantages and disadvantages and this thesis introduces the approaches egg companies can take, to decide which approach would fit best to their production line needs. Finally, the possibility of bio-fortification of farmed salmon was investigated with UVB (central wavelength 296 nm), UVA (central wavelength 338 nm) and blue light (central wavelength 454 nm).

The present chapter is the result of interdisciplinary research collaboration between DTU Fotonik, and DTU Food (Line Lundbæk Barnkob, Anja Hvonbech Pedersen and Jette Jakobsen).

4.2. Investigation of the effect of UV-LED exposure conditions on the production of vitamin D in pig skin

The suggested daily intake for vitamin D is 10-20 μg [4.3], however, the world recorded vitamin D intake is well below that value. A way to improve the daily vitamin D intake is dietary supplement, unfortunately though, the uptake from supplements does not normally exceed 40%. Black et al. [4.4] reported in 2012, that vitamin D status could be improved by consuming “enriched vitamin D” food products.

The present section focuses on the possibility of increasing vitamin D contents in the edible parts of pork skin by illuminating tissue. The ideal conditions of UV exposure for achieving that, by using LEDs, are investigated.

Direct illumination of human skin as a vitamin D source could be dangerous if not applied with precautions. On the other hand, consumption of edible biofortified pork products produced by UVB irradiation excludes any risk (cancer development, irritation of skin etc.) of direct skin exposure to UVB.

In terms of market product development the solution suggested here, namely edible biofortified pork products, by UV LEDs which are easily compatible with food production lines, add an innovative aspect that has not been presented before, and has several advantages over solutions presented in the past. For example, UV LEDs may be effortlessly implemented in existing food production facilities, without major modifications to the processes or the processing equipment.

Finally, it must be mentioned that according to the Worldwatch Institute [4.5] pork is the most widely consumed meat in the World.

4.2.1. Materials and Methods

4.2.1.1. Irradiation setup

The experimental setup is shown in Fig. 4.1, and was located in the sample preparation room of the National Food Institute (DTU Food). The ability to transfer the setup physically close to the laboratories where the vitamin D analysis was performed was of major importance, since it enabled an undisturbed and convenient workflow. All exposures were performed in the same period and under the same environmental conditions. The objective was to determine how 1) wavelength, 2) incident radiant exposure (dose) and 3) irradiance influence the vitamin D production, when pig skin is exposed to UV. The distance between the LEDs and the sample of pig skin was kept constant for all exposures at 1.5 ± 0.1 cm. All exposures were repeated on two samples of pig skin (n=2) to test reproducibility of the outcome.

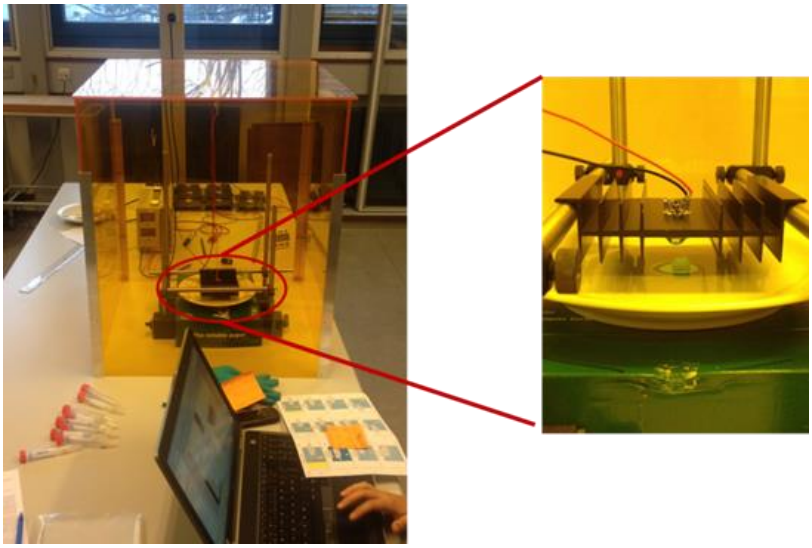

Fig. 4.1: The setup for irradiation of pig skin samples with UV light. The orange box is opaque to UV light and is used for protection from the irradiation. The distance between the light source and the surface of the sample was kept constant in all experiments. The zoom in section shows the pig skin sample under irradiation generated by an LED light source.

4.2.1.2. Pig skin samples

The skin samples were taken from the back of a slaughtered mini pig which had not been exposed to UV irradiation; it spent all its life indoors without access to UV irradiation. The carcass had been stored at -20 °C for 2 years before the removal of the skin took place. Hair and subcutaneous fat were cautiously removed from the skin. Total hair removal was not possible as shown in Fig. 4.2, though, the remaining hair was not considered to be a detrimental bias for the outcome of the study. A scalpel and a ruler were used to cut the skin into 1x1 cm pieces. The average weight of the pig skin samples was 0.498±0.015 g. All samples were kept at -20 °C before and after exposure to UV irradiation. Before exposure the samples were left to reach room temperature. After the exposure the samples were kept in

airtight nitrogen flushed bags. Control-samples (samples not exposed to UV irradiation), were included in the investigation. All samples were kept in an UV free environment, both before and after the experiment**.**

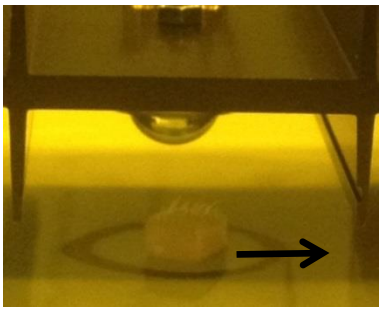

Fig. 4.2: Typical picture of pig skin sample demonstrating that total hair removal was impossible. The remaining hairs are indicated with a black arrow. The remaining hairs are considered to be an insignificant bias to the final outcome of the experiment.

4.2.2. Results

4.2.2.1. Identifying the optimal wavelength

Twelve UV-LEDs (purchased from SETi, Columbia, SC, USA), emitting with central wavelengths in the range 280-340 nm, were used for investigating the effect of wavelength on the production of vitamin D in pig skin. The effect was determined at two different incident radiant exposures, namely 300 J/m^2 and 7.000 J/m^2, to ensure the observation of vitamin D increase; while avoiding observing saturation. The LEDs were operated at constant current mode, in the region between 100-600 mA. Operating only within this current regime should ensure a good viability of the LEDs according to LED provider. The exact operation current, irradiance and exposure time are presented in table 4.1 for each incident radiant exposure. The precision of the exposure time was estimated to ±0.5 sec to cover the experimentalist's response time to the timer.

Table 4.1: The effect of wavelength on the production of vitamin D in pig skin was determined at two different incident radiant exposures (doses) 300 J/m^2 and 7.000 J/m^2. The exact operation current, the irradiance and exposure time for each of the (central) wavelengths of the LEDs are given for each of the doses.

	300 J/m^2			7.000 J/m^2		
central wavelength (nm)	current (mA)	Irradiance (W/m^2)	exposure (sec)	current (mA)	Irradiance (W/m^2)	exposure (sec)
281	100	10	31	200	21	330
285	100	11	28	200	23	304
292	200	12	26	200	14	500
296	500	11	26	200	3	2188
300	300	11	26	200	8	854
306	400	10	29	200	6	1167
310	400	9	32	200	6	1250
313	400	9	32	200	6	1250
318	300	12	24	200	9	778
330	600	8	37	200	2	3500
336	200	11	26	200	11	625
338	200	10	31	200	10	729

The spectral distribution of the UV-LEDs was measured by an External Optical probe (EOP-146, Instrument Systems GmbH, Munich, Germany) and a monochromator (bandpass: 1 nm, scan step: 1 nm, detector: Photomultiplier). The spectrometer, coupled to the monochromator, was a SPECTRO 320 (D) Release 5 (Instrument Systems GmbH) and operated in the wavelengths between 200 nm and 900 nm. The measurements were performed in close proximity between the detector and the light source, and subsequently a correction was introduced for the distance introduced between the sample and light source. The relation between irradiance percentage and distance was measured and is displayed in Fig. 4.3. The spectral distribution obtained with each of the LEDs is presented in Fig. 4.4.

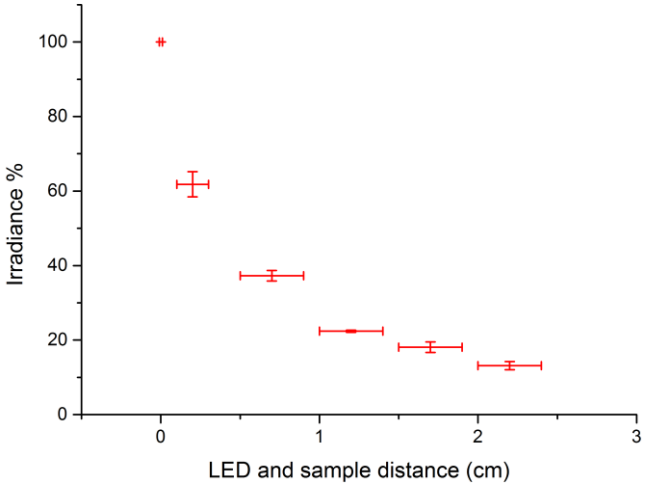

Fig. 4.3: Dependence relation between total irradiation percentages delivered on the sample and distance between UV LEDs and sample.

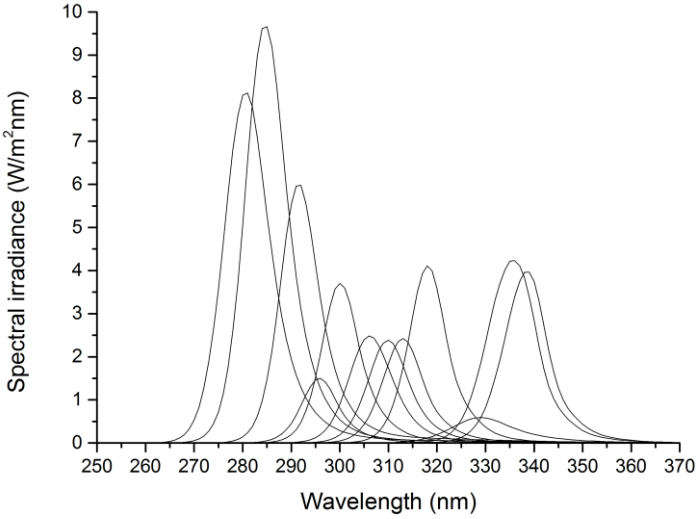

Fig. 4.4: Spectral distribution of the various UV-LEDs used in the experiments. The specific spectral irradiances are obtained from UV LEDs operating at 200mA, in close proximity with the detector.

Based on the Gaussian fit (with OriginPro 9.0 software) the central wavelength, the area and full width half maximum (FWHM) were

estimated. The estimated values are displayed in Table 4.2. The range was determined as plus/minus three standard deviations (SD). Irradiance of the exposures was calculated by taking the integral of spectral irradiances (area) of all emitted wavelengths for each LED and by adjusting with a correction factor, based on figure 4.3, for the distance introduced during exposures.

Table 4.2: The central wavelength, full width at half maximum (FWHM), and range (±3 SD.) were estimated based on the Gaussian fit of the spectral distributions for each of the 12 LEDs.

Central wavelength (nm)		FWHM	
Purchased as	Measured as	(nm)	Range (nm)
280	281	11	266-296
285	285	11	270-300
290	292	10	280-304
295	296	9	284-308
300	300	10	288-312
305	306	11	291-321
310	310	10	298-322
315	313	10	301-325
320	318	10	306-330
330	330	16	309-351
335	336	12	321-351
340	338	11	323-353

The content of vitamin D in the pig skin as a function of wavelength is displayed in Fig. 4.5; for incident radiant exposures of 300 J/m^2 and 7.000 J/m^2. The curves for both doses have similar shape, with maximum around 296 nm, but differing in the maximum vitamin D content (some saturation is observed at 7.000 J/m^2). Minor amounts of vitamin D were produced at 318 nm, while no vitamin D production was observed at or above 330 nm. The quantification limit for vitamin D was 3 ng/cm^2 pig skin. The content of vitamin D in the control sample (not exposed) was 5 ng/cm^2.

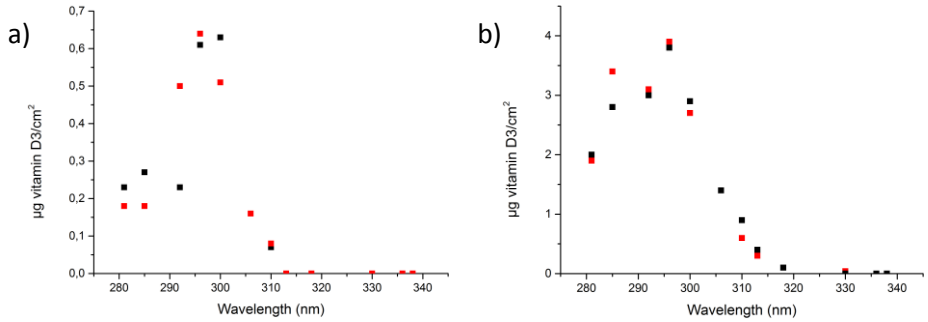

Fig. 4.5: Content of vitamin D in pig skin as function of wavelength after incident radiant exposures of a) 300 J/m^2 (281-338 nm) and b) 7000 J/m^2 (281-338 nm). No vitamin D production was observed at or above 330 nm. The maximum vitamin D production was observed around 296 nm. The two different replicates are indicated by red and black [0.2].

4.2.2.2. Effect of dose (with the optimal wavelength)

We used the optimal LED (296 nm central wavelength) to determine the effect of incident radiant exposure (dose) on the vitamin D production in pig skin. The skin samples were exposed to doses in the interval 200-20.000 J/m^2. For all tests the LED was run at 600 mA. The exposure times and incident radiant exposure are shown in Table 4.3.

Table 4.3: The exact exposure details for the determination of the effect of dose are presented.

Incident radiant exposure (J/m^2)	exposure (sec)
210	14
1.010	68
2.000	135
6.000	405
10.000	675
20.000	1.350

The LED was operated at a constant current mode and the irradiance arriving at the sample surface was approx. 15 W/m^2. The content of vitamin D resulting from the different doses is presented in Fig. 4.6. The relation between vitamin D content and dose seems to follow logarithmic kinetics. The content of 7-DHC (provitamin D) in control skin samples (unexposed samples) was found to be 79±6 μg/cm^2 (n=3). The highest obtained content of vitamin D in the pig skin was found to be between 3.5-4 μg/cm^2, which was around 4 % of the 7-DHC content in control skin. Thus, the capacity for increase of vitamin D is expected to have additional potential.

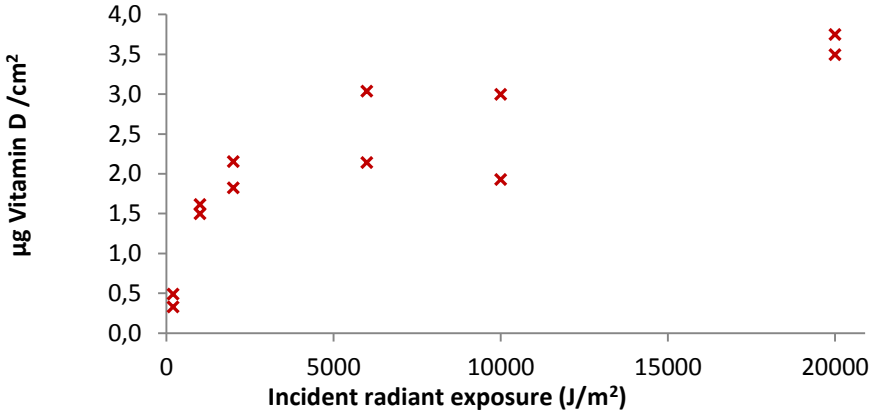

Fig. 4.6: Production of vitamin D in pig skin as a function of incident radiant exposure (dose). The pig skin samples are irradiated with a UV LED exhibiting central wavelength at 296 nm, which was determined as the optimal wavelength for pig skin bio-fortification [0.2].

In the past [4.6], human skin, obtained by surgery, was exposed to different doses of UV irradiation in the interval 10.000-300.000 J/m^2 using a wavelength of 295 nm; total conversion of provitamin D to vitamin D was not reached, despite the fact that the highest dose applied was 300.000 J/m^2. At this dose of 300.000J/m^2 approx. 70 % of the initial 7-DHC was converted to vitamin D [4.6]. There is agreement in the literature [4.6, 4.7] that higher dose of UV will result in a higher content of vitamin D, and at some point a plateau will be reached (logarithmic kinetics).

4.2.2.3. Reciprocity: effect of irradiance and exposure time

In photobiological processes it is often assumed that the extent of a response should depend on stimulus extent, rather than on the rate the stimuli is delivered, or duration of exposure to the stimuli. This hypothesis is called reciprocity [4.2]. However, responses of cells and tissues to electromagnetic radiation frequently involve a cascade of biological interactions making a linear dose-time relationship less likely. Therefore, reciprocity must be tested. In order to test the reciprocity, the irradiance emitted by the UV LEDs was varied between 0.1-43 W/m^2 (at four different levels) by adjusting the operation current at the interval 8 to 600mA; and the production of vitamin D content was subsequently measured. The test was performed with three different LEDs exhibiting central wavelengths: 292 nm, 296 nm, and 300 nm, around the identified optimal wavelength. The delivered stimulus (incident radiant exposure) was approx. 300 J/m^2. The specific LED settings used for each exposure are presented in Table 4.4.

Table 4.4: The exact exposure details for testing reciprocity are presented.

Central Wavelength (nm)	Current (mA)	Irradiance (W/m^2)	Exposure (sec)
292	8	0.1	3.000
	70	3.0	100
	400	27.2	11
	600	43.0	7
296	30	0.1	3.000
	200	3.0	100
	400	8.4	36
	600	14.8	20
300	10	0.1	3.000
	100	2.4	125
	300	11.4	26
	600	26.8	11

The results for the production of vitamin D are shown in Table 4.5. One-way ANOVA (two tailed) [2.71] was conducted, for each of the wavelengths, to test the null hypothesis of no difference between the different levels of irradiance used. For the tested range of irradiance values, no clear deviation from reciprocity is evident (null hypothesis is accepted $p>0.05$), and therefore, it is possible to deliver a specific dose of UVB over a short or long exposure and achieve the same vitamin D level (at least within the tested range of irradiance values).

Table 4.5: The content of vitamin D is presented after incident radiant exposure approx. 300J/m^2 (295-302 J/m^2). Reciprocity was tested with LEDs at central wavelengths 292, 296 and 300 nm; at four different levels of irradiance. P-values from one-way ANOVA (two tailed), testing for no differences between irradiances, at each of the wavelengths, are shown.

Wavelength (nm)	Irradiance (W/m^2)	Vitamin D (μg /cm^2)		*P*-value
292	0.1	0.57	0.41	0.62
	3.0	0.46	0.36	
	27.2	0.46	0.45	
	43.0	0.53	0.57	
296	0.1	0.31	0.83	0.96
	3.0	0.43	0.63	
	8.4	0.63	0.61	
	14.8	0.53	0.58	
300	0.1	0.47	0.58	0.06
	2.4	0.71	0.77	
	11.4	0.56	0.43	
	26.8	0.57	0.52	

4.2.3. Discussion and conclusion

4.2.3.1. Discussion

Studies have shown that UVB exposure of dairy cows and pigs can enrich milk and pork with vitamin D [4.8]. However, to apply this method in the food production necessitates the development of light sources that can comply with all requirements existing in food production lines.

UV-LEDs as light sources are suitable to fit into a food production line, due to their compact design and low energy consumption. Furthermore, LEDs can easily be implemented in industrial settings; to the contrary traditional bulky sources of narrowband UV can only be practical for laboratory use. LEDs allow spectral selectivity of the emitted light, and can be effortlessly integrated into electronic systems for automation. Moreover, LED technology can provide dust- and moisture - proof solutions, as well as, ensure lack of toxic compounds, and mechanical stability. Furthermore, LEDs produce minimal radiant heat, in comparison to other UVB-light sources and the non-desirable surface heating can be avoided [4.9].

Energy consumption and safety are some of the first challenges that need to be addressed when installing UV-light sources in a food production facility. Up-front costs of installing an UVB-LED based lighting system are at present high. However, costs are expected to fall in the near future [4.10], and LED performance is expected to continue to advance [4.11, 4.12]. LED systems have longer expected lifetimes, and lower maintenance costs than other UVB-light sources. Therefore, the specific application potential of the emerging technology of UV-LEDs cannot be overlooked.

According to the observations, vitamin D in a food product containing pig skin can be modulated by adjusting the applied exposure to the UVB irradiation. Moreover, since the vitamin D content at a specific dose is independent of the inversely related parameters total irradiation and exposure time (up to the irradiance values studied in this work), the exposure time can be freely designed to fit the needs of the specific production line.

Fortification in terms of addition of vitamin D to the “end product” has been introduced in several countries. The option of bio-fortification, by adding more vitamin D to the feed of animals has expanded further the

acceptance. Though, in Europe the addition of vitamin D in feed of animals is restricted within specific limits [4.13]. The alternative principle of biofortification by usage of UV irradiation of animals or food, is approved for use in the production of vitamin D both in the United States [4.14] and in the European Union [4.15], and imposes no restriction as normal biofortification, through feed, does.

The novelty proposed here for the first time is the ability of production of vitamin D biofortified pork products, with a light source (consisting of UV LEDs) that could easily become compatible with the requirements of a food production line.

Additionally, the UV LED found to be the optimal for biofortifying with vitamin D, could delay or even eliminate undesirable microbial growth (see chapter 3). Finally, considering the significant problem arising in pig farms with antibiotic resistant bacteria like MRSA and the demand for higher quality pork meat, in this work some substantial steps were taken towards the development of an LED lighting system that will be able to cover these needs and also being environmentally friendly.

4.2.3.2. Conclusion

In this Chapter we have shown that food products containing pork skin can be enriched by UVB LED exposure to elevate their content of vitamin D. The optimal wavelength for the production of vitamin D in pig skin irradiated with LED-UV was determined to be 296 nm. The effect of dose on the production of vitamin D in pig skin followed logarithmic kinetics, and the maximum incident radiant exposure (dose) used (20 kJ/m^2) resulted in a vitamin D content of 3.5-4 $\mu g/cm^2$.

It was confirmed that the reciprocity hypothesis is valid (for the tested irradiances), and therefore, the exposure duration needed to obtain a specific content of vitamin D can be freely selected; within the limits that the power of the LEDs dictate.

It was demonstrated that a good level of vitamin D enrichment (0.5 $\mu g /cm^2$) of pig skin can be achieved with UV LEDs only by a few seconds

exposure (7 sec), even though currently available UV LEDs are limited in output power.

4.3. Investigation of the effect of LED irradiation in the UVB, UVA and blue range on the production of vitamin D of farmed salmon skin

The present section focuses on the possibility to increase vitamin D content in farmed salmon skin (S. salar) by irradiation in the UVB, UVA and blue range. Salmon is known to contain high amount of vitamin D. However, several studies have reported that farmed salmon contains less vitamin D than wild salmon, ranging from 1.6-7.6 μg/100g in farmed salmon, to 9.6-26.5 μg/100g in wild salmon [4.16-4.19].

Recently, it was reported that it was possible to increase the vitamin D content of trout skin by exposure to solar spectrum or by exposure to blue light [4.20]. Moreover, *Tilapia* after exposure to UVB irradiation was reported to increase its vitamin D content up to three times [4.21]. Though, photolysis of vitamin D by sunlight, in fish skin, is not expected to be a key source for vitamin D in fish. UV rays from sunlight are expected to penetrate only the upper levels of ocean waters (50 m), where the marine photosynthesis happens [4.22].

Salmon consumption needs are mainly covered by farmed salmons [4.19]. Therefore, it is interesting to investigate if it is possibile to biofortify farmed salmon skin by implementing a specially designed LED lighting system (UVB, UVA or blue). In terms of market demand it would be even more interesting if biofortification could take place in the fish farm, while the fish were alive. Therefore, the fish samples were also placed under water, to test if biofortification is totally prohibited when water is present.

4.3.1. Material and methods

A summary of the exposure details for investigating the possibility of biofortifying farmed salmon is presented in table 4.6. The exposure of the

skin was performed in laboratory glassware/beaker containing cold tap water and the fish sample was positioned approx. 1 cm underneath the air-water interface. The radiant exposure reported was the one incident to the air-water interface. To secure the fish samples at a certain position, a thick layer of adhesive tape was located in the beaker (Fig. 4.7) and two needles were used for clamping the fish skin. The fish samples were cut in pieces of approx. 1x2cm^2. The central 1cm^2 piece of the fish skin was used for the vitamin D analysis, while the excess ends of the samples were only used for attachment to the tape layer. The needles were disinfected with ethanol and cleaned from vitamin D traces every time before "pinching". Similarly, clean water and tape layer was introduced every time in the beaker, before exposure. The weight of 1 cm^2 salmon skin varied between 0.08 g to 0.19 g. Pieces for control and exposure were cut from the same skin area (e.g. back (BA) or belly (BE)) but opposite fish part (left (L) and right (R)). The controls were taken from left side and test samples from right side. It was assumed that BA and BE could exhibit different amount of vitamin D content, due to proximity to

Table 4.6 : The exposure details for testing probable biofortification of farmed salmon.

	UVB (cw 296 nm)		UVA (cw 338 nm)		Blue (cw 454 nm)		
Radiant exposure (J/m$^{2)}$	6.000	60.000	6.000	60.000	6.000	60.000	120.000
Irradiance (W/m^2)	14.8	14.8	9.8	36.2	40	40	40
replicates	3	3	3	2	3	3	2

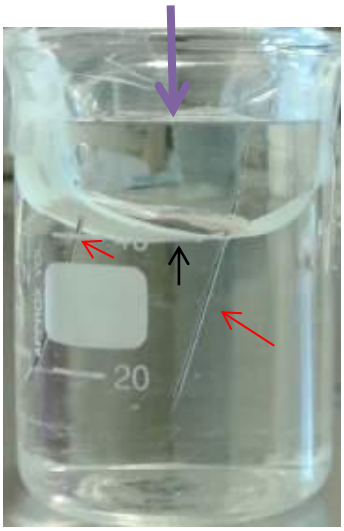

Fig. 4.7: The fish skin sample prepared for exposure. The skin is resting on the tape layer (black arrow) with the help of two needles (red arrows); the fish flake- surface is facing the air-water interface (purple arrow).

different organs of the fish. L and R side of the fish are not expected to exhibit any difference in vitamin D content due to inherent symmetry.

All samples were kept in a UV free environment before and after exposure. After exposure the samples were kept in airtight nitrogen flushed bags, and until the analysis of vitamin D they were kept at -20 °C. The set up for UV irradiation was the same as shown in Fig. 4.1. The set up and the spectral irradiance of the blue LED used for the exposure is presented in Fig. 4.8. The blue LED was purchased from Philips (Royal Philips, Amsterdam, The Netherlands), and was controlled by the hue Philips app. The spectral distribution of the UVB (296 nm) and UVA (338 nm) LEDs are the same as described in 4.2.2.1.

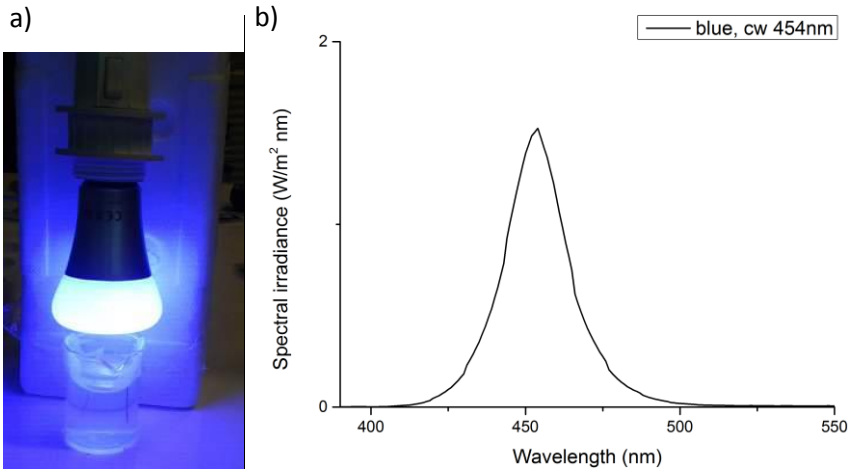

Fig. 4.8: a) Setup for blue light exposure. b) Spectral irradiance of the blue LED used for exposure of fish skin.

4.3.2. Results

The assumption that belly and back of the fish could exhibit different content of vitamin D was tested by a one way ANOVA (two tailed). The content of vitamin D at the two fish parts (left back (LBA), n=8 or left belly (LBE), n=10) is presented in figure 4.9. It was demonstrated that the vitamin D content was independent of the fish part the sample was taken from p=0.5. Hypothesis of no difference for the mean value of vitamin D content between fish-part was accepted. In general, the variance from fish-to-fish sample was observed to be as big as 0.07 μg/cm^2; see spread of points Fig. 4.9. Therefore, in the following analysis effects are considered significant, only if they are bigger than this fish-to-fish variation. The content of vitamin D found in the skin of salmon before exposure (control) and after exposure to UVA (338 nm), UVB (296 nm) and blue light (454 nm) is shown in table 4.7. The raw data are presented in Fig. 4.10. Since no significant difference was found in the average content of vitamin D in the controls, taken from back and belly, it was decided to group all the samples (independently of the fish part they were taken) into one group.

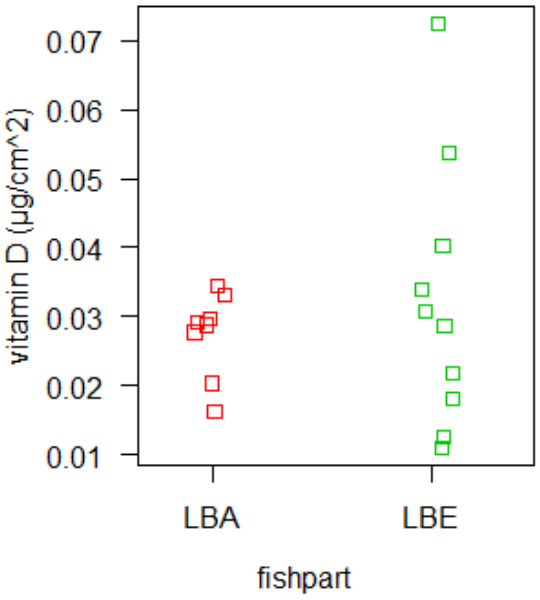

Fig. 4.9: The content of vitamin D at the two fish-parts left back (LBA), n=8 and left belly (LBE), n=10 are presented respectively in red and green color.

Table 4.7: The content of vitamin D found in the skin of salmon before exposure (control) and after exposure to UVA (338 nm), UVB (296 nm) and blue light (454 nm) presented together with standard deviation (SD).

	Radiant exposure (J/m^2)	Vitamin D ($\mu g/cm^2$)	SD of Vitamin D ($\mu g/cm^2$)
Non exposed	0	0.030	0.015 (n=18)
UVB (cw 296 nm)	6.000	0.037	0.003 (n=3)
	60.000	0.143	0.045 (n=3)
UVA (cw 338 nm)	6.000	0.012	0.004 (n=3)
	60.000	0.023	0.000 (n=2)
Blue (cw 454 nm)	6.000	0.015	0.008 (n=3)
	60.000	0.021	0.007 (n=3)
	120.000	0.014	0.002 (n=2)

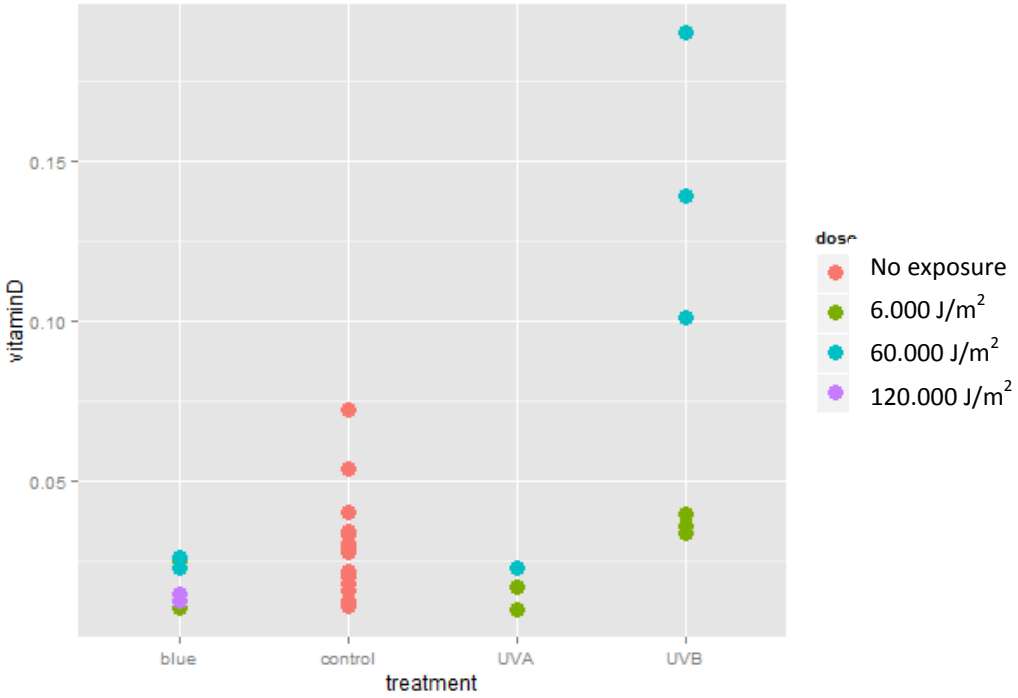

Fig. 4.10: The content of vitamin D (μg/cm^2) of salmon, after the various treatments were applied. The different radiant exposures (doses) are indicated by the different colors.

T-pairwise tests among the different treatments showed that only the UVB (60.000 J/m^2) was significantly different from all other treatments with p<<<0.001. The increase in vitamin D content achieved by this treatment, compared to unexposed salmon, was 0.10 μg/cm^2. Based on the 95% CI the increase achieved could be as much as 0.14 μg/cm^2 or as little as 0.09 μg/cm^2. UVA and blue exposure didn't increase significantly the vitamin D content compared to the control, independently of the exposure applied.

Finally, the water was removed from the beaker and exposure with UVB was performed (on three samples with 6.000 J/m^2; and one sample with 60.000 J/m^2), as before. The influence of the presence of water during exposure on the vitamin D content of salmon is presented in Fig. 4.11. Anova analysis accepted the hypothesis (both for 6.000 J/m^2; p=0.38 and 60.000 J/m^2; p=0.75) that the medium (water or absence of water;

indicated as dry) as applied here, imposed no significant changes at the vitamin D outcome; dry/wet difference (approx. 0.02 μg/cm^2) was much less than fish-to-fish variation).

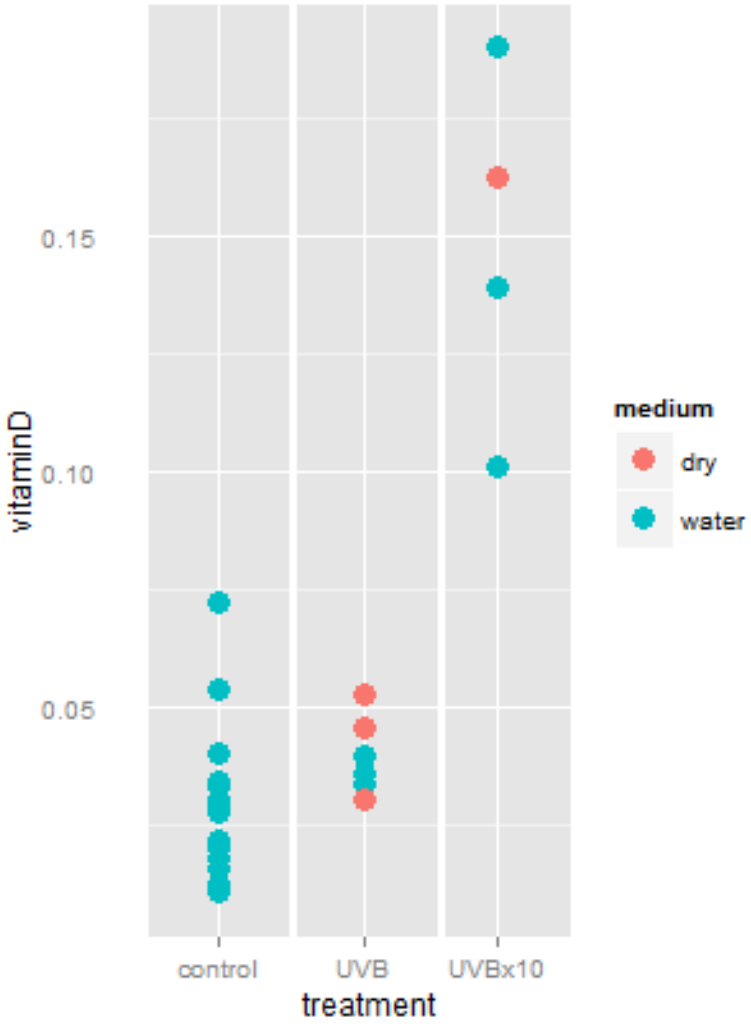

Fig. 4.11**:** The content of vitamin D (μg/cm^2) of salmon, after UVB treatments were applied. The presence or absence of water (indicated as “water” or “dry”) is indicated by the different colors.

4.3.3. Conclusion

It was demonstrated that farmed salmon skin can be biofortified by UVB LED illumination. An exposure of 60.000 J/m^2 was able to increase vitamin D content in average by 0.1 μg/cm^2. However, the vitamin D levels reached were not comparable to those obtained by exposure of pig skin. UVA and blue irradiation did not affect the vitamin D content in the range of exposures applied in this experiment. Moreover, the presence of approx. 1 cm of water above the sample imposed no significant changes at the vitamin D outcome.

4.4. Vitamin D biofortification in eggs with UV LEDs: indirectly by illuminating hens or directly on egg content

According to the present European legislation, it is not allowed to further increase the vitamin D content in eggs through feed, because the level of vitamin D added to the feed contains already the maximum permitted amount. Illumination with UVB-LEDs has potential to be used as an alternative or supplementary fortification method in egg farms, since requirements in terms of safety, energy and maintenance, could easily align with the advantages LED technology offers. Bio-fortification of eggs could possibly raise the vitamin D status in the global population since their consumption is very widespread. The reason why eggs are of special interest in regards to bio-fortification is the fact that they are easily accessible at a reasonable price to the majority of people, and additionally is a product which is palatable and easily digestible [4.23]. Moreover, hen's eggs, when compared with other natural food products, are rated very high as sources of both vitamin A and D.

Our ambition was to investigate the possibility of increasing the vitamin D content in eggs by exposing (vitamin D) supplemented hens to UVB from above using LED technology. The scenario of convincing egg companies to adopt only the alternative (vitamin D) biofortification method, on non (feed) supplemented hens could be considered too unrealistic. Moreover, if UVB-treatment is to be implemented in egg production facilities it would be

necessary to develop solutions where the hens are irradiated from above, to avoid the vast amount of cleaning and maintenance that would be required if the illumination was from below.

LED technology offers the chance to choose a narrower wavelength range than with traditional UV-light sources. As shown in the previous section 4.1, the optimal wavelength for achieving maximum increase of vitamin D when irradiating through skin is around 296 nm. Moreover, compared to other UV light sources LED technology provides high degree of control over the directionality of the output beam; greatly reducing delivery of light outside the region of interest.

Finally, the idea about increasing the vitamin D content of eggs by direct illumination (section 4.3.2) on the egg yolk and egg white was tested, and the penetration depth of UVB light in egg yolk, egg white and egg mix was investigated.

Since UVB irradiation can also be used successfully for killing bacteria (see chapter 3), egg products would be ideal candidates for UVB irradiation processing, during pasteurization or packaging, able to assist both in terms of vitamin D enrichment and lower bactericidal load.

4.4.1. Indirect biofortification of eggs by illuminating hens

4.4.1.1. Materials and Methods

4.4.1.1.1. Experimental setup

40 Lohmann-LSL layers (type of laying hens) were reserved from a herd of 62.000 hens in enriched cages (eating eniriched food) and delivered by Hedegaard A/S, Denmark. The hens were 28 weeks of age upon arrival and their average weight was 1.67 kg ± 0.14 kg (as measured in the herd). The hens were placed in the same type of cages as Hedegaard A/S uses in the production (type Euro SO 10, Hellmann Poultry, Germany). Each cage could house up to 10 hens and the cage dimensions were 120.5 cm in length and 62.5 cm in depth. A total of 753 cm^2 per bird was available; for a cage hosting 10 hens. There was a nesting area in the cages, with a red curtain in front and on top of it there was located a scratching area. The cages were linked two and two and shared the water drinking nipples. The cage is

shown in Fig. 4.12. UV opaque material was placed between the cages in order to avoid UV "contamination" (Fig. 4.13). The feeding tray was placed along the complete length of the cage.

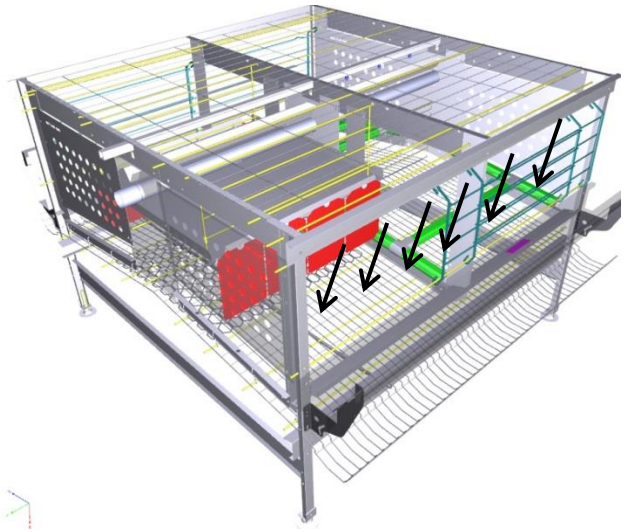

Fig 4.12: A three dimensional sketch of the hens cage**.** The irradiation was entering the cage as indicated by the black arrows. A nesting area was separated by a red curtain.

The hens were fed a standard feed which contained 3000 IU/kg vitamin D (Hedegaard-Agro, Denmark). 1 IU is the biological equivalent of 0.025 μg cholecalciferol (one of the D vitamins). Feed and water was offered ad libitum and the feed intake was determined on a week-basis.

General illumination was on from 01:30-16:30 each day, as in the production facilities. In this way it was ensured that the hens would be laying their eggs in the morning. Fluorescent tubes were used for the general illumination of the location that the experiment took place; again same type as used in the production. No dimmer was available in the existing illumination system therefore the light was dimmed by using white paperboard. The usage of paperboard did not change the spectral distribution of the lamps (as confirmed by a handheld spectrometer, UPRtek (MK350, Zhunan, Taiwan)). The illuminance at eye level of the hens was measured to be 6 lx. This level of illuminance was comparable to the level used in the production at Hedegaard A/S (6 lx). The acclimatization period was 2 weeks. General illumination is a critical factor in poultry since

cannibalism and aggressive behaviours have been reported in the past in bright environments [4.24, 4.25].

The Danish Animal Experiments Inspectorate provided the needed ethical approval. The authorization number given was 2014-15-0201-00254 C1 and the experiments were administered by the National Food Institutes in-house Animal Welfare Committee for animal care and use.

The UVB LED source was attached to the cages as shown in Fig. 4.13. Sixteen UVB-LEDs were purchased from Sensor Electronic Technology, Inc (SETi, TO3 package, flat window, half angle 60 degrees) and were assembled in two modules of eight diodes to fit the cage dimensions. The spectral distribution of the 16 LEDs is shown in Fig. 4.14. The average central wavelength of the UVB-LEDs was 307 ± 2 nm (std.dev.) with range 290-335 nm and was determined from the Gaussian fit of the spectral distributions. The resulting mean irradiance, of the two modules was respectively 0.76W/m^2 and 1.06W/m^2. The irradiance was measured at a distance of 25 cm which was the average distance between the hens and the LEDs; which was determined by observation of the daily activity of the hens (average distance between moving hens and light source, when accounting that hens move towards the feed tray and stay there with head downwards quite often ¾ of activity, or to the drinking nipples ¼ of activity). These data came from regular observation (10-15 minutes every 3-4 days) of hens in the created environment. The measurements were done using an integrating sphere and a spectrometer (QE 65000, Ocean Optics). The range of the analysis was 200-700 nm.

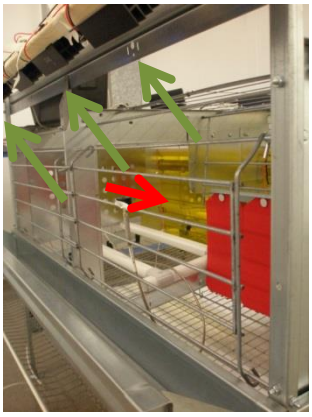

Fig. 4. 13: Picture of the hens' cage with "UV opaque wall"; red arrow. Green arrows show the attached LEDs.

The two LED assemblies (LED module 1, LED module 2) were designed with the intention to create an identical 3D irradiance pattern in the two cages. The 8 LEDs in the two irradiance groups were

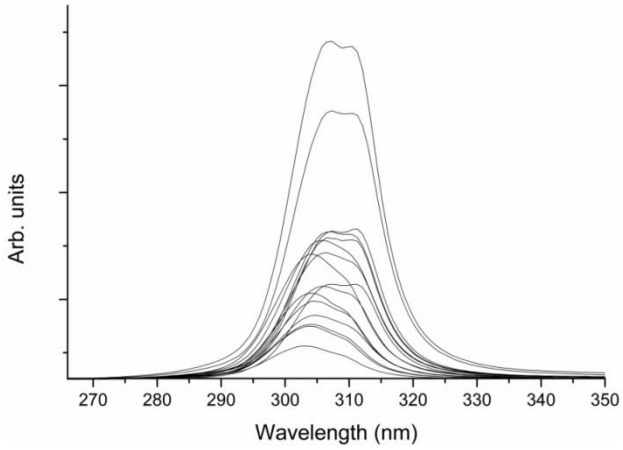

Fig. 4. 14: The spectral distribution of the 16 LEDs used to assemble the two modules used to illuminate hens from above.

placed at the top front of their cage respectively. 3D measurements with a cosine diffuser were performed on location to confirm that the irradiance patterns were comparable. Moreover the measurements showed that no UVB irradiation was accessing the nesting area (behind the curtain).

4.4.1.1.2. Irradiation protocol on hens

An overview of the irradiation protocol followed in the experiments with hens with goal to biofortify eggs by implementation of UVB illumination from above is presented in Fig. 4.15. The original plan to run 2 experiments each for the duration of a month and have a weekly collection of eggs was unfortunately not followed, due to unexpected problems.

The UVB light was delivered continuously in the first phase of the trial (from 04:00-11:38, for the 29.000J/m^2/day exposure, and from 03:00-15:47 for the 35.000J/m^2/day). In the second phase of the trial, the time schedule for the turning on/off of the UVB irradiation has been calculated to

maximize the “rest” between exposures of 20 minutes. In the third phase of the trial the exposure was split into time intervals of 1 min spread evenly over the entire daylight period (12 min exposure in total).

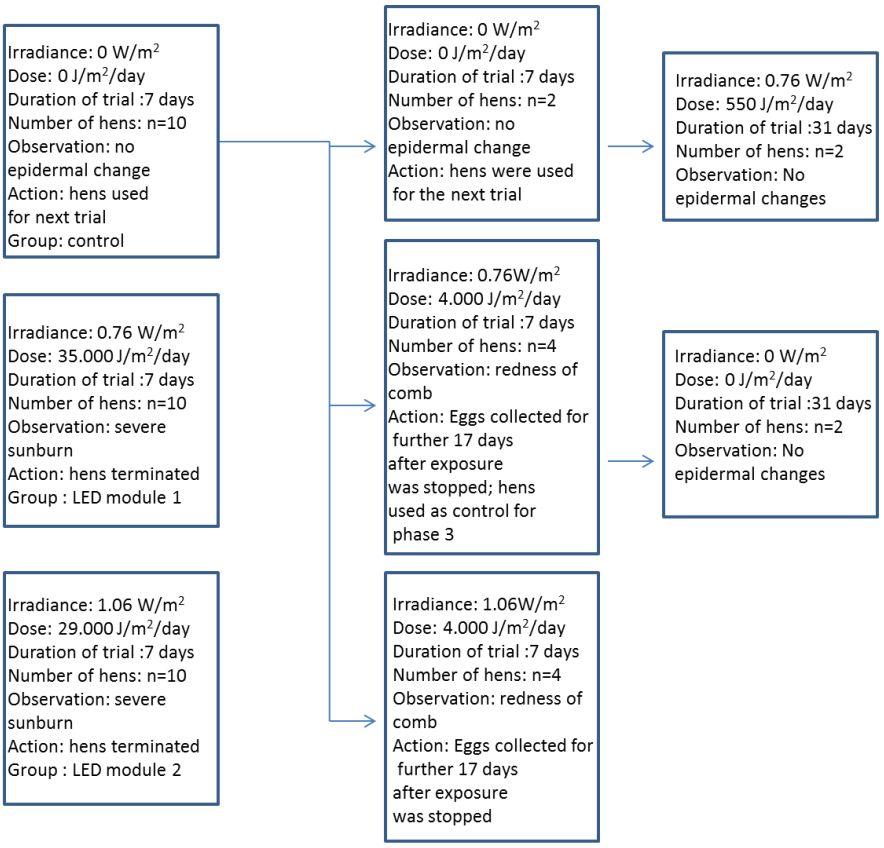

Fig. 4.15: Schematic presenting an overview of irradiation protocol on hens, in three phases of the trial (shown as separate columns). Information about irradiance, incident radiant exposure (dose), duration of trial-phase, size of hens’ group, visual observation about the condition of hens and action taken, is given.

4.4.1.2. Results

The content vitamin D and 25(OH)D determined in each egg yolk, after trial phase one, is shown in Table 4.8. The increase in vitamin D content of the eggs (the hens were laying) was in average 85-93% in phase one of trial, compared to eggs from non-illuminated hens. Unfortunately severe sunburns were observed on the irradiated hens, and therefore the (irradiated) hens were terminated and the trial was redesigned. There were no significant increase in the content of 25(OH)D in the treatment groups compared to the control. 25(OH)D is usually used to determine the vitamin D status of an organism. No significant difference between the LED-UVB treatments was observed.

Additionally, UV irradiation at a dose of 19.000 J/m^2/day was delivered at a separate hens group with a UVB-tube; the vitamin D content of egg yolk in that case was increased by 45%.

Table 4.8: Content of yolk vitamin D and 25(OH)D in eggs from hens after trial phase one. The exposure lasted 7 days.

Dose J/m^2/day	Irradiance W/m^2	25(OH)D ng/g			D ng/g		
		ng/g	average	std. dev.	ng/g	average	std. dev.
0	0	16.4	16.6	1.6	37.1	34.6	5.2
		17.7			32.0		
		18.0			40.4		
		14.4			28.7		
29.000	1.06	18.5	18.7	3.1	58.5	64.1	8.3
		21.1			52.0		
		23.4			76.6		
		16.4			65.9		
		17.6			64.5		
		15.1			67.2		
35.000	0.76	18.3	18.8	1.5	62.5	66.9	9.3
		19.6			65.7		
		18.6			68.7		
		17.1			54.0		
		21.4			82.3		
		17.9			68.3		

Then, at the second phase of the trial, a lower dose (4.000 J/m^2) was addressed and the eggs reached a 51% increase in their vitamin D content compared to eggs from non-illuminated hens, but still indications of dried skin and moderate sunburn were observed. It was interestingly observed that the vitamin D content of eggs continued to increase even after the UVB irradiation was stopped as shown in Fig. 4.16.

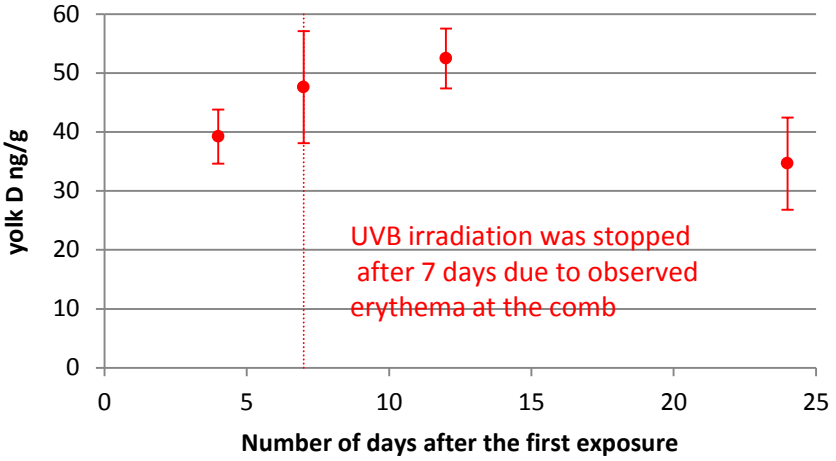

Fig. 4.16: Vitamin D content in egg yolk (± SD) as a function of number of days after first exposure; 2nd trial phase. The dose used in the UVB-treatment was 4.000 J/m^2/day. The UVB-treatment was stopped after 7 days of exposure, due to observed erythema at the hens' comb.

Further decrease of the dose in phase three of the trial resulted in completely healthy chicken even after 4 weeks of exposure, though no significant increase in vitamin D content was observed compared to eggs from non-illuminated hens. The detailed data are presented in table 4.9.

Table 4.9: The content of vitamin D and 25(OH)D in egg yolks; 3rd phase of trial.

Dose (J/m^2/day)	24 days of exposure		28 days of exposure	
	yolk vitamin D (ng/g)	yolk 25(OH)D (ng/g)	yolk vitamin D (ng/g)	yolk 25(OH)D (ng/g)
0	26.4	12.0	24.4	10.7
	36.8	16.4	34.5	15.0
547	32.6	13.5	28.7	11.8
	24.0	12.8	24.9	14.5

4.4.1.3. Discussion

Basic guidelines regarding the suitable dose and way of delivery (continuously "light on" versus interrupted mode with introduction of "rest periods") were introduced. We believe that a dose higher than 550 J/m^2 and lower than 3.500 J/m^2 would be appropriate to serve the purpose of biofortifying eggs without harming the specific type of "all white" grown indoors hens (this type of hens has not been exposed to sunlight for several generations). Probably an adaptation period to UVB irradiation, where the UV-light is gradually increased, would help hens' skin to accept without side effects the intervention.

With these studies we realized that it is much more economical (the cost for animal care, feed and host was very high) and much less dangerous if we aim for increasing the vitamin D content in dead tissue (like pig skin, or salmon skin) than live organisms (hens that produce eggs).

In the present study, vitamin D supplemented cage hens were used as a model system, as it is an easy environment to manipulate in regards to UVB exposure. However, as mentioned in the introduction, barn hens and free range hens are the future.

Directing the UVB irradiation at the feet is reported to be a very effective way of increasing the vitamin D in eggs [4.26, 4.27]. However implementing UVB light sources directed at the feet of the hens in a barn is a very challenging task. If light sources are placed near the floor, they will get dirty and a vast amount of cleaning will be necessary. Additionally, only the hens in close proximity to the light source will be exposed, making it hard to control the exposure each hen receives; thereby introducing variations in the vitamin D content and erythema side effects. It would be possible to install UVB-light sources directed at the feed of hens in cages, but as discussed above the sales of eggs from this type of production is diminishing and taken over from free range hens. If UVB-treatment is to be implemented in egg production facilities it is essential to develop illumination solutions where the hens are irradiated from above, in order to meet future market demands.

Hens are known to be extremely sensitive to their illumination environment therefore it was of vital importance to secure minimal interference; when comparing large scale egg production facilities to our testing facilities.

Extreme behavioral changes, as well changes in eating and laying habits have been reported in the past after shifting illumination environment of hens [4.28-4.30].

No behavioral changes (including eating, drinking, laying habits, and productivity of eggs) were observed during UV irradiation in these experiments, based on visual observation and measurement of feed intake.

4.4.2. Biofortification of eggs by direct UVB irradiation

The ability to increase the vitamin D content of eggs by direct illumination to the egg would solve many of the issues that arise when trying to bio-fortify eggs by illuminating hens. In addition UVB irradiation could also be used successfully for killing bacteria relevant in egg industry. Therefore, it was tempting to investigate the penetration depth of UVB irradiation in egg products namely egg yolk, egg white and egg mix (yolk and white) and find out if UVB processing could become a sensible dual method for bio-fortification and pasteurization.

4.4.2.1. Materials and methods

The penetration depth of different UVB wavelengths in egg products namely egg yolk, egg white and egg mix (yolk and white) are determined by using a UV spectrophotometer, UVB LEDs as light sources and the Beer–Lambert–Bouguer law. This law states that the intensity (I) of a light wave inside a material (I) is reduced exponentially from the value at the surface (I_0), as shown in the equation:

$$I(d) = I_0 e^{-\alpha d} \quad (1)$$

where α is the absorption coefficient of the substance, and d is the distance the light travels through the material. The penetration depth is a measure of how far light can penetrate into a material and is defined as the depth at which the intensity of the light inside the material falls to 1/e (about 37%)

of the value at the surface. The penetration depth is equal to the inverse of the absorption coefficient.

The experimental setup is shown in Fig. 4.17. The egg product was inserted in the quartz container (square cross section) at room temperature and the liquid was spread, so that a thin film of uniform thickness was formed at the middle region of the cuvette. The exact volumes of the different egg products used and the respective layer thicknesses are presented in Table 4.10.

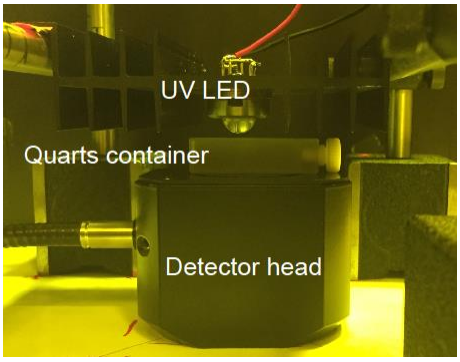

Fig. 4.17: The setup for testing the penetration depth of different liquid egg products in the UVB range.

Table: 4.10: The exact used volumes of liquid egg products and respective thicknesses; used to determine penetration depth.

Liquid egg product	used volume (ml)	thickness of egg yolk (cm)
Egg yolk	0	0
	0.1	0.027
	0.2	0.055
	0.3	0.083
	0.4	0.111
	0.5	0.139
	0.7	0.194
	1.1	0.305

Egg white	used volume (ml)	thickness of egg white (cm)
	0	0
	0.5	0.139
	1	0.277
Egg mix	used volume (ml)	thickness of egg mix (cm)
	0	0
	0.3	0.083
	0.4	0.111
	0.6	0.166

4.4.2.2. Results

A typical example of how the intensity decreases with increased thickness of liquid egg product is presented in Fig. 4.18.

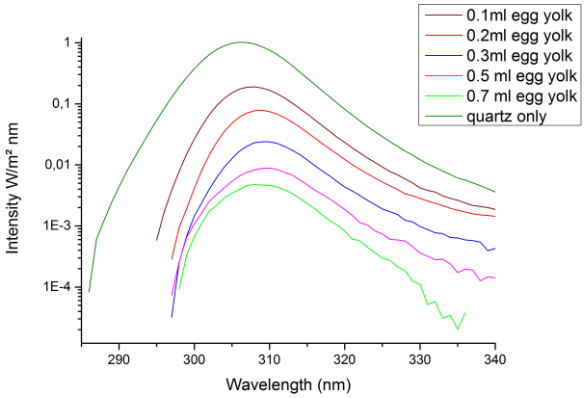

Fig. 4.18: Graph exhibiting a typical example of how the intensity decreases with increased thickness of liquid egg product, in this case egg yolk.

The penetration depth as determined for the different liquid egg products and at different UVB wavelengths is shown in Fig. 4.19. The penetration depth as determined by Geveke et al. [4.31] at 254 nm for egg mix and egg white is also shown (Fig.4.19). The vitamin D content after the UV

processing (central wavelength 296 nm) is shown in Table 4.11. The egg product layers exposed had a thickness around 3-4 mm.

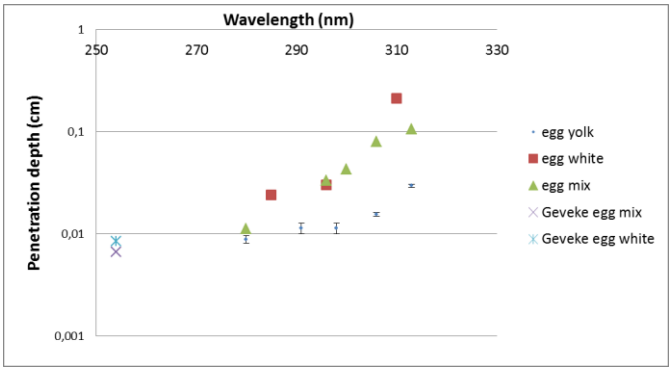

Fig. 4.19: The penetration depth as determined for the different liquid egg products, at different wavelengths.

Table 4.11: The vitamin D content in egg products; as acquired by UV thin film processing.

Egg product	Radiant exposure (J/m^2)	Vitamin D (µg/g)
Egg mix	0	0,011
	300	0,020
		0,026
	3.000	0,043
		Lost sample
Egg yolk	0	0,052
	300	0,076
		0,075
	3.000	0,207
		0,171

4.3.2.3 Discussion

For the wavelength region (290-306 nm) that would be interesting to process eggs with, in order to achieve the dual effect of biofortification and reducing bacterial load (chapter 3) the penetration depth was determined to be around 0.01-0.08 cm. This result indicates that the egg UVB processing is only sensible if it happens on thin films of liquid egg product or if a stirring process was taking place.

The concept for thin film biofortification of egg yolk and egg mix was demonstrated by irradiating layers of 3-4 mm, using a UV diode with central wavelength 296 nm. Any bubbles were removed from the surface using a needle.

Up to a 4-fold increase in the vitamin D content in both egg products was achieved after UV processing that lasted less than 3.5 minutes; egg white was not tested since its potential for biofortification is much lower. The reduction of bacterial load was not studied on egg product thin films, after UVB processing, though the results of chapter 3 strongly suggest that it will be possible to also disinfect from some types of bacteria.

4.4.3. Conclusion

Vitamin D biofortification of eggs is considered to be a strategy that would improve the status of the European population related to vitamin D deficiency. Evidence of the broad harmful effect vitamin D insufficiency/deficiency has on general health is growing. Therefore, it is of outmost importance to raise the vitamin D level of the population [4.1].

Here, two methods based on UVB LED technology were suggested for biofortifying eggs: 1) illumination from above for supplemented hens and 2) direct processing of thin film (3-4mm) egg products.

It was shown that the radiant exposure delivered on the hens is of critical importance for the welfare of the hens, especially if the “hen type” is such

that has never been exposed to sunlight for several generations. The acceptable limits for operation were found to be between 550-3.500 J/m^2 (daily exposure) and it is suggested that an adaptation period to UVB irradiation should be introduced in order to avoid sunburn of hens. A 4.000 J/m^2 exposure to the hens resulted in an increase of egg vitamin D content up to 51%, but also some erythema was observed at the comb of the hens which was not easy to evaluate if it was normal.

Direct UV processing of thin film (3-4 mm) egg products resulted in a 4 fold increase in the vitamin D content. It was found that the penetration depth of egg products (egg yolk, egg white and egg mix) in the UV region 290-306 nm is 0.01-0.08 cm. Taking into account the inactivation ability of this UVB band on biofilms (chapter 3), the possibility of UVB processing of eggs with dual functionality, namely biofortification and inactivation of bacteria could be considered as an interesting possibility for UVB LEDs in the egg industry.

The two methods presented here for egg biofortification have both advantages and drawbacks; therefore, the choice of way depends strongly on the details of specific potential application.

4.5. Novelty of the Chapter

UV exposure of farm animals [4.27] and mushrooms [4.32, 4.33] with UV lamps was proposed in the past as an alternative approach (biofortification) to solve the vitamin D deficiency problem. Here, UV LED technology is suggested as a more appropriate light source for this concept, since the requirements for safety and optimization existing in industrial settings can be much better aided by LEDs.

Evaluation of UV LEDs for production of vitamin D have been reported before by A.K. Ravichandran after direct human skin illumination and in vitro on solutions (ampoules of 7-DHC) [4.34]. Direct illumination of human skin as a vitamin D source could be dangerous if not applied with extreme precautions. Consumption of biofortified edible products produced by UVB irradiation, as suggested here, is excluding all dangers (cancer development, irritation of skin etc) of direct skin exposure to UVB.

Specifically for salmon skin the possibility of biofortification with blue light was investigated as suggested by Pierens et al [4.20], however, such a

response was not observed. Among the tested irradiations, UVA, UVB and blue, only UVB was able to increase significantly the vitamin D content.

Regarding biofortification of eggs, illumination for supplemented hens has been shown to be an effective method when directed to the hens' feet [4.26, 4.27, 4.35]. However, if UVB-treatment is to be implemented in egg production facilities, it is essential to develop illumination solutions that can meet future market demands. The two methods based on UVB LED technology that were suggested here 1) illumination from above for supplemented hens and 2) direct processing of thin film egg products meet this criterion. Especially direct processing of thin film eggs could additionally offer the advantage of lower bacterial load.

The novelties, related to UV LEDs and vitamin D biofortification achieved by the author of this thesis are presented below:

- Conceptualization and execution of direct processing of thin film eggs
- systematic investigation of the biofortification efficacy of UV LEDs, on pig skin, in the UVB and UVA range
- Development of irradiation protocol for biofortifying edible pig skin
- Identification of irradiation protocol limitations, for Illuminating hens for above, targeting enhanced vitamin D content in eggs.

4.6. Summary

A vitamin D biofortification method is introduced here and its applicability is discussed for three different food products types, namely pig skin, salmon skin and eggs. The optimal wavelength for achieving vitamin D enrichment in pig skin was investigated, and it was demonstrated that by using an LED with central wavelength around 295 nm a good level of vitamin D enrichment (0.5 μg /cm^2) can be achieved only by a few seconds exposure (7 sec). UVA and blue light were not able to biofortify salmon skin at the doses delivered, while UVB (central wavelength at 296 nm) irradiation enhanced the vitamin D levels in average by 0.1 μg /cm^2. These results were not in agreement with Pierens et all [4.20 or 1.4], that observed biofortification of fish by blue light. Egg biofortification was attempted by two ways. Direct illumination of egg products resulted up to a 4 fold increase in vitamin D content. While illumination of supplemented hens

from above, exhibited a potential for vitamin D enrichment up to 51%, but erythema was observed at the comb of the hens raising questions about the wellbeing of the flock. A summary table of the biofortification results achieved by LEDs on the different food product types is presented below (Table 4.12).

Table. 4.12: Biofortification results achieved by LEDs on various food product types.

Illumination type	Type of food	Dose (J/m^2)	Vitamin D content (μg/g)
UVB	pig skin [0.2]	0	0.005
		300	1
		2.000	3.6
UVA		7.000	Insignificant increase
UVB	salmon	60.000	0.7-1.75
		0	0.16-0.375
Blue or UVA		60.000	Insignificant increase
UVB	Egg product	0	0.05
		3.000	0.2
UVB	Egg from hens	0	0.035
		4.000	0.052

References

4.1. Gröber, U. et al., 2013. Vitamin D: Update 2013: From rickets prophylaxis to general preventive healthcare. Dermato-endocrinology, 5(3), pp.331–47.

4.2. Bunsen R, Roscoe HE, Photochemische Untersuchungen, Poggendorff´s Annalen 1855: 96: 373-394, 1857: 100: 43-88 and 481-516, 1857: 101: 235-263, 1859: 108: 193-273.

4.3. Institute of Medicine. (2011). Dietary Reference Intakes for Vitamin D and Calcium. Washington DC: The National Academies Press.

4.4. Black, L. J., Seamans, K. M., Cashman, K. D., & Kiely, M. 2012. An updated systematic review and metaanalysis of the efficacy of vitamin D food fortification. The Journal of Nutrition, 142(6), pp. 1102–1108.

4.5. http://www.worldwatch.org/global-meat-production-and-consumption-continue-rise

4.6. MacLaughlin, J. A., Anderson, R. R., & Holick, M. F., 1982. Spectral character of sunlight modulates photosynthesis of previtamin D3 and its photoisomers in human skin. Science, 216(4549), pp. 1001 – 1003.

4.7. Lehmann, B., Knuschke, P., & Meurer, M., 2007. The UVB-induced synthesis of vitamin D3 and 1α,25-dihydroxyvitamin D3 (calcitriol) in organotypic cultures of keratinocytes: Effectiveness of the narrowband Philips TL-01 lamp (311 nm). Journal of Steroid Biochemistry and Molecular Biology, 103(3-5), pp. 682–685.

4.8. Burild, A., Frandsen, H. L., Poulsen, M., & Jakobsen, J., 2015. Tissue content of vitamin D3 and 25-hydroxy vitamin D3 in minipigs after cutaneous synthesis, supplementation and deprivation of vitamin D3. Steroids, 98, pp. 72 – 79.

4.9. Souza, C. D., Yuk, H., Khoo, G. H., & Zhou, W., 2015. Application of light-emitting diodes in food production, postharvest preservation, and microbiological food safety. Comprehensive reviews in food science and food safety, 14, pp. 719 – 740.

4.10. Bergh, A. 2004. Blue laser diode (LD) and light emitting diode (LED) applications. Physica Status Solidi (A) Applied Research, 201(12), pp. 2740 – 2754.

4.11. Nishida, T., Saito, H., & Kobayashi, N., 2001. Efficient and high-power AlGaN-based ultraviolet light-emitting diode grown on bulk GaN. Applied Physics Letters, 79(6), pp. 711 – 712.

4.12. Yam, F. K., & Hassan, Z., 2005. Innovative advances in LED technology. Microelectronics Journal, 36(2), pp. 129 – 137.

4.13. EEC. (2004). List of the authorised additives in feedingstuffs published in application of Article 9t (b) of Council Directive 70/524/EEC concerning additives in feedingstuffs. Official Journal of the European Union, C50/1, pp. 1 – 144.

4.14. Food and Drug Administration. 2012. Food additives permitted for direct addition to food for human consumption; Sec. 172.381 Vitamin D2 bakers yeast. Federal Register, 77(168), pp. 52228–52232.

4.15. EFSA NDA Panel. 2014. EFSA Panel on Dietetic Products, Nutrition and Allergies. Scientific Opinion on the safety of vitamin D-enriched UV-treated baker's yeast. EFSA Journal,12(1), pp. 3520 – 3539.

4.16. J. Jakobsen, P. Knuthsen, and C. Smith, 2015. Salmon and trout- wild and farmed - what's the content of vitamin D?. unpublished.

4.17. U. Ostermeyer and T. Schmidt, 2006. Vitamin D and provitamin D in fish: Determination by HPLC with electrochemical detection. Eur. Food Res. Technol., vol. 222, no. 3–4, pp. 403–413.

4.18. M. Malesa-Ciecwierz and Z. Usydus, 2015. Vitamin D: Can fish food-based solutions be used for reduction of vitamin D deficiency in Poland?. Nutrition, vol. 31, no. 1, pp. 187–192.

4.19. Seafish, 2012. Responsible Sourcing Guide: farmed Atlantic salmon. Grimsby, UK.

4.20. Pierens, S.L. and Fraser, D.R., 2015. The origin and metabolism of vitamin D in rainbow trout. The Journal of steroid biochemistry and molecular biology, 145, pp.58-64.

4.21. D. S. Rao and N. Raghuramulu, 1997. Vitamin D3 in Tilapia mossambica: Relevance of Photochemical Synthesis. J Nutr Sci Vitaminol, vol. 43, pp. 425–433.

4.22. S. Johnsen and H. Sosik, 2004. Shedding Light on Light in the Ocean. Oceanus Magazine, vol. 43, no. 2, p. 5.

4.23. Bethke, R.M., Kennard, D.C. & Sassaman, H.L., 1927. THE FAT-SOLUBLE VITAMIN CONTENT OF HEN ' S EGG YOLK AS AFFECTED BY THE RATION AND MANAGEMENT OF THE LAYERS. JOURNAL OF BIOLOGICAL CHEMISTRY, 72, pp.695–706.

4.24. Prayitno DS, Phillips CJC and Stokes DK. 1997. The effects of color and intensity of light on behavior and leg disorders in broiler chickens. Poultry Science, 76, pp. 1674-1681.

4.25. Sultana S, Hassan MR, Choe HS and Ryu KS. 2013. The effect of monochromatic and mixed LED light colour on the behaviour and fear responses of broiler chicken. Avian Biology Research, 6, pp. 207-214.

4.26. Kühn, J. et al., 2015. Non-linear increase of vitamin D content in eggs from chicks treated with increasing exposure times of ultraviolet light. The Journal of Steroid Biochemistry and Molecular Biology, 148, pp.7–13.

4.27. Schutkowski, A. et al., 2013. UVB exposure of farm animals: study on a food-based strategy to bridge the gap between current vitamin D intakes and dietary targets. PloS one, 8(7), p.e69418.

4.28. Sultana, S., Hassan, M.R., Choe, H.S., Kang, M.I., Kim, B.S. and Ryu, K.S., 2013. Effect of various LED light color on the behavior and stress response of laying hens. The Indian Journal of Animal Sciences, 83(8), pp. 829–833.

4.29. Karakaya, M., Parlat, S.S., Yilmaz, M.T., Yildirim, I. and Ozalp, B., 2009. Growth performance and quality properties of meat from broiler chickens reared under different monochromatic light sources. British poultry science, 50(1), pp.76-82.

4.30. Huber-Eicher, B., Suter, A. and Spring-Stähli, P., 2013. Effects of colored light-emitting diode illumination on behavior and performance of laying hens. Poultry science, 92(4), pp. 869-873.

4.31. Geveke, D.J., Boyd, G. and Zhang, H.Q., 2011. UV penetration depth in liquid egg white and liquid whole egg. Journal of Food Processing and Preservation, 35(6), pp.754-757.

4.32. Mau, J.L., Chen, P.R. and Yang, J.H., 1998. Ultraviolet irradiation increased vitamin D2 content in edible mushrooms. Journal of Agricultural and Food Chemistry, 46(12), pp.5269-5272.

4.33. Jasinghe, V.J. and Perera, C.O., 2006. Ultraviolet irradiation: the generator of vitamin D 2 in edible mushrooms. Food chemistry, 95(4), pp.638-643.

4.34. Ravichandran, A.K., 2015. Evaluation of a novel light-emitting diode device for producing vitamin D (Doctoral dissertation, SCHOOL OF MEDICINE Thesis EVALUATION OF A NOVEL LIGHT-EMITTING DIODE DEVICE FOR PRODUCING VITAMIN D by AJAY KUMAR RAVICHANDRAN BS, University of Maryland–Baltimore County).

4.35. Lietzow, J. et al., 2012. Effect of short-term UVB exposure on vitamin D concentration of eggs and vitamin D status of laying hens. Journal of agricultural and food chemistry, 60(3), pp.799–804.

Chapter 5

5. VIS LED lighting systems and their potential benefit to populations with special health care needs

Motivation

Solid state lighting technology has offered innumerable choices regarding indoor general illumination. However, the culture about how to implement the available lighting choices for best benefit of wellbeing is not yet formed. Generation of evidence and statistical proof that specific lighting scenarios, generated by LEDs, can benefit general health could have impact on society, especially for populations with special health care needs.

Related PhD publications: ***0.1, 0.3, 0.7 , 0.11, 0.12, 0.15.***

5.1. Introduction

The present chapter is concerned with the usage of VIS LED lighting systems for meeting specific needs of populations with a distinct health care profile. The intention is to provide empirical evidence and demonstrate statistically that specially designed VIS LED lighting systems can be beneficial to populations with special health care needs.

More specifically, the sleep quality and wellbeing of healthy elderly (older than 65 years) was investigated by changing the indoor lighting at their homes. Moreover, potential benefits during birth labor, both for the mothers and the midwives, are discussed after testing the specially designed lighting during the birth, versus normal fluorescent light which is the norm for birth clinics. The measurable effects, of the specially designed lighting, on the birth are to be presented in an upcoming publication [0.7].

Light interventions on elite athletes (Danish Olympic swimmers) were also evaluated as a potential tool to improve sleep patterns on occasions of disturbed circadian rhythm conditions (e.g. different time zones, inconvenient competition times). The lighting system used for the interventions of athletes was designed by Jakob Hildebrandt Andersen for his project with Team Denmark that the author of this thesis was co-supervising**.** Moreover, a preliminary testing was performed with blue light intervention and its potential effect on reaction time.

Finally, the ability of humans to identify veins was studied under different illumination conditions as a (example) paradigm that direct visual perception of biosamples can be improved if suitable general lighting is applied.

The present chapter is the result of interdisciplinary research collaboration between DTU Fotonik, and Nordsjællands Hospital-Hillerød (T. Wrønding and E. C. L. Løkkegaard), Glostrup Hospital (B. Sander, L. Kessel), Gate 21, Team Denmark (L. Johansen, A. T. Adler), Aalborg University (J. Markvart, K. Johnsen) and DTU Compute (L. K. H. Clemmensen).

5.2. VIS LED lighting systems and elderly citizens' sleep quality and wellbeing [0.3]

The present section focuses on the potential to improve the sleep quality and wellbeing of elderly healthy citizens by employing specially designed indoor lighting [0.3]. It is known that the spectral retinal illumination is changing with age, blue light is transmitted less [5.1-5.3]; and that the eye lens aging can play an important role in systemic health [5.4, 5.5]. Moreover, for elderly people the life is mostly spent indoors; and that can result in the absence of a timely sequence of light intensity with which, so wisely, evolutionary adaptation entrained the human circadian rhythm. Disturbed circadian rhythms can increase the risks for diabetes and hypertension [5.6-5.8] and affect the mood.

Therefore, it was interesting to explore if any benefits, in terms of sleep quality and wellbeing, would come up by exchanging existing luminaires in private homes of healthy elderly citizens with commercial LED luminaires that enabled control over spectral characteristics and light intensity.

5.2.1. Materials and Methods

5.2.1.1. Experimental design

Twenty-nine participants (twenty similar private houses) were exposed to two light scenarios in a randomized cross-over design, followed by 1 week pause. Each light scenario was applied for 3 weeks from 8 am to 1 pm. One light scenario was blue-enriched (280 lx) and another blue-suppressed (240 lx). In all cases the illuminance was reduced to approx. 140 lx blue-suppressed, after 1 pm. Data were collected at baseline (existing illumination setting) and at the end of each light epoch.

Elderly subjects suffering from depression and/or taking medication known to influence the circadian rhythm were excluded from the study. The study was performed in accordance with the policies of international chronobiological standards [5.9]. Constraints on daily schedule were not enforced. However, the participants were encouraged to spend time indoors until midday. All participants lived in homogeneous houses (rooms positioned in alternative geometries and minor differences in size).

Changes in terms of wellbeing and sleep quality were evaluated by using diaries filled by the participants. Self-reported diaries are reported to be an

effective method for evaluating sleeping habbits [5.10]. Additionally, the Pittsburg sleep index (PSQI) [5.11] and the Morningness–Eveningness questionnaires were used to assess sleep quality. PSQI≥5 indicated "bad sleepers". According to the Morningness–Eveningness score (MEscore) participants were categorized as "morning types" (score bigger than 59), "neutral types" (score between 42 and 58) or "evening types" (score smaller than 41) [5.12]. Sleep duration and rest-time were cross tested by an Actiwatch (monitoring system) that the participants were wearing.

In order to obtain a subjective evaluation of the change in light environment, all participants were asked to give a score (to the light environment change) from 0 to 10. A score of zero indicated high "unlikablility" (not acceptable light) while a score of ten high "likability". The experimental light was compared to their previous habitual light (pre-experimental light), and the blue-suppressed and blue-enriched scenarios were compared with each other.

For the data analysis normal distribution was assumed for the subjects' response, and pairwise t-tests were performed to compare the outcomes from the different light epochs. The significance level was set to 0.05.

5.2.1.2. Light conditions

The indoor sunlight levels were assessed to be insignificant for the outcome of the experiment. The pre-experimental light distributed in general limited light at the position of the cornea (below 100 lx). The experimental light was Philips Hue light bulbs (http://www2.meethue.com/en-us/this-is-hue/). The 3 bulbs were placed in 3 globe-shaped frosted glass pendants in the central room of the house, i.e. where the dining table and/or living room was located and in close proximity to the kitchen. The specific light location was chosen to maximize the hours spent by the participants near the experimental light.

In order to increase the light exposure and to avoid contrast problems an LED uplight was mounted (Philips, SkyRibbon IntelliHUE Wall Washing Powercore © Eindhoven, the Netherlands) that illuminated the ceiling and added indirect light to the exposure zone. The same light sequence was followed both from uplight and the HUE light bulbs. From 8 am to 1 pm, the illuminance of the light system was controlled to reach approx. 280 lx (blue enriched) and 240 lx (blue suppressed), at the position of the cornea, measured half a meter away from the frosted glass pendants. After 1 pm,

the illuminance was reduced to approx. 140 lx blue-suppressed in both light epochs. From 6 pm until bedtime the setting was approx. 100 lx blue-suppressed. During the night the participants could switch the light on and off to meet their needs. If the light was turned on during night hours, the illuminance level was set at 100 lx and spectrum-wise it was blue-suppressed.

The light setting measurements were performed on location (after sunset) with a handheld spectrometer from UPRtek (MK350, Zhunan, Taiwan). The efficacy was measured by a Yokogawa WT3000 power analyzer and an Elgar CW1251P power supply, in the laboratory. The summary of light characterization is presented in table 5.1. The light spectra were selected to achieve a color rendering index (CRI) over 80. The spectral irradiance for blue enriched, blue suppressed and afternoon light are shown in Fig. 5.1. The spectral radiant power is presented in Fig. 5.2.

Table 5.1: Summary of light characterization; population of houses studied n=4 (correlated color temperature (CCT), CRI, illuminance, efficacy, radiant power and irradiance). The light intensities are measured at cornea level. The morning scenarios were applied from 8 am to 1 pm and were either blue-enriched or blue-suppressed. The afternoon scenario was applied from 1 pm to 6 pm and was blue-suppressed [0.3].

	CCT (K) (average; SD)	CRI	Illuminance (lx) (average; SD)	Efficacy (lm/W)	Radiant power (W) (average; SD)	Irradiance (mW/m^2) (average; SD)
Morning-blue enriched	5.100; 300	82	280; 35	85	1.47; 0.02	920; 170
Morning-blue suppressed	2.800; 30	92	240; 31	79	1.14; 0.01	710; 110
Afternoon	2.800; 30	92	140; 16	75	0.59; 0.01	392; 48

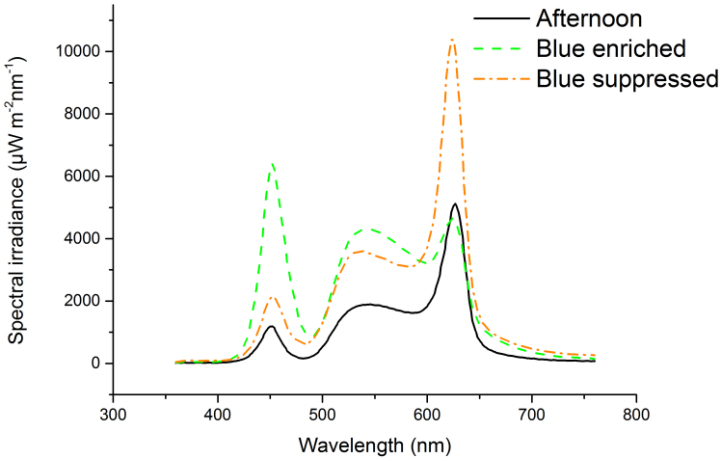

Fig 5.1. Spectral irradiance for blue-enriched, blue-suppressed and afternoon light. The blue-enriched and blue-suppressed light conditions were applied with irradiance approximately 700–900mW/m^2 during morning until 1 pm in the participant's living room. From 1pm, the afternoon light conditions were applied (irradiance approximately 400mW/m^2). [0.3]

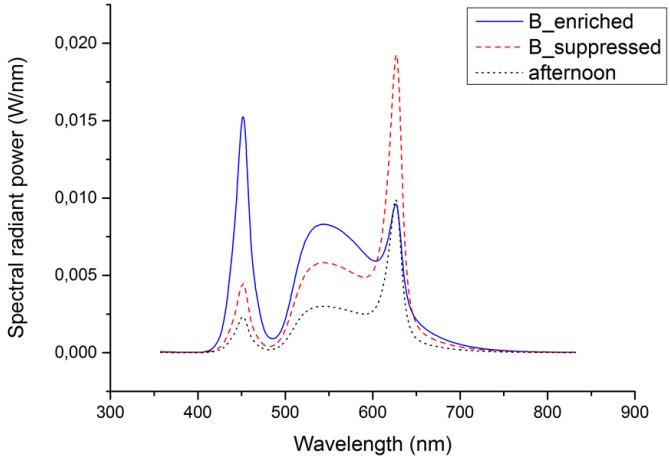

Fig 5.2. Spectral radiant power for blue-enriched, blue-suppressed and afternoon light.

5.2.2. Results

The average age of the participants in the study was equal for the males and females, 69.5 years (67.5–71.4, taking into account the 95% CI).

According to the randomization procedure, equal number of males and females were receiving a specific light scenario in the first or second experimental period (p>0.8; balanced design). The results from the PSQI questionnaires are presented in table 5.2. Females were positively affected by the installation of experimental light, and their PSQI score decreased significantly (p=0.007). Males did not experience significant changes (p=0.7). It is important to mention that at baseline only 19% of males were identified as "bad sleepers", to the contrary the majority of females 62% were identified as "bad sleepers" at baseline (p=0.009). After the light intervention the status of females and males was indistinguishable (p>0.05).

Table 5.2: PSQI for the subjects at baseline and during blue-enriched and blue-suppressed light epochs reported as average values, [standard error] and 95% CI; together with p. values for the various comparisons performed [0.3].

	Baseline	Blue-enriched	Blue-suppressed
PSQI (males)	4.06 , [0.67] 2.64-5.49	4.31, [1.04] 2.09-6.54	4.13, [0.97] 2.06-6.20
PSQI (females)	7.62, [1.14] 5.13-10.00	5.62, [0.87] 3.71-7.52	5.85, [0.88] 4.02-7.67
P. value (compared genders)	0.009	0.36	0.20
P. value (males compared to baseline)	Not applicable	0.721	0.78
P. value (females compared to baseline)	Not applicable	0.007	0.08

The summary results for sleep duration, sleep quality and MEscores are shown in table 5.3. No significant differences were found between the different light scenarios for the sleep time, as reported in the diary

(p=0.85); and the MEscore indicated participants, in both scenarios, as "morning types" (p=0.3). Moreover, no significant changes were observed for the occurrence of nightly awakenings (p=0.14) neither for the occurrence of daily naps (p=0.24). Similarly for the time spent on computers or television (p=0.84). Unfortunately, important data from the baseline period were not collected which prevented all possible comparisons to be performed.

Table 5.3: Results for 29 subjects at baseline and after each type light epoch as derived from diary and Actiwatch data. Results are given as mean, [standard error] and 95% confidence limits. The p. values as obtained from the pairwise t-tests, between blue enriched and blue suppressed scenarios, are also included [0.3].

	Baseline	Blueenriched	Bluesuppressed	p-value
Sleep/ rest				
Sleep hours (diary)		7.44, [0.15] 7.14-7.74	7.31, [0.15] 7.01-7.62	0.29
Rest hours (diary)	Not applicable	8.00, [0.20] 7.59-8.41	7.88, [0.20] 7.47-8.29	0.26
Rest hours (Actiwatch)		7.91, [0.16] 7.58-8.24	7.75, [0.18] 7.40-8.11	0.18
Quality of Sleep				
PSQI	5.66, [0.07] 4.22-7.09	4.90, [0.70] 3.47-6.32	4.93, [0.66] 3.58-6.28	0.90
Poor sleeper occurrence (percentage)	17/29 (59%)	13/29 (45%)	11/28 (39%)	0.67
Circadian rhytm				
MEscore, mean (SE) 95% CI	61.14 (1.36) 58.35-63.92	59.62 (1.52) 56.51-62.73	60.29 (1.38) 57.47-63.12	0.32

Finally, the subjective evaluation showed that the participants favored the experimental light compared to habitual light, with an average score of 7.84. The blue enriched and blue suppressed light scenarios were equally "likable"; score 4.95.

5.2.3. Conclusion

It was found that females had a significantly worse baseline PSQI score than males. After the light intervention, the PSQI score of females reached almost normal values (around 5). This positive outcome can be a result of the fact that habitual indoor lighting was exchanged with the experimental LED light that allowed illuminance and spectral modulation throughout the day. However, no improvement was observed for the sleep duration, sleep quality and circadian rhythm parameters between the blue enhanced scenario and the blue suppressed (applied during morning hours). Placebo affects were not investigated by this study.

Secondary beneficial effects related to the exchange of the pre-experimental luminaires with LEDs, was the fact that the energy consumption of the houses was reduced and that the participants enjoyed the upgraded light environment in their houses.

5.3. VIS LED lighting systems in the delivery room [0.7]

It is known that for first time mothers, the labor occurs primarily in the night-morning hours [5.13]. These hours of the day where natural sunlight is very dim and has very little percentage of blue wavelengths, melatonin exhibits its peak concentration in the human body, due to maximum excretion. Melatonin acts in synergy with oxytocin to promote contractions of the uterus and thereby momentum of the birth.

Special LED lighting systems designed by Wavecare and Philips have been installed in delivery rooms at Hillerød hospital, with the scope to allow

ambient interventions by audiovisual stimulation. These delivery rooms are called sensory delivery rooms (in opposition to standard delivery rooms). The present chapter section focuses on characterizing the differences between illumination characteristics of sensory versus standard delivery rooms, and discussing the possible positive implications on labor [0.7] and on midwives wellbeing, related to the special light surrounding created by the LED system.

5.3.1. Materials and methods

5.3.1.1. Light characterization: Sensory versus standard delivery rooms

In the sensory rooms, a special illumination system is accompanied with a big illumination-alive screen. The system is controlled through a touch panel which allows choices among 5 preset programs, namely “arrival” program, “breathing” program, “atmospheric” program, “relaxing” program, and “white light no sound” program. Inside each program further adjustments can be made by separately controlling the light at four specific locations, namely the entrance (white light, able to be dimmed), ceiling (white light, able to be dimmed), wall (colored light), spot light (colored light). The colored light is interchangeable among the following colors blue, yellow, red, white, and green. The curtains were closed during the measurements to simulate night hours (darkness outside the window). The light characterization measurements were performed on location with a handheld spectrometer from UPRtek (MK350, Zhunan, Taiwan).

The light environment under the five preset programs in the sensory room is shown in Fig. 5.3. It can be seen that the presence of the screen, introducing a blurred visual dynamic stimulus, influences significantly the atmosphere created by the LED illumination system.

The spectral distributions of the different light programs of the sensory rooms, as perceived at the level-height of the cornea at three different locations namely on the bed, in the bath tub and standing, are presented in Fig. 5.4. The woman undergoing labor is expected to “freely” move or be located at any of the three locations in the room and similarly for the

midwife. Moreover, the spectral power distribution of a standard delivery room is presented (compact fluorescent light). In the standard labor room there was also a dimming option, therefore, we present here the irradiance, as measured under fully dimmed conditions (min. irradiance) and under full power conditions (max. irradiance).

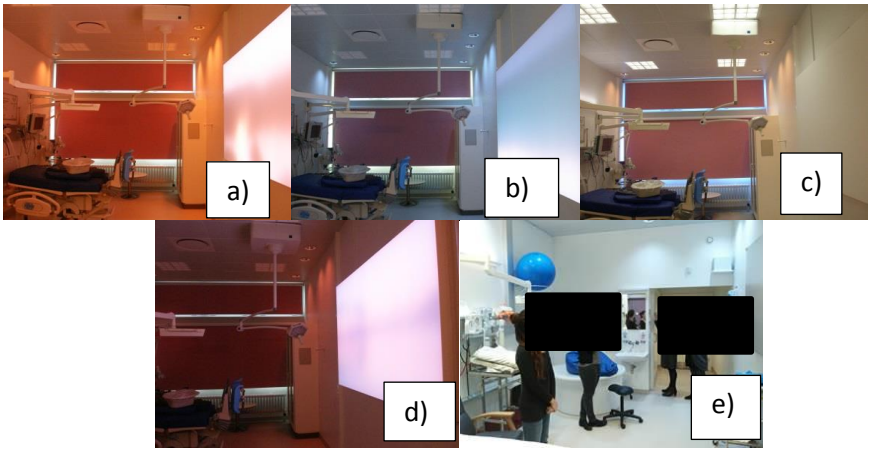

Fig. 5.3: Photos of a sensory room as an illustration of the lighting environment under the preset programs: a) arrival program b) breathing program c) atmospheric program d) relaxing program and e) white light no sound program.

Among the preset light programs, the one called “white light no sound” was observed to have much higher irradiance around 900 mW; and illuminance 280 lx in the bed position. The relaxing program had the next highest irradiance 170 mW; illuminance 39 lx in bed position. The arrival (31 lx; bed position) and atmospheric (41 lx; bed position) programs were alike in terms of irradiance 110-130 mW. The breathing program had the lowest irradiance among the preset programs (around 80 mW) and illuminance 22 lx in bed position. The location in the room is not substantially changing the spectral distribution but affects the irradiance of light; especially standing position affects most the intensity of light perceived. The light intensity at standard labor rooms was reaching the same levels (irradiance around 500 mW; and illuminance 260 lx) as the “white light no sound” program in the sensory room.

It must be highlighted here that the “white light no sound” program is very rarely used during the labor, when compared to the frequency of usage of the rest preset programs arrival, breathing, atmospheric, relaxing (see section 5.3.1.2). Hence, the average irradiance and illuminance level in

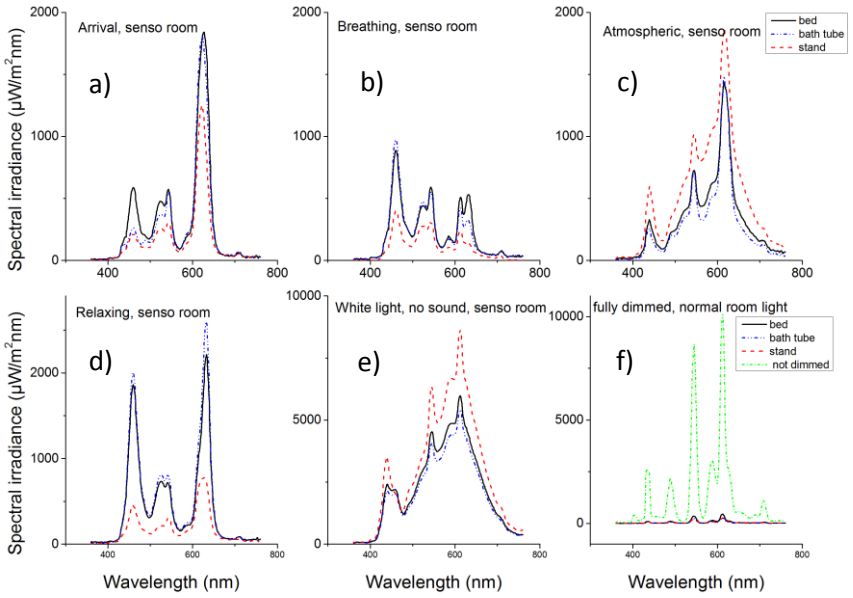

Fig. 5.4: Spectral irradiance of the different preset light programs at three locations, in bed, in bath tub, and standing, in the sensory room. a) arrival program, b) breathing program, c) atmospheric program, d) relaxing program and e) white light no sound program. f) Spectral irradiance of the normal labor rooms, here irradiance is measured under fully dimmed conditions and in not dimmed mode.

the sensory delivery room is much lower than in standard labor rooms, if the dimming option (in the standard delivery room) is not used. Dimming option also exists in the sensory delivery rooms.

Color control within a preset program can result in a further shift in the illumination environment, as illustrated in Fig. 5.5.; as an example, we present here the shift in the preset program “breathing”. The breathing program was the most used among preset programs both in phase 2 and 3 of labor [see section 5.3.1.2]. The consequential shift happening, after changing the preset program, is not significant in terms of changes in irradiance. However, the balance among colors (spectral distribution) can be significantly affected (Fig. 5.6).

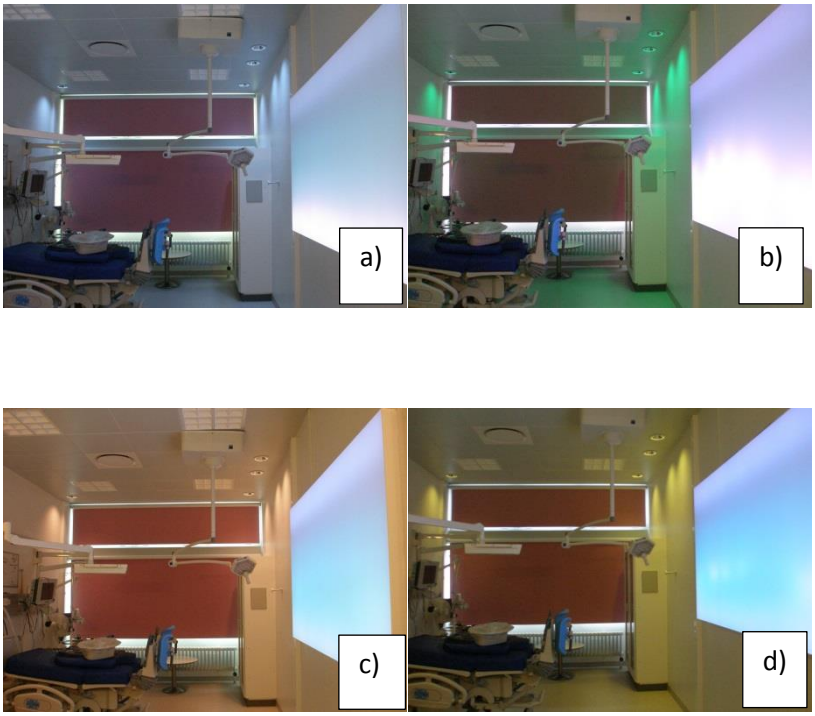

Fig. 5.5: Photos of the sensory room as an illustration for the light environment, after changing the preset program breathing. a) breathing program as preset, b) breathing program, with color set to green (at spot lights), c) breathing program with color set to red (at spot lights), d) breathing program, with color set to yellow (at spot lights). The breathing program with the color set to blue is not presented, since it was almost identical to the breathing preset. More specifically, the preset breathing program is a dimmed version of breathing with blue.

The characterization of illumination at the two different types of delivery rooms, sensory vs standard, revealed that the available light settings in the sensory room could potentially act as facilitators for secretion of melatonin, as well as, provide a colorful and playful ambient environment adaptable to personal preferences. These qualities, which the LED lighting system offers could potentially have beneficial effects both on the medical personnel working in these rooms but also on the labor itself.

Therefore, the authors decided to conduct an observational retrospective cohort study to investigate if any measurable parameters of labor were different, in a sensory versus a standard labor room [0.7].

Additionally, we decided that a questionnaire should be filled by midwives to recover some fundamental information concerning the way they were using the illumination possibilities in the sensory room and get feedback about their experiences of working in the sensory, versus a standard delivery room.

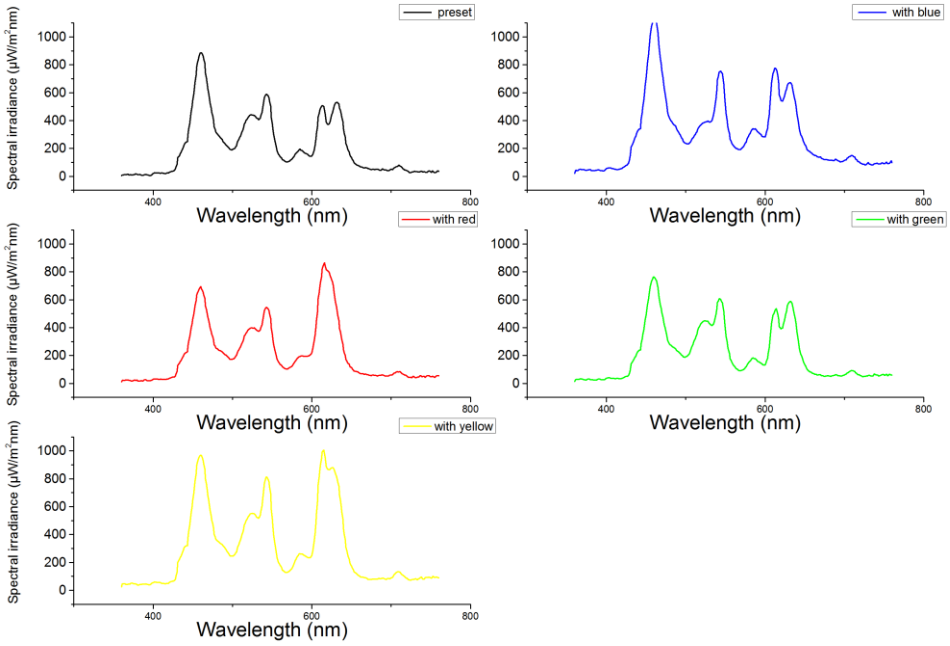

Fig. 5.6: Spectral irradiance of breathing program as preset, and with blue, or red, or green, or yellow settings for the spotlights.

5.3.1.2. Midwives questionnaire

A questionnaire was filled by 50 midwives in order to find out the way the midwives were using the illumination possibilities in the sensory room; and

get feedback about their experiences of working in the ambient environment the LED lighting system was creating.

Half of the midwives (n=25) answered that are choosing the lighting program depending on the labor phase. The occurrence, with which the midwives use the different preset lighting programs in the different phases of labor, is shown in Fig. 5.7. More than one program might be chosen at the same birth phase. The relaxing program is the one used mostly in the labor process. While the white light no sound program is the one used least. The breathing program is the one used most during phases 2 and 3 of labor. For latency and phase 1 the most used programs were reported to be the arrival and relaxing, while after birth the atmospheric program.

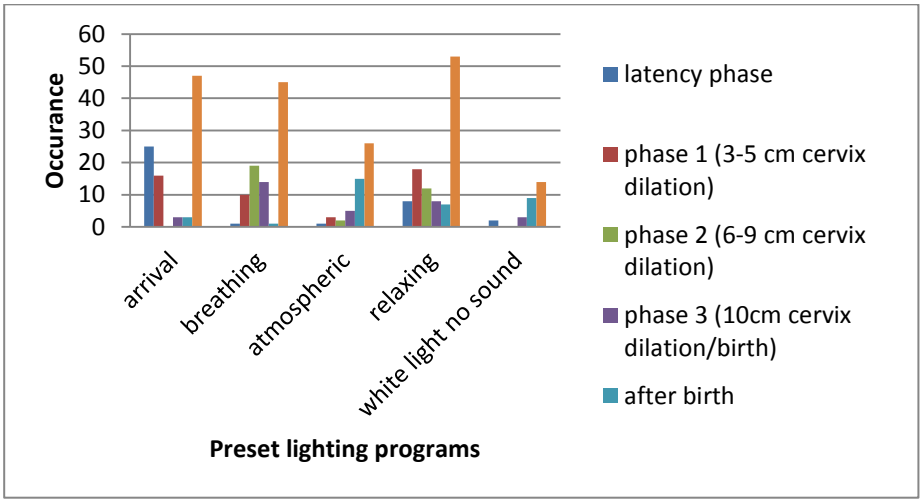

Fig. 5.7: Graph showing the usage of the preset programs by the midwives during the phases of labor.

74% of the midwives answered that they were changing the preset programs and the colors they were most frequently changing were blue and white (most altered colors); and changing them into (introduced colors) red

and yellow (Fig. 5.8). So the tendency was to alter preset programs towards more reddish tints.

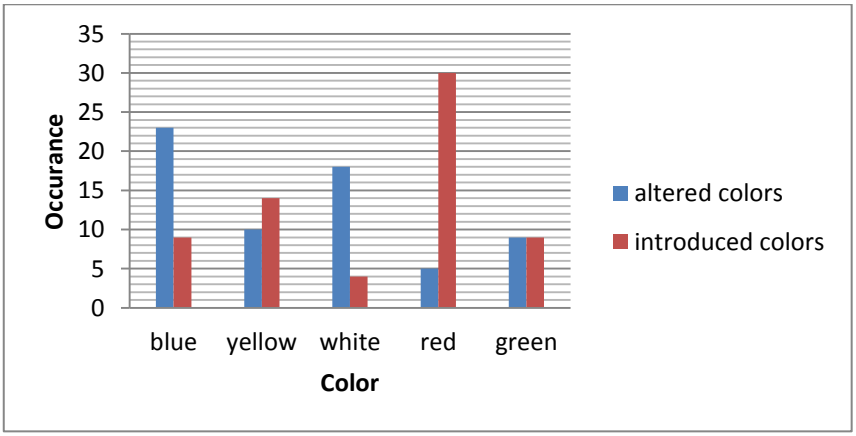

Fig. 5.8: Graph presenting the way midwives where altering the preset programs by altering and introducing colors into the settings. Red color is altered least among the colors and introduced most. Blue and white are altered most among colors and introduced least.

5.3.2. Results

It was found that the light in the sensory delivery rooms is different from the light in standard delivery rooms both in terms of spectral distribution, illuminance and irradiance. The light environment created by the LED lighting system is dynamic, playful and is adaptable to personal preferences. If taking into account the manner the midwives used the preset programs during the birth phases in the sensory delivery room, there was a trend for blue suppressed illumination during the initial phases of labor, but a bluer tint in phase 2 and 3, while compared to a standard delivery room throughout the whole labor process the irradiance and illuminance level were lower.

The observational retrospective cohort study [0.7] demonstrated that the risk for a caesarean section was significantly lower (OR 0.57; 95% CI 0.33-0.97) when giving birth in a sensory delivery room (6.4%) compared to a typical delivery room (10.7%). Furthermore, the midwives majorily answered positively on the experience of working in the sensory delivery room compared to a typical room. According to the midwives' statements "working in the sensory room was less tiring and less stressful".

5.3.3. Conclusion

There are a number of indications that the qualities the LED lighting system offered in the delivery rooms, namely:

- Suppressed blue wavelengths at the initial phases of labor
- Bluish tints during phases 2 and 3
- Lower illuminance and irradiance throughout the whole labor process
- Ability for dynamic and colorful lighting environment
- Adaptable lighting conditions to personal preferences

can benefit both the medical personnel working in these rooms, but also promote the labor process itself (lower risk for cesarean section [0.7]).

5.4. VIS LED lighting systems for athletes

Sleep quality and quantity is undoubtedly related to increased potential for achieving a top performance [5.14, 5.15]. Especially, for elite athletes where the time difference between an unsatisfactory performance and a world record or medal can be a matter of milliseconds. In the present section the potential of using light interventions for sustaining sleep quality and quantity of elite swimmers under conditions of shifted circadian rhythm is investigated.

Light is known to be one of the strongest zeitgebers that entrain the biological rhythms; other zeitgebers of secondary importance are food

ingestion, exercise, social activites, etc. [5.16]. The circadian response to light intervention is dependent on the intensity and spectral distribution of the stimulus and on the timing it is applied.

If external desynchrony occurs due to time zone transitions or abrupt shifts in work times, our internal clock adapts slowly and usually it feels easier to delay the clock than to advance it. Light interventions could accelerate the process and make the alignment, upon forced desychrony, smoother.

Furthermore, a light intervention for improving reaction time was designed based on the background that blue wavelengths might impose alerting effects, not only related to melatonin suppression (circadian pathway) [5.17- 5.19] but through different transmitters (limbic pathway) [5.20-5.22].

5.4.1. Sleep pattern [0.15]

5.4.1.1. Materials and methods

Six elite swimmers were monitored for their sleep patterns throughout two different phases: the baseline period, registered both before and after the intervention; and the preparation period (intervention). The intervention took place in Bermuda in a preparation/training camp; mimicking the conditions expected in the 2016 Summer Olympics in Rio (5 hours shift in circadian rhythm - Denmark is 5 hours ahead of Bermuda, warmer climate, etc.). The intervention period consisted of two phases T1 and T2. At phase T1, athletes were training at normal training times (transition period) 9-11 and 18-20, despite the 5 hours circadian rhythm shift, where also a camp effect is expected due to sudden absence of daily routines. At phase T2, the athletes were training 4 hours later (competition times) 13-15 and 22-24, to fit the time that the Olympic Games would take place (late at night). The time to go to sleep was exactly the same local time (22:40) in Denmark and Bermuda. Only, during phase T2, the time to go to sleep was 3 hours later.

The light interventions comprised of a strict time schedule with alternating blue enhanced white light (CCT: 8000K, cold blue light), blue suppressed white light (CCT: 1200K, warm orange light), daylight and total darkness. The light intervention time schedule is presented in Fig. 5.9. The light bulbs used for executing the light program were LIFX color 1000; and the

predefined light scheme was running by using a user-friendly application dedicated to the light bulbs. Moreover, when using screens (computer, iPad and other electronic devices) the f. lux software was used, to avoid unwanted exposure.

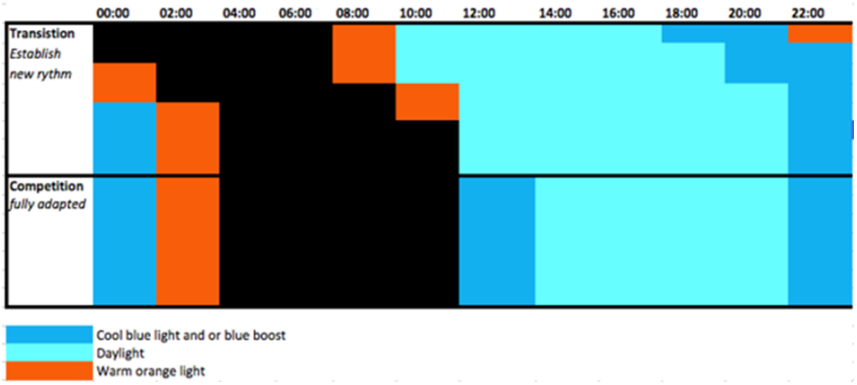

Fig. 5.9: Light intervention time schedule for phase T1 (transition) and T2 (competition), from Jakob Hildebrandt by permission. The black color indicates hours of total darkness [0.15].

For monitoring the sleep patterns of the swimmers, a smart armband system (SenseWear Armband) was used. Sleep duration, efficiency and latency, as well as the percentages of light, deep or REM sleep were the variables under investigation.

To analyze the sleep output, analysis of variance (ANOVA) was used with a significance level of 0.05, using a mixed model with subject (individual swimmers) as a random effect and phase of experiment (baseline or intervention phases T1 and T2) as a fixed effect.

5.4.1.2. Results

It was observed that the light program during the intervention phase significantly enabled the conservation of sleep quantity and quality of the swimmers, despite the shifted circadian rhythm. The results of the ANOVA

showed an insignificant effect of the phase of experiment on all sleep output variables of the swimmers. The hypothesis of no effect of phase of experiment on sleep duration (p=0.17), efficiency (p=0.53), latency (p= 0.90), percentage of light (p=0.38), deep (p= 0.57) and REM (p= 0.52) sleep, were all accepted. The boxplots for the various variables under investigation are presented in Fig. 5.10 (a-f).

The swimmers commented only positively on the light interventions and decided to use them at Rio Olympics 2016. No side effects were observed.

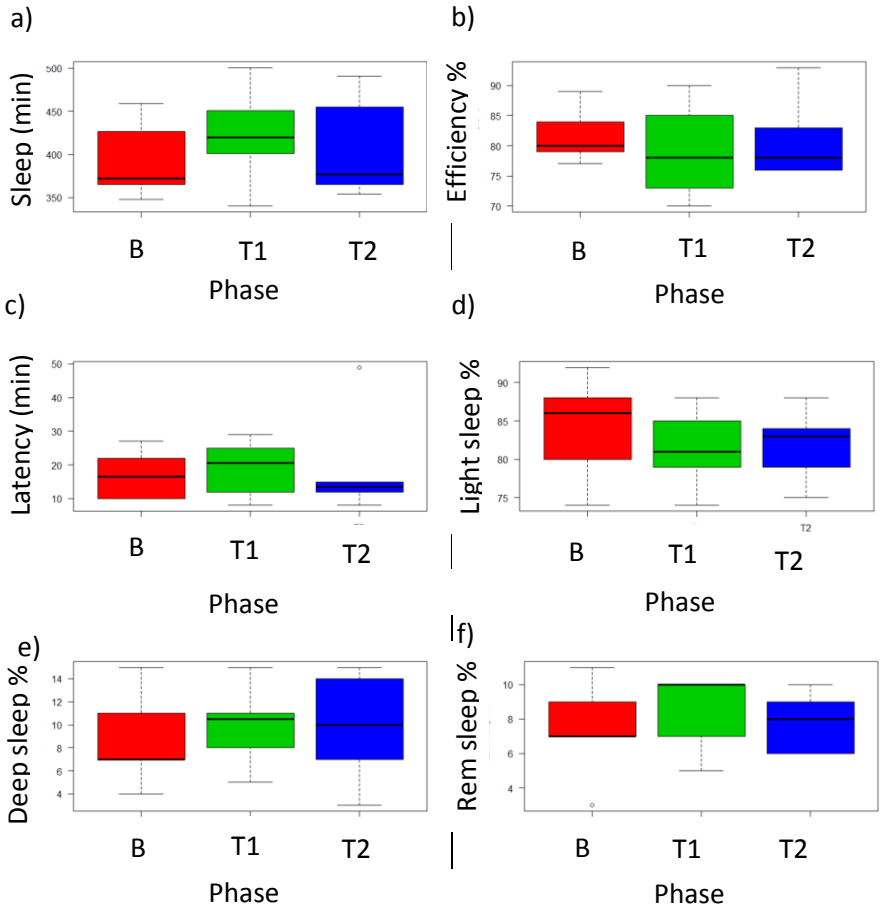

Fig. 5.10: Boxplots of various sleep variables under investigation, at the three different experimental phases (baseline B, intervention phase T1, and intervention phase T2). a) Sleep duration (min). b) Sleep efficiency percentage. c) Latency (min). d) Light sleep percentage. e) Deep sleep percentage. F) REM sleep percentage [0.15].

5.4.1.3. Discussion

The design of this light intervention study was dictated 1) by the fact that everything should be ready within a few weeks to manage to be ready for Olympic competition preparation camp; and 2) that the best possible performance should be intended for all participants. This restriction demanded that all participants received the same treatment (no option of separating a control group to observe potential placebo effects). Individual differences in a complex system like circadian rhythm adaptation are very pronounced; therefore, in order to test them, much bigger populations should be investigated. Furthermore, several repetitions would be needed to confirm the outcome.

On the other hand, exactly the rarity of this study is also its most fundamental strength. It is a very unusual setting that one has the opportunity to test an alternative approach like light intervention on world-class elite athletes, which could be considered the optimal version of the human organism.

The sleep patterns in such circumstances of somatic exhaustion can easily be disturbed; on this occasion despite the presence of jetlag [5.23, 5.24] and by no pharmacological means, the sleep pattern was sustained.

5.4.2. Reaction time

Some preliminary testing was performed with blue light (Philips HF3430/01 GoLight Blu) short exposures (session of 15 minutes) and possible effect on reaction time after an auditory stimuli was delivered versus absence of exposure. The spectral distribution of the illumination arriving at the eye, both in case of exposure (blue) and without (normal), is shown in Fig. 5.11. The blue light was dimmed to a comfortable level to the participant's eyes. The testing was performed with Jeanette Ottensen, a Danish competitive swimmer who participated at the 2004, 2008, 2012 and 2016 Summer Olympics. She currently holds the Danish record in the 100 m butterfly events, both long course and short course. The testing was performed

before the Olympic Games in Rio. The scatterplots and boxplots showing her reaction times, after the blue exposure and without (normal), are presented in Fig. 5.12. In average, the reaction time was reduced by 16.4 ms after the blue light exposure ($p=3.4*10^{-6}$). Taking into account a 95% CI when applying no treatment, the reaction time could be slower by 9.5 ms up to 23.3 ms.

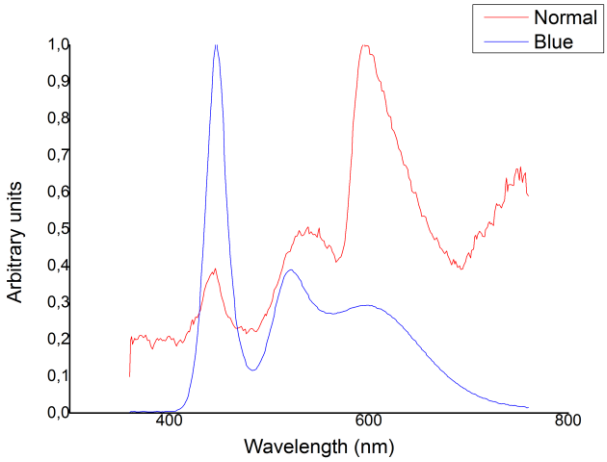

Fig. 5.11: Spectral distribution of the illumination arriving at the eye of the participant for 15 minutes before performing the reaction test. The intensity of the blue light source was dimmed to the level that was comfortable for the participant's eyes.

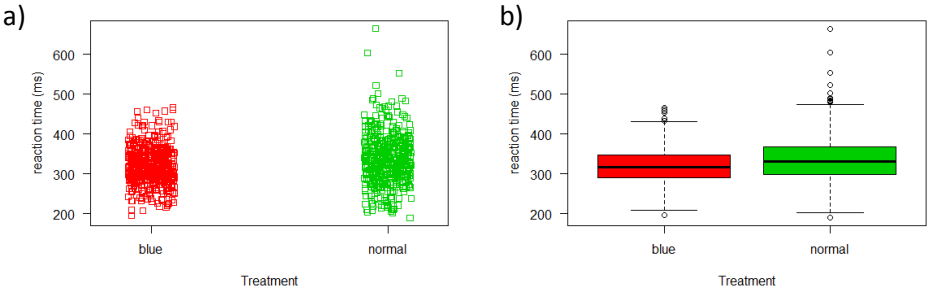

Fig. 5.12: Reaction time in milliseconds after an auditory stimuli is applied after exposure to blue light is performed; and without (exposure to blue light). a) Scatter plot b) Boxplot.

Since the results were encouraging, it was decided to repeat the test on 10 individual adults, defining themselves as “Gamers” with a visual stimulus instead. The results are shown in Fig. 5.13.

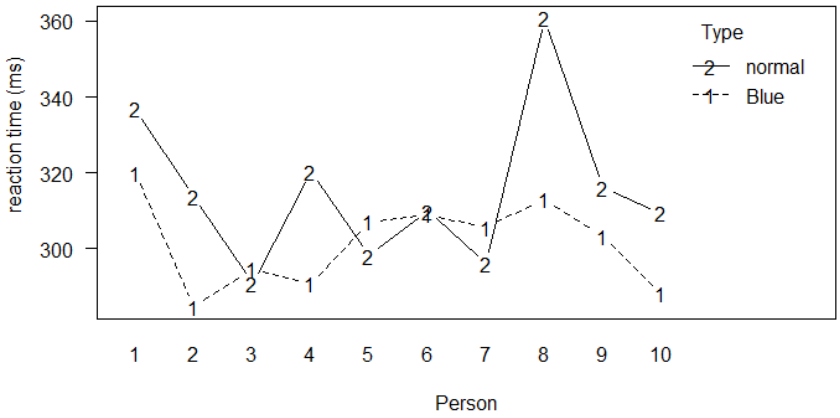

Fig. 5.13: Reaction times for the 10 individual adults after a visual stimulus is applied under normal conditions (normal;2) and after blue enhanced illumination is applied (Blue;1).

Gamers are expected as a group to be quite quick on responding at visual stimuli. Therefore, if any improvement would be made for this group, that already is trained to respond quickly, stronger potential would be anticipated for a group with lower performance records. On average the reaction time was improved by 13.6 ms after the blue light exposure (95% CI 2.3- 25.0 ms). Acclimatization to the reaction test was implemented on other days than the day of gathering the data. The assignment of which exposure took place first (normal or blue), was random. The participants were not informed about the possible effects of light on their performance. The results acquired indicated that there might be some potential in using blue enriched light (15 minutes exposure) for improving reaction times after a stimulus is applied (auditory or visual). However, for reaching significance a more detailed design would be needed, with bigger population and more repetitions.

5.4.3. Conclusion

Light interventions could become a supplementary basic tool for elite swimmers and coaches to improve sleep patterns in circumstances of disturbed circadian rhythm conditions (uncomfortable competition times, different time zones, etc.). In opposition to other methods for improving sleep pattern (e.g. sleeping pills), light interventions impose minimal risk for causing severe side effects [5.15]. Moreover, light interventions are short acting, inexpensive and can easily become a part of the daily routine.

Blue light interventions (short term exposure of 15min) have been demonstrated to show some potential for improving reaction time after a stimulus, auditory or visual, was applied. Since the exposure is short term the effect is not believed to be related to melatonin suppression. However, in order to reach significance and verify that melatonin suppression is not the reason why reaction time can be decreased after the blue light intervention is completed, further research is needed.

5.5. Visual perception of hand veins: an example of the light-source choice importance [0.1, 0.11, 0.12]

Simulation programs have been reported to be able to predict the needed spectral power distribution for achieving optimal immediate visual clarity [5.25-5.27]. However, due to the complexity of how colors are perceived by human eyes, there can be a shift when comparing reality and simulation [5.28]. Therefore, visual inspection of real objects and with real illumination is crucial for developing light sources that can serve the purpose of enhanced immediate visual clarity.

Especially in the case of biosamples where the diversity and complexity of existent nuances is inevitable, the need for human eye evaluation is stronger. Furthermore, immediate visual examination is the first tool used by medical practitioners in every occasion; and one could also claim that there are occasions where performance in medical practice, is determined by good visibility. For example extended vision to surgeons with usage of endoscopes has revolutionized modern medicine [5.29]. On the other hand

imaging techniques that offer high contrast and resolution are often expensive and the maintenance of the equipment might be challenging.

In the present section the intention is to provide empirical evidence and demonstrate statistically that the spectral distribution of an LED lighting system, providing white light, can affect the ability of humans to identify veins. Inner hand vasculature is an easily accessible biosample that is used as a demonstration paradigm. Apart from that, accessibility of veins is an everyday issue in hospital environments [5.30-5.32], and an LED lighting system developed for easier identification of veins could be a potential candidate for addressing such issues. Equipment for easier identification of veins is already commercially available [5.33-5.35], but currently is very costly.

In the past, several studies have been carried out concerning subjective performance of lighting conditions based on questionnaires [5.36-5.38]. In this section the evaluation of the lighting is assessed by human eye perception and is coupled with a "handling task" that involves time constraints and is not subjective. Non-subjective tests, d2-alertness and concentration test [5.39], have been used for measuring and testing concentration under different lighting conditions [5.40].

5.5.1. Materials and methods

5.5.1.1. Lighting system

An LED multichannel lamp with color rendering index (CRI) ranging from 84 to 95 was developed that allowed ramping the correlated color temperature within the limits 2600-5700 K. The illuminance was kept within 40±9 lx, a level that would not influence the circadian rhythm of medical personnel in case of implementation during night hours. Seven illumination settings were tested in total.

The different LEDs were controlled individually by a Lab VIEW program interface, and mixing was done by a reflector painted with barium sulfate ($BaSO_4$). The light was transmitted through a 3mm thick plastic diffuser. The spectra from the individual LEDs are presented in Fig. 5.14, while the final spectral distributions of the white settings that were tested for their

efficiency in improving direct visual perception, are shown in Fig. 5.15. Among the seven different white

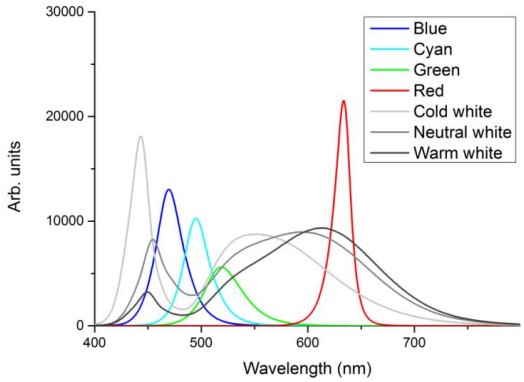

Fig. 5.14: Spectral distribution of the individual LEDs existing in the LED illuminant. All LEDs were measured at 45% of their maximal performance [0.1].

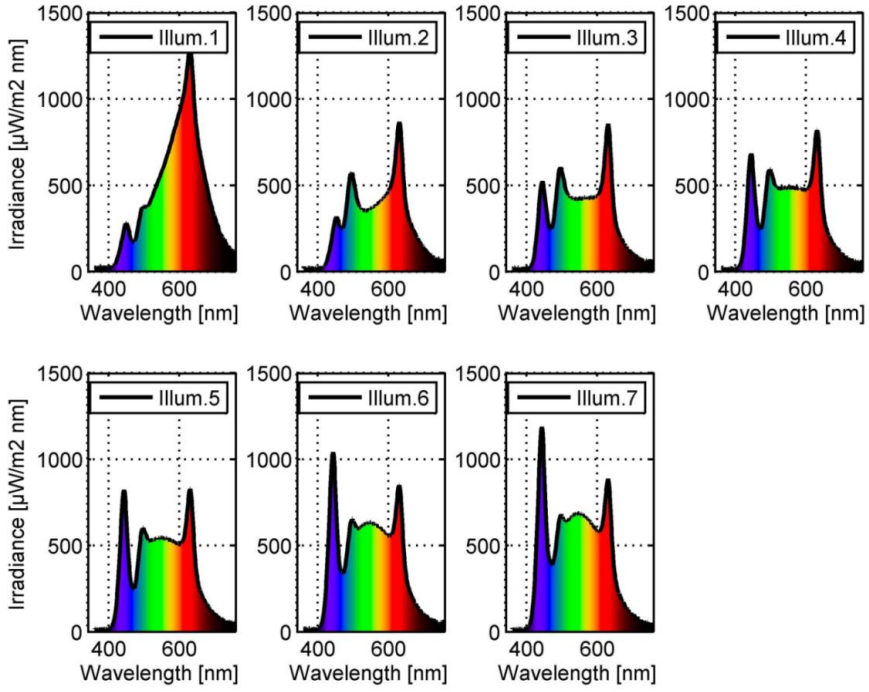

Fig. 5.15: Spectral distribution of white light settings tested for their efficacy to improve direct visual perception [0.1].

illumination settings, Setting 1 (48 lx) was the only one resembling incandescent light but also providing a warm relaxed environment, where the observer could feel calm. Setting 2 (31 lx) was completing the same purpose but without resembling incandescent. Settings 6 (44 lx) and 7 (47 lx) were more imposing a cold clean environment. And settings 3-5 (33-39 lx) were somewhere in between covering a CCT region from 4000-5000 K. At this region RGB LEDs can result in optimal color enhancement ability for early detection of oral cancer [5.41]. An illustration of the environment, as created by the different white illumination settings, is reproduced by images and shown in Fig. 5.16. A color chart is positioned within the field of view to support the illustration of the color shift as achieved; due to the alternation in the spectral power distribution of the white light settings.

External distractions are minimized by placing the lamp within a black painted box. Surrounding illumination is eliminated for the same reasons (no interferences from external light sources). The experimental setup is presented in Fig 5.17.

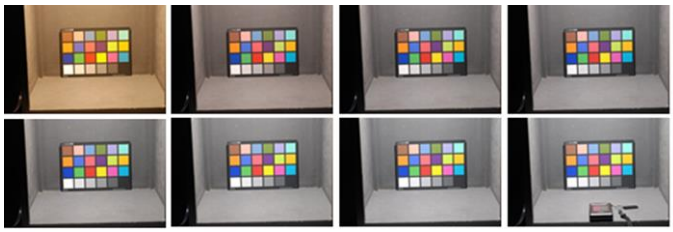

Fig. 5.16: Illustration of the environment created by the different white illumination settings as captured by a camera. The camera is operated under the same settings. The color chart in the field of view facilitates a better perception of the color shift; happening due to the alternation of the white spectral distribution settings [0.1].

Fig. 5.17: The experimental setup. The vein identification process is taking place within a black box created to eliminate external distractions.

5.5.1.2. Method for quantifying ability to identify veins

The human ability to identify veins was quantified in terms of vein identification output; determined as the number of lines drawn by the participant in order to mimic the vein pattern he/she was observing. The drawing was performed on an A4 printing paper and a blue pen was used for the drawing process. The systematic approach followed to estimate the vein identification output achieved under the different illumination settings was the following. 1) The drawings of one person were gathered (both for the reference and the random hand), 2) the optimal and poorest performances were identified for the same object, 3) The intermediate performances were ordered from poorest to best, 4) The medium performance was identified; named MVIO standing for medium vein identification output, and scored by counting the line entities present on the drawing. The MVIO was a relative measure for evaluating performance among different illuminations for the same person and object (random or reference hand), 5) The vein identification output was then calculated by identifying lacking lines and subtracting from the MVIO for the poorer performances; or by identifying additional lines and adding to the MVIO for better performances. The vein identification output score is a measure to express how badly or optimally a pattern, like inner hand vasculature, was perceived visually by the participants due to different illumination settings.

5.5.1.3. Drawing procedure

The instructions given to the thirty-four observers that joined the experiment were as mentioned in Argyraki et al [5.42]: 1) “Draw as many veins as you can see. You will have 1.5 minutes. I will give notice at the initialization and the end of each round.” (2) “You have the freedom to move the hand around for optimal performance.” (3) “Try not to recall where the veins were.” (4) “Draw only the veins you can see and try to replicate the shape/curvature of veins as well as possible.”

These instructions were accompanied by a distraction period where the observer was asked to draw the periphery of the hand to be observed,

before the drawing process itself was started. A typical example of how drawings were looking like is presented in Fig. 5.18.

The procedure was designed in order to minimize carryover effects (learning effects, section 5.4.5.3). The process of copying a pattern with the original design still in view does not involve any conscious effort to retain information in the long term, and also does not demand any organization of material held in memory, resulting in a minimization (if not total elimination) of learning effects. A randomized process, for the sequence of the illumination settings applied for each observer, was adopted to diminish any subconscious learning effects.

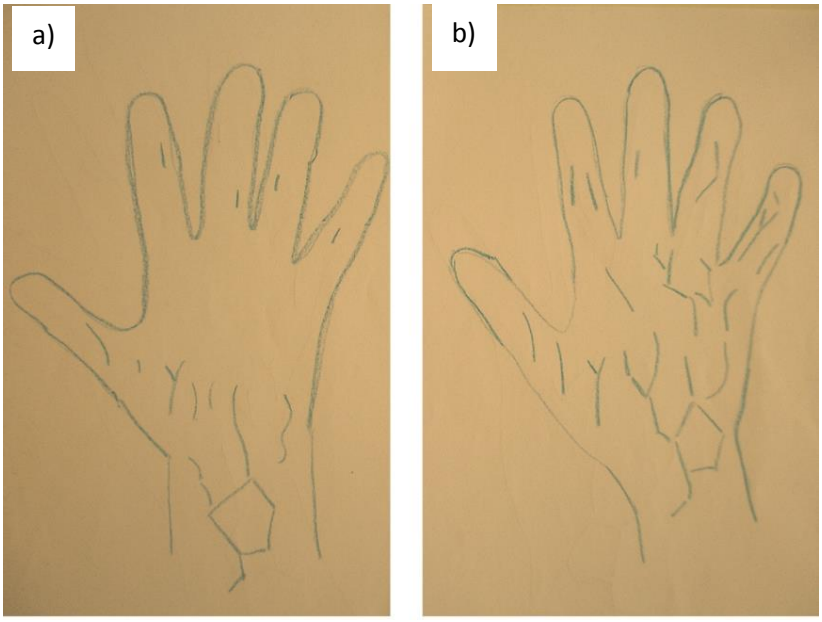

Fig. 5.18: Reproduction of two drawings as created by an observer for random hand. Veins are drawn as lines. a) The drawing was identified as the MVIO and was acquainted with illumination setting 7; and scored with 21. b) Optimal performance drawing under illumination setting 4, exhibiting a VIO of 38. Seventeen additional entities were identified in this case [0.1].

5.5.1.4. Statistics

The population of observers joining the experiment was thirty four, twenty nine of the participants were men and five were women. Thirteen of the men were above 40 while all women were below 40. Around the age of 40, the eye lens of the human eye is expected to transmit less of the blue wavelengths [5.2], therefore the age group could be considered as a confounder variable. Similarly, gender was considered as a confounder. However, no special concerns for data acquisition were taken to assure a "balanced design"; therefore confounders were introduced as fixed effects [5.43].

Since the goal was to simulate a real life situation, observers with abnormal visual acuity were not excluded by the study but just allowed to keep their corrective lenses on. Observers with abnormal color vision were excluded from the sample population.

The analysis of the vein identification output was done with a significance level of 0.05. Analysis of variance (ANOVA) was performed using a mixed model with illumination setting as fixed effect [5.43, 5.44], (similarly for confounders) and subject as random effect. To avoid comparison of illumination settings to darkness an intercept was introduced. Pairwise t-tests were used to find differences among performances with the different white illumination settings, after taking into account the differences among individuals [5.45]. The statistical software was R [5.46] and the functions used were lmer [5.47, 5.48], ANOVA and t- test.

5.5.2. Results

5.5.2.1. Reference hand

On the reference hand the illumination settings tested were 1, 2, 4, and 7. A significant effect of illumination setting on the vein identification output was found ($p=4.8*10^{-7}$). The detailed results are presented in table 5.5. Illumination setting 1 was the illumination under which the majority of observers performed worst, only for 5.9% of the population that was not

true. The distribution of the population for the different illumination settings and optimal performance is presented by a histogram (Fig. 5.19).

Table 5.5: Summary results for vein identification output as obtained for the reference hand. The improvement percentage is calculated in relation to illumination 1, which resembled incandescent light, and was found to result in the worst performance for the majority of observers [0.1].

Illumination setting	Average vein identification output	Standard deviation of vein identification output	Average Performance improvement %
1 (CCT: 2600 K)	19.3	0.9	Not applicable
2 (CCT:3700 K)	22.5	2.3	16.6
4 (CCT:4700 K)	24.0	2.3	24.3
7 (CCT: 5700 K)	23.1	2.3	19.7

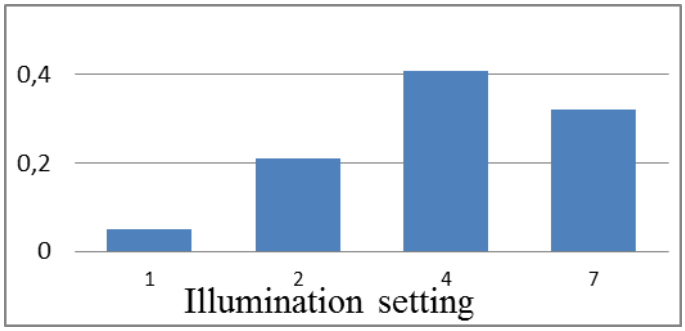

Fig. 5.19: Histogram showing the population distribution at the various illumination settings and optimal performance for reference hand [0.1].

The p. values from the t-pairwise analysis for identifying differences in the vein identification output among illumination settings are presented in table 5.6. Only illumination setting 1 was resulting significantly different vein identification output.

Older observers in average performed (numerically) worse on the task (score reduced by 2.4), though significance levels were not reached (p=0.16). Male observers also performed on average worse (numerically) than females (score reduction by 1.9), but significance levels were not reached (p=0.42). Women in that study were all young (below 40) so the increased performance can be explained by the age related trend.

Table 5.6: Results from t-pairwise test on reference hand. Only illumination setting 1 was identified significantly different from rest illumination settings [0.1].

	Illumination setting 1	Illumination setting 2	Illumination setting 4	Illumination setting 7
Illumination setting 1	1	3^{-5}	3^{-6}	5^{-5}
Illumination setting 2	3^{-5}	1	0.13	0.43
Illumination setting 4	3^{-6}	0.13	1	0.29
Illumination setting 7	5^{-5}	0.43	0.29	1

5.5.2.2. Random hand

A significant effect of illumination setting on the vein identification output was found also with the random hand (p= 0.029). The detailed results are presented in table 5.7. The best performance was observed under illumination setting 4. 35% of the participants reached their optimal performance under this setting. The distribution of the participants for the different illumination settings and optimal performance is presented by a histogram (Fig. 5.20). For 23.4% of the participants, the maximum performance was observed in more than one illumination settings. Pairwise t-tests showed significant differences only between illumination setting 1 and each of the other settings (p= 0.01).

Table 5.7: Summary results for vein identification output as obtained for the random hand. The improvement percentage is calculated in relation to illumination 1 [0.1].

Illumination setting	Average vein identification output	Standard deviation of vein identification output	Average Performance improvement %
Illumination setting 1	17.1	2.6	Not applicable
Illumination setting 2	19.2	3.5	12.3
Illumination setting 3	18.2	3.5	6.4
Illumination setting 4	20.2	3.5	18.1
Illumination setting 5	19.1	3.5	11.7
Illumination setting 6	18.6	3.5	8.8
Illumination setting 7	18.6	3.5	8.8

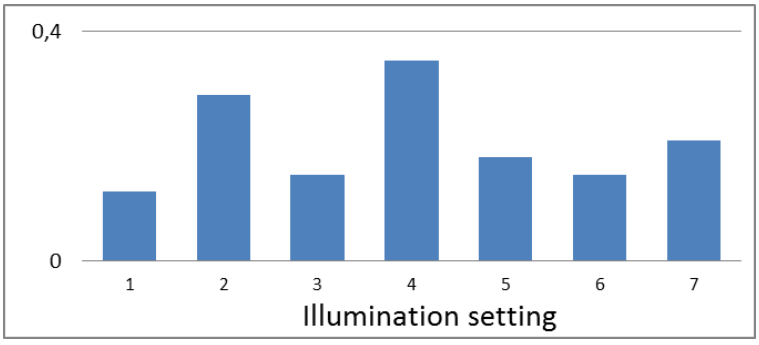

Fig. 5.20: Histogram showing the population distribution at the various illumination settings for optimal performance [0.1].

It is worth mentioning that lower illuminances are not likely to improve visualization. The fact that illumination setting 1 (providing the highest illuminance) resulted in the poorest performance supports the hypothesis that visualization of veins can be improved by applying illumination settings with another spectral distribution either at the same illuminance like illumination setting 7 or even at lower illuminance levels like illumination settings 2, 3, 4, 5, and 6.

Vein identification output of older observers was reduced when performing the test on random hands by 3.6. Significance levels were not reached (p=0.09); and similarly when comparing genders (p= 0.98).

5.5.2.3. Learning effects

To test if any learning effect was present at the process, and possibly introducing a bias for the outcome, we investigated for 70% of the population (remaining data were not available) if the average VIO was increased as a function of the order in which the illumination setting was applied both for the reference and random hand (Fig. 5.21). Additionally the average VIO across all participants' kth drawing was calculated (table 5.8). None of the analysis indicated that significant learning effects could create bias to the outcome.

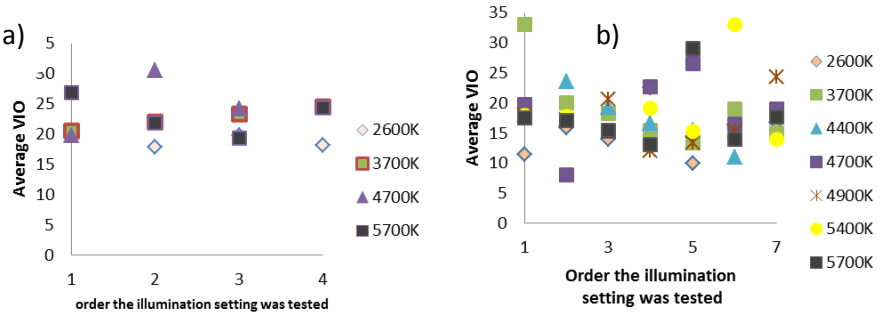

Fig. 5.21: Vein identification output as a function of the order in which the white illumination settings were applied a) on a reference hand b) on a random hand. No significant upward tendency is observed as the order is increased, supporting insignificant learning effects [0.1].

Table 5.8: Summary table with averages of VIOs across all participants' kth drawing: both on reference and random hand [0.1].

	Drawings' order						
object	1st	2nd	3rd	4th	5th	6th	7th
Random hand	17.33	17.13	17.50	17.58	17.08	16.27	18.67
Reference hand	21.14	21.75	22.3	22.3	Not applicable		

5.5.3. Discussion

In the present section a paradigm was presented; that the choice of the spectral distribution of a light source can significantly affect the ability of humans to identify critical biological entities in a body. For the first time that was done not by simulation programs and computing, but through constructing a real LED light source and then evaluating statistically the performance of human eyes on a specific task. The white light settings tested were all targeting to generate a good color rendering as well as disturb the circadian rhythm of the user as little as possible.

Old lighting technologies (fluorescent lamps, halogen lamps, etc.) are expected to be exchanged soon by LED lighting technology due to the lower energy consumption they can offer. In that perspective, LED light sources can both support energy saving needs but also optimize direct visual perception.

However, due to the infinite color palette existing in the potential applications (not necessarily only biomedical application) the optimization process should be application specific.

5.5.4. Conclusion

It was demonstrated that the specific spectral distribution of the light source can alter the direct visual perception of humans and affect their performance on a specific task.

5.6. Novelty of the chapter

Brainard et al [5.49] presented for the first time in 2001 evidence for a novel photoreceptor in the retina that could stimulate production of hormones. Since then, a huge amount of research has been performed, with the scope to understand how light regulates hormone suppression and consequently the circadian rhythm [5.50-5.53, 5.18].

Here, for the first time we study broadly how LED lighting systems, that enable spectral regulation and dynamic modulation of general illumination throughout the day, could be used as a light intervention tool that could benefit populations with special health care needs, namely non-institutionalized elderly, women in labor, and elite athletes.

Effects of light on the elderly have been reported before [5.54] but the light interventions were not an integrated aspect in their daily activities installed in their homes [5.55, 5.56]. Women and light has been studied in the past especially for the correlation observed between night shifts and breast cancer [5.57-5.59]. Here, a new angle namely light interventions as a tool for improved birth labor is investigated. Furthermore, light interventions in sports [5.19, 5.60] are for the first time incorporated in the preparation and execution of the training program of elite athletes that competed in Olympic Games (2016).

Finally, it is for the first time demonstrated that white illumination settings can affect the human ability to identify biosamples. The statistical confirmation of the superiority of the “optimal illuminant” was done by human eye perception.

The novelties, related to VIS LEDs and improved human health or optimization of health care applications, achieved by the author of this thesis are presented below:

- Conceptualization and execution of statistical evaluation of LED light source for improved visualization of biosamples [0.1]
- Investigation and analysis of light environment differences between sensory and standard delivery rooms [0.7]
- Conceptualization of light intervention for improved reaction time of athletes.

5.7. Summary

Light interventions with VIS LED lighting systems can become beneficial for populations with special health care needs. A table summarizing the different specific populations tested and the respective positive outcome is presented below (table 5.9.). The LED lighting systems used for the different interventions were characterized in terms of their spectral distribution, illuminance, irradiance, and sometimes efficacy.

Light interventions as applied here are non-invasive, relatively inexpensive and are expected to result in no or minor side effects. In the perspective that older general lighting technologies are out-phased due to their higher energy consumption, it is worth investigating the additional potential benefits that LED technology can offer, apart from the environmentally friendly profile.

Table: 5.9: Summary of benefits of light interventions on populations with special health needs. All light interventions were performed with VIS LED lighting systems [0.1, 0.3, 0.7, 0.11, 0.12, 0.15].

Illumination type	population	Parameters that improved	Outcome
Modulated spectral distribution (SPD) throughout the day, low illuminance and irradiance in the afternoon	Active elderly [0.3]	Sleep quality	Better PSQI score for females which were identified as poor sleepers at baseline
		Preference: Likeability +	Majority of participants preferred the experimental light compared to their usual light
		Practical issues	Power efficacy of experimental light was over 75%

Modulated SPD throughout labor, adapted by midwives	Women in labor [0.7]	Caesarean section frequency	Only 6.4% in the delivery room with light intervention, compared to 10.7% in standard delivery room
Adaptable lighting in working environment	Midwives	Stress factor (self evaluation)	Less stressful to work in room with experimental light
		Tireness factor (self evaluation)	Less tiring to work in room with experimental lighting
Light schedule that follows activities	Elite athletes + Gamers	Sleep pattern [0.15]	Sleep quality and quantity was conserved despite shifted circadian rhythm
Short blue light exposure		Reaction time	Potentially improved reaction time after a stimulus, auditory or visual, is applied
White light SPD that does not resemble incandescent light, and low illuminance to disturb minimally circadian rhythm	Medical personnel doing night shifts	Direct vision [0.1, 0.11, 0.12]	Improved performance in identification of veins up to 24%

References

5.1. Brøndsted AE, Lundeman JH, Kessel L., 2013. Short wavelength light filtering by the natural human lens and IOLs – implications for entrainment of circadian rhythm. Acta Ophthalmol. 91, pp. 52–7.

5.2. Kessel L, Lundeman JH, Herbst K, et al., 2010. Age-related changes in the transmission properties of the human lens and their relevance to circadian entrainment. J. Cataract Refract Surg. 36, pp. 308–12.

5.3. Turner Pl, Mainster MA. 2008. Circadian photoreception: Ageing and the eye's important role in systemic health. Br. J. Ophthalmol. 92, pp. 1439–44.

5.4. Kessel L, Siganos G, Jørgensen T, et al, 2011. Sleep disturbances are related to decreased transmission of blue light to the retina caused by lens yellowing. Sleep. 34, pp. 1215–19.

5.5. Kim Y.H., Jung K.I., Song C.H., 2012. The effect of cataract on sleep time and quality in late adulthood. Aging Clin. Exp. Res. 24, pp. 663–8.

5.6. Gordijn M.C.M., Meesters Y., 2012. The effects of blue-enriched light treatment compared to standard light treatment in seasonal affective disorder. J. Affect Disord. 136, pp. 72–80.

5.7. Lee TM, Chan CC, Paterson JG, et al., 1997. Spectral properties of phototherapy for seasonal affective disorder: A meta-analysis. Acta Psychiatrica Scand. 96, pp. 117–21.

5.8. Sharkey KM, Pearlstein TB, Carskadon MA., 2013. Cirdadian phase shift and mood across perinatal period in women with a history of major depressive disorder: A preliminary report. J. Affect Disord. 150, pp. 1103–8.

5.9. Portaluppi F, Smolensky MH, Touitou Y., 2010. Ethics and methods for biological rhythm research on animals and human beings. Chronobiology. 27, pp. 1911–29.

5.10. Levenson JC,Troxel WM, Begley A, et al., 2013. A quantitative approach to distinguishing older adults with insomnia from good sleepers controls. J. Clin. Sleep Med. 92, pp. 125–31.

5.11. Buysse DJ, Reynolds CF, Monk TH, et al., 1988. The Pittsburg sleep quality index: A new instrument for psychiatric practice and research. Psychiatry Res. 28, pp. 193–213.

5.12. Horne, JA, O¨ stberg O., 1976. A self-assessment questionnaire to determine morningness-eveningness in human circadian rhythms. Int. J. Chronobiol. 4, pp. 97–110.

5.13. Cagnacci A, Soldani R, Melis GB, Volpe A., 1998. Diurnal rhythms of labor and delivery in women: modulation by parity and seasons. American journal of obstetrics and gynecology. 178(1 Pt 1), pp. 140-5.

5.14. Samuels, C., 2009. Sleep, recovery, and performance: the new frontier in high-performance athletics. Physical medicine and rehabilitation clinics of North America, 20(1), pp.149-159.

5.15. Golden, R.N., Gaynes, B.N., Ekstrom, R.D., Hamer, R.M., Jacobsen, F.M., Suppes, T., Wisner, K.L. and Nemeroff, C.B., 2005. The efficacy of light therapy in the treatment of mood disorders: a review and meta-analysis of the evidence. American Journal of Psychiatry, 162(4), pp. 656-662.

5.16. Arendt, J., 2010. Shift work: coping with the biological clock. Occupational medicine, 60(1), pp. 10-20.

5.17. Nathan J, Reh R, Ankoudinova I, Ankoudinova G, Chang B, Heckenlively J, Hurley JB., 2006. Scotopic and photopic visual thresholds and spatial and temporal discrimination evaluated by behavior of mice in a water maze. Photochemistry and Photobiology 82, pp. 1489–1494.

5.18. Cajochen C, Münch M, Kobialka S, Kräuchi K, Steiner R, Oelhafen P, Orgül S, Wirz-Justice A., 2005. High sensitivity of human melatonin, alertness, thermoregulation, and heart rate to short wavelength light. J Clin Endocrinol Metab 90, pp. 1311–1316.

5.19. Knaier, R., Meister, S., Aeschbacher, T., Gemperle, D., Rossmeissl, A., Cajochen, C. and Schmidt-Trucksäss, A., 2016. Dose–response relationship between light exposure and cycling performance. Scandinavian journal of medicine & science in sports. 27(6), pp. 794–801.

5.20. Lehrl, S., Gerstmeyer, K., Jacob, J.H., Frieling, H., Henkel, A.W., Meyrer, R., Wiltfang, J., Kornhuber, J. and Bleich, S., 2007. Blue light improves cognitive performance. Journal of neural transmission, 114(4), pp. 457-460.

5.21. Alkozei, A., Smith, R., Pisner, D.A., Vanuk, J.R., Berryhill, S.M., Fridman, A., Shane, B.R., Knight, S.A. and Killgore, W.D., 2016. Exposure to Blue Light Increases Subsequent Functional Activation of the Prefrontal Cortex During Performance of a Working Memory Task. Sleep, 39(9), pp. 1671-80.

5.22. Rautkyä E, Puolakka M, Halonen L., 2012. Alerting effects of daytime light exposure-a proposed link between light exposure and brain mechanisms. Light Res Technol 44, pp. 238–52.

5.23. Manfredini, R., Manfredini, F., Fersini, C. and Conconi, F., 1998. Circadian rhythms, athletic performance, and jet lag. British journal of sports medicine, 32(2), pp.101-106.

5.24. Lee, A. and Galvez, J.C., 2012. Jet lag in athletes. Sports health, 4(3), pp.211-216.

5.25. M. Litorja, S. W. Brown, C. Lin, and Y. Ohno, 2009. Illuminants as visualization tool for clinical diagnostics and surgery," Proc. SPIE 7169, 71691B.

5.26. M. Litorja and B. Ecker, 2010. Use of a spectrally tunable source to explore improvement in chromatic contrast for illumination of tissues," Proc. SPIE 7596, 759607.

5.27. W. Davis and Y. Ohno, 2005. Toward an improved color rendering metric. Proc. SPIE 5941, 59411G.

5.28. S. M. C. Nascimento and O. Masuda, 2014. Best lighting for visual appreciation of artistic paintings—experiments with real paintings and real illumination. J. Opt. Soc. Am. A 31, pp. A214–A219.

5.29. K. Gono, T. Obi, M. Yamaguchi, N. Ohyama, H. Machida, Y. Sano, S.Yoshida, Y. Hamamoto, and T. Endo, 2004. Appearance of enhanced tissue features in narrow-band endoscopic imaging. J. Biomed. Opt. 9, pp. 568–577.

5.30. K. Scales, 2005. Vascular access: a guide to peripheral venous cannulation," Nurs. Stand. 19, pp. 48–52.

5.31. L. Dougherty and J. Lamb, 2009. Intravenous Therapy in Nursing Practice, Wiley.

5.32. L. Dougherty, 2008. Peripheral cannulation. Nurs. Stand. 22, pp. 49–56.

5.33. R. K. Miyake, H. D. Zeman, F. H. Duarte, R. Kikuchi, E. Ramacciotti, G. Lovhoiden, and C. Vrancken, 2006. Vein imaging: a new method of near infrared imaging, where a processed image is projected onto the skin for the enhancement of vein treatment. Dermatol. Surg. 32, pp. 1031–1038.

5.34. V. Zharov, S. Ferguson, J. Eidt, P. Howard, L. Fink, and M. Waner, 2004. Infrared imaging of subcutaneous veins. Lasers Surg. Med. 34, pp. 56–61.

5.35. H. D. Zeman, G. Lovhoiden, C. Vrancken, and R. K. Danish, 2005. Prototype vein contrast enhancer," Opt. Eng. 44, 086401.

5.36. P. R. Boyce and C. Cuttle, 1990. Effect of correlated colour temperature on the perception of interiors and colour discrimination performance. Lighting Res. Technol. 22, pp. 19–36.

5.37. C. L. B. McCloughan, P. A. Aspinall, and R. S. Webb, 1999. The impact of lighting on mood," Lighting Res. Technol. 31, pp. 81–88.

5.38. Á. Logadóttir, J. Christoffersen, and S. A. Fotios, 2011. Investigating the use of an adjustment task to set the preferred illuminance in a workplace environment. Lighting Res. Technol. 43, pp. 403–422.

5.39. R. Brickenkamp, K. H. Hängsen, T. Merten, and K. D. Hängsen, D2 Aandachts en concentratie test [D2 Alertness and Concentration Test] (Hogrefe Uitgevers, 2007).

5.40. P. J. C. Sleegers, N. M. Moolenaar, M. Galetzka, A. Pruyn, B. E. Sarroukh, and B. van der Zande, 2013. Lighting affects students' concentration positively: findings from three Dutch studies. Lighting Res. Technol. 45, pp. 159–175.

5.41. H. C. Wang and Y. T. Chen, 2012. Optimal lighting of RGB LEDs for oral cavity detection," Opt. Express 20, pp. 10186–10199.

5.42. Argyraki, A., Clemmensen, L.K.H. and Petersen, P.M., 2016. Does correlated color temperature affect the ability of humans to identify veins?. JOSA A, 33(1), pp.141-148.

5.43. M. J. Crawley, Statistics: An Introduction Using R (Wiley, 2005), Chap. 1.

5.44. M. J. Crawley, Statistics: An Introduction Using R (Wiley, 2005), Chap. 9.

5.45. M. J. Crawley, Statistics: An Introduction Using R (Wiley, 2005), Chap. 6.

5.46. R Core Team, "R: A language and environment for statistical computing. R foundation for statistical computing," Vienna, Austria, 2014, http://www.R‐project.org/.

5.47. D. Bates, M. Maechler, B. Bolker, and S. Walker, "lme4: Linear mixed-effects models using Eigen and S4. R package version 1.1-7," 2014, http://CRAN.R‐project.org/package=lme4.

5.48. D. Bates, M. Maechler, B. Bolker, and S. Walker, 2015. Fitting linear mixed-effects models using lme4. J. Stat. Soft. 67, pp. 1–48.

5.49. Brainard, G.C., Hanifin, J.P., Greeson, J.M., Byrne, B., Glickman, G., Gerner, E. and Rollag, M.D., 2001. Action spectrum for melatonin regulation in humans: evidence for a novel circadian photoreceptor. Journal of Neuroscience, 21(16), pp.6405-6412.

5.50. Lockley, S.W., Brainard, G.C. and Czeisler, C.A., 2003. High sensitivity of the human circadian melatonin rhythm to resetting by short wavelength light. The Journal of clinical endocrinology & metabolism, 88(9), pp. 4502-4502.

5.51. Berson, D.M., Dunn, F.A. and Takao, M., 2002. Phototransduction by retinal ganglion cells that set the circadian clock. Science, 295(5557), pp. 1070-1073.

5.52. Zeitzer, J.M., Dijk, D.J., Kronauer, R.E., Brown, E.N. and Czeisler, C.A., 2000. Sensitivity of the human circadian pacemaker to nocturnal light: melatonin phase resetting and suppression. The Journal of physiology, 526(3), pp. 695-702.

5.53. Lockley, S.W., Evans, E.E., Scheer, F.A.J.L., Brainard, G.C., Czeisler, C.A. and Aeschbach, D., 2006. Short-wavelength sensitivity for the direct effects of light on alertness, vigilance, and the waking electroencephalogram in humans. SLEEP-NEW YORK THEN WESTCHESTER-, 29(2), p. 161.

5.54. Sloane, P.D., Figueiro, M. and Cohen, L., 2008. Light as therapy for sleep disorders and depression in older adults. Clinical geriatrics, 16(3), p. 25.

5.55. Lovell, B.B., Ancoli-Israel, S. and Gevirtz, R., 1995. Effect of bright light treatment on agitated behavior in institutionalized elderly subjects. Psychiatry research, 57(1), pp. 7-12.

5.56. Riemersma-Van Der Lek, R.F., Swaab, D.F., Twisk, J., Hol, E.M., Hoogendijk, W.J. and Van Someren, E.J., 2008. Effect of bright light and melatonin on cognitive and noncognitive function in elderly residents of group care facilities: a randomized controlled trial. Jama, 299(22), pp. 2642-2655.

5.57. Hansen, J. and Stevens, R.G., 2012. Case–control study of shift-work and breast cancer risk in Danish nurses: impact of shift systems. European journal of cancer, 48(11), pp. 1722-1729.

5.58. Ijaz, S., Verbeek, J., Seidler, A., Lindbohm, M.L., Ojajärvi, A., Orsini, N., Costa, G. and Neuvonen, K., 2013. Night-shift work and breast cancer—a systematic review and meta-analysis. Scandinavian journal of work, environment & health, pp. 431-447.

5.59. Bullough, J.D., Rea, M.S. and Figueiro, M.G., 2006. Of mice and women: light as a circadian stimulus in breast cancer research. Cancer Causes & Control, 17(4), pp. 375-383.

5.60. Beaven, C.M. and Ekström, J., 2013. A comparison of blue light and caffeine effects on cognitive function and alertness in humans. PloS one, 8(10), p. e76707.

6. Conclusion and outlook

6.1. Conclusion

The present thesis was concerned with the potential health benefits that LED implementation can stimulate/generate, both as a tool of general illumination, but also as an electromagnetic radiation source. Direct and indirect pathways for improving human health and performance were considered.

A main part of the work involved application of UV LEDs for UV irradiation exposures to combat biofilms or to improve vitamin D content in various food products. A portable setup has been fabricated for performing UV irradiation exposures and UV irradiance measurements. The ability to transfer the setup physically into the laboratories where the different analyses were performed was of foremost importance for conducting the studies. Different irradiation protocols and treatments were developed depending on the specific bioapplications.

More specifically, after a systematic study for the identification of the optimal wavelength for combating multiple species of biofilms (*E. faecalis* [0.6]; and *P. Aeruginosa*), it was found that a wavelength around 296 nm is the most promising in a range from 250 nm to 340 nm for inactivating 24h grown gram negative biofilms (*P. aeruginosa*); and for gram positive (*E. faecalis*) the optimal wavelength region is 280-296 nm (peak performance at 285 nm).

The treatment defined as a “natural treatment” (UVB, central wavelength 296 nm, 20.000 J/m^2) for inactivating biofilms was compared to the “traditional choice” of UVC irradiation 260-265 nm (around 20.000 J/m^2), on biofilms different maturity stages (24h, 48h or 72h grown), and it was

confirmed that the "natural treatment" was more efficient than UVC also for mature biofilms [0.9, 0.17, 0.5]. However, neither of the treatments was reaching adequate levels of inactivation (99.9%) on mature biofilms.

Furthermore, the "natural treatment" was compared to conventional antibiotics [0.13] and photodynamic therapy [0.6, 0.16]. It was demonstrated that it was more efficient than the antibiotic monotherapies and photodynamic therapy, independently of the maturity stage of the biofilms. Though, when the "natural treatment" was compared to combinatory antibiotic treatment, they were found equally inadequate to combat mature biofilms (p=0.12); the 99.9% inactivation goal was not reached.

Light assisted antibiotics were suggested for the first time as a method for combating resistant biofilms. It was demonstrated that when antibiotics (tobramycin 100 MIC) are combined with light (UVB irradiation), the concentration of the antibiotic could be reduced by ten-fold without compromising the inactivation output even for mature biofilms. Furthermore for mature biofilms, tobramycin monotherapy at a concentration of 100 MIC, had no significant inactivation effect; but when the same treatment was assisted by light the inactivation output was 3 log (95% CI 2.4 –3.1), while the UVB treatment alone resulted in a 1.1 log inactivation (95% CI 0.58 – 1.30). This indicates that there is a synergetic effect of light and antibiotics. Light assisted antibiotics managed to reach the 99.9% inactivation goal also on mature biofilms.

Nanoscale topography was discussed as tool for implant improvement and a method for fabricating cost effectively nano-topographies was introduced [0.10, 0.14]. The method can also be used for improving light extraction efficacy of LEDs [0.4].

Biofortification protocols involving UV LEDs were developed, for increasing the vitamin D content in various food products: pig skin [0.2], salmon skin, eggs; and with the scope to fit into food production lines. It was demonstrated that the vitamin D content could be increased from 0.005 to 3.6 μg/g for the pig skin [0.2], and from 0.05 μg/g to 0.2 μg/g for egg yolk, after a moderate exposure (approx. 2.000-3.000 J/m^2). For the salmon skin, even after an exposure of 60.000 J/m^2 the increase was from 0.16 μg/g to 1.75 μg/g.

Vitamin D increase in salmon skin by blue light, as suggested previously in the literature, was not confirmed. For the egg biofortification two

methods were presented and both have advantages and drawbacks, the choice of method to be employed should strongly depend on the details of the specific application. Moreover, it was confirmed that the reciprocity hypothesis holds for irradiances in the regime 0.1-43 W/m^2 and the relation between the vitamin D content and the incident radiant exposure was shown to follow logarithmic kinetics expected. The LED with central wavelength at 296 nm was found to be optimal for vitamin D production in pig skin, among twelve LEDs in the range 280 nm-340 nm (approx. step 5 nm).

The success of UV LEDs to disinfect biofilms and bio-fortificate food products, as demonstrated, indicate a promising future for UV LED devices within bioapplications. Especially for occasions where the dual functionality of UVB irradiation (wavelength around 296 nm) becomes relevant, like improved farming environment or special dermatological treatment, one would expect several advances in the near future.

Another main part of the present work was the optical characterization of several commercial LED systems and their positive impact on populations with special health care needs. Regulation of several hormones can be modulated by light, and the conditions under which indoor illumination can assist humans' daily life still remain to be exploited. Here, four occasions were presented, where the illumination environment, as created, by specially designed LED lighting systems promoted wellbeing, compared to typical illumination solutions:

- Elderly women experienced better sleep, PSQI score decreased significantly by 2 units (p=0.007) [0.3]
- Women in labor experienced lower risk for caesarean section (OR=0.57)[0.7]
- Midwives experienced less tiring and less stressful shifts
- Athletes managed to conserve their sleeping patterns, despite the shifted circadian rhythm [0.15].

It was also demonstrated that the specific spectral distribution of the light source can alter the direct visual perception of humans and affect their performance on a specific task [0.1, 0.11, 0.12].
Efforts to improve reaction time by light interventions indicated that there might be some potential in the idea, but significance has yet to be established.

The author of this PhD envisioned to merge knowledge from diverse medical fields and to identify how photonics and LEDs could make a positive impact in medical science. This goal was to an extent achieved.

Although UV LEDs are not yet mature technologically, several steps were taken in this work to explore the effects of their narrowband spectrum and reveal some of the new opportunities they offer in bioapplications.

Concerning VIS LED systems, their technological maturity is inevitable and continues growing. However, the culture about how to implement the available LED lighting systems for best benefit of wellbeing is not yet formed. In this work, considerable steps were taken towards this direction by generating evidence and demonstrating statistically that specially designed light interventions can impose positive impact on human health and performance.

6.2. Outlook

Although several steps have been taken in this work towards the exploration of usage of LEDs for the benefit of human health and wellbeing, many aspects of the underlying mechanisms causing these reactions are not yet clearly understood; and the irradiation processes are still to be optimized. Therefore, several directions could be pointed out for continuation of the present work.

Experiments regarding light assisted antibiotics and inactivation of mature biofilms indicated that a synergetic effect might take place between UVB and tobramycin. Tobramycin alone had no significant inactivation effect on mature biofilms, UVB alone resulted a 1.1 log inactivation, while the light assisted treatment caused a 3 log inactivation. The reasons for this synergy are still to be understood. The author can only speculate some thoughts that the pretreatment with UVB brings the biofilm “community” into a state of emergency, the biofilm in order to fix/counteract the induced mutagenic and cytotoxic DNA lesions shifts/increases its metabolic activity and that makes tobramycin’s operation more effective. To test this hypothesis a trustable method for real-time monitoring of the metabolic activity of biofilms should be developed. Real-time monitoring of the metabolic activity of periodontopathic bacteria has recently been reported by Ishiguro

et al. [6.1]. Another possible pathway would be that the UVB pretreatment reduces the oxygen limitation within the biofilm. Profiling of oxygen distribution in biofilms has recently been reported by usage of microelectrodes [6.2]. The path of light assisted antibiotic treatments has just been approached and only the future can reveal its true potential as a method for combating resistant biofilms.

Additionally, the exact relationship between thickness of biofilm, maturity of biofilm, bacterial species present and optimal wavelength for inactivation should be discovered; as well as the exact radiant exposure for achieving optimal inactivation with minimal risk for the surrounding healthy tissue. The irradiation treatments suggested could be tested in all relevant medical fields providing access of operation like dentistry, dermatology or otorhinolaryngology.

The dual effect of biofortification and disinfection by UV LEDs in the range of 296-300 nm could be further tested and utilized in industrial environments for egg production, as a potential solution to MRSA-infected farm-pigs, or even as a fridge food conservation solution.

With respect to VIS light interventions, the positive impact on labor, namely the lower risk of cesarean section (occurrence of caesarian section: 10.7% for standard and 6.4% for a sensory delivery room) as obtained by an observational retrospective cohort study was impressive [0.7]. However, further validation of the findings, and better understanding of the effects of visible light on the hormones of labor by controlled randomized studies, are necessary. Possible effects of blue light on reaction times of athletes could be tested on bigger populations to reach significance levels and also under more appropriate surroundings during real training conditions; possibility of placebo effects could also be investigated.

Finally, the ability to enhance visualization just by modifying the spectral distribution of the light source illuminating the object could be further explored for a range of biosamples and tested in real medical environments.

References

6.1. Ishiguro, K., Washio, J., Sasaki, K. and Takahashi, N., 2015. Real-time monitoring of the metabolic activity of periodontopathic bacteria. Journal of microbiological methods, 115, pp. 22-26.

6.2. Moya, A., Guimerà, X., Del Campo, F.J., Prats-Alfonso, E., Dorado, A.D., Baeza, M., Villa, R., Gabriel, D., Gamisans, X. and Gabriel, G., 2015. Profiling of oxygen in biofilms using individually addressable disk microelectrodes on a microfabricated needle. Microchimica Acta, 182(5-6), pp. 985-993.